



**Groundwater Exploration, Development and
Management in NIASM Watershed,
Malegaon Khurd, Baramati**
with special emphasis on
characterising Abiotic Stresses



In collaboration with
Department of Geology, University of Pune

National Institute of Abiotic Stress Management
(Deemed University)
Indian Council of Agricultural Research
Malegaon, Baramati - 413115, Pune, Maharashtra

About the NIASM

Recognizing the importance of influence of climatic change on the already mounting adverse effects of abiotic stresses of climate, water, edaphic factors, etc. on various sectors of agriculture, horticulture, livestock, fisheries, birds, etc., on 19th January 2009, the Union Cabinet approved in XI plan establishment of National Institute of Abiotic Stress Management (NIASM), with a status of Deemed-to-be University, initiated on the recommendation of Shri Moily Oversight Committee on the Implementation of the Reservation Policy in Higher Education (2006). Its foundation stone was laid by Shri Sharadchandraji Pawar, Hon' Minister of Agriculture, GOI on 21st February 2009, at Malegaon Khurd, Baramati, Pune District, Maharashtra. This is a 'Dream Project' of the Council. Wisely the Council vested the responsibility with Natural Resource Management Division to define the target areas to bio and other technologists by bridging the gap to meet the mandate. The mandate of the institute is

- To undertake basic and strategic research on management of abiotic stresses of crop plants, animals, fishes and micro-organisms through genetic, biotechnological and nano technological tools and agronomic methods for enhanced sustainable productivity, food/feed quality and farm profitability adopting integrated interdisciplinary approaches
- To develop a Global Center of Excellence by establishing linkages and networking with national and international Institutes/agencies, and
- To act as repository of information on abiotic stress and management

Presently the science is progressing from the functions of individual genes to behaviours of complicated systems that emerge from the interactions of a multitude of factors. These recent developments necessitate the promotion of a combination of approaches collectively called "Systems Biology." It aims to acquire an insight into background, hypotheses to mitigate, strategies to incorporate with a foresight to practice climatically adaptable farming systems for building sustainable and profitable livelihood in stressed environments and constitutionally acceptable policy issues. Long-term goal is to develop agricultural commodities neutral or adoptable to mounting abiotic stresses under climate change using bio-nano-technologies and other scientific frontier tools without any reduction in productivity to meet food security.

Visit us on WebCampus: www.niam.res.in for more information on the NIASM.



**Groundwater Exploration, Development and
Management in NIASM Watershed,
Malegaon Khurd, Baramati**
with special emphasis on
characterising Abiotic Stresses

by

UK Maurya
RA Duraiswami
KPR Vittal
NR Karmalkar
SV Ghadge



In collaboration with
Department of Geology, University of Pune

National Institute of Abiotic Stress Management
(Deemed University)
Indian Council of Agricultural Research
Malegaon, Baramati - 413115, Pune, Maharashtra

January, 2012

Published by

Director
National Institute of Abiotic Stress Management
Malegaon, Baramati- 413 115, Pune, Maharashtra

Phone: 02112- 254055/57/58, Fax: 02112- 254056

E-mails: niamdirector@gmail.com

Website: www.niam.res.in

Documentation

AK Sharma

Technical Assistance

Pravin More

Santosh Pawar

Citation: Maurya, UK., Duraiswami, RA., Vittal, KPR., Karmalkar, NR., Ghadge, SV. (2012). *Groundwater Exploration, Development and Management in the NIASM Watershed, Malegaon Khurd, Baramati with special emphasis on characterizing Abiotic Stresses*. NIASM Technical Bulletin-4, National Institute of Abiotic Stress Management, Baramati, **p.

© by the author

All rights reserved. No part of this publication may be reproduced, stored in a retrieval system, or transmitted, in any forms or by any means, electronic, mechanical, photocopying, recording, or otherwise, without written permission of the publisher.

First Edition 2012

Cover Photos:

Hard pan in the open well along the NIASM Site

Back Cover Photos:

Photographs of lava features from the Main Pit at NIASM site.

Preface

The National Institute of Abiotic Stress Management (NIASM), with a status of deemed-to-be university was established in the year 2009 to realise the importance of influence of climatic change on the already mounting adverse affects of abiotic stresses of climate, water, edaphic factors etc. on various sectors of agriculture, horticulture, livestock, fisheries, birds etc. The mandate of the institute is to enhance the capacity for abiotic stress management through basic, strategic, and policy support research.

The publication on *Groundwater Exploration, Development and Management in the NIASM Watershed, Malegaon Khurd, Baramati with special emphasis on characterizing Abiotic Stress* is a baseline document that characterises various agroclimatic-abiotic stress factors in the NIASM watershed. This document will help the Graduate/Post Graduate students of agriculture, earth sciences and engineering who are studying the different aspects of soil and water conservation measures in different agro-climatic regions with variable abiotic stresses in the country. The publication will also be of helpful to the administrator/planner for their future activities on watershed development and management. It is envisaged that this publication will serve as an inspiration to students and academia to take up similar projects in diverse agroclimatic zones of India.

Dr. KPR Vittal
Director, NIASM

Contents

Preface

1 Introduction

2 The study area

2.1 Climate

2.2 Land use/ Land cover

2.3 Geology

2.4 Hydrogeology

3 Petrography

3.1 Primary mineral constituents of Basalt

3.2 Secondary mineral constituents of Basalt

3.3 Mineralogical alteration, Transformation and Abiotic Edaphic Stresses

4 Rock Geochemistry and Weathering

4.1 Geochemical variations in Major oxide content

4.2 Geochemical variations in Trace Element content and their role in the Abiotic Stresses

4.3 Weathering of Basalts

5 Groundwater Quality

5.1 Groundwater characteristics

5.2 Evaluation of groundwater for irrigation

5.3 Groundwater facies

6 Geophysical Surveys

6.1 Electrical Resistivity Method (ERM)

6.2 Results and Data Processing

7 Development of Piezometers and Groundwater Management

8 References

List of Tables

- 2.1 Hydrometeorological data from Padegaon Sugarcane Research Station, Baramati
- 2.2 Established geochemical- and lithostratigraphy in the western Deccan Traps
- 2.3 Geological logs from main pit at NIASM site
- 2.4 Geological logs from the different boreholes
- 2.5 Geological logs from various random locations
- 4.1 Major oxide geochemistry and CIPW norms of samples from main pit
- 4.2 Major oxide geochemistry and CIPW norms of samples from the boreholes
- 4.3 Major oxide geochemistry and CIPW norms of random samples
- 4.4 Trace element concentrations (ppm) of samples from main pit
- 4.5 Trace element concentrations (ppm) of samples from the boreholes
- 4.6 Trace element concentrations (ppm) of random samples
- 5.1 Geochemical analysis of groundwater
- 5.2 Classification of groundwater quality in DPR, Maharashtra for irrigation purpose
- 6.1 Latitude and longitude of Electrical Resistivity Survey observation points
- 6.2 Modelled electrical resistivity data output at various locations (1-46) of NIASM site

List of Figures

- 2.1 Location of study area Malegaon in Pune District
- .2 Location map with water abstractions structures in the study area
- 2.3 Climatic conditions recorded from hydro-meteorological lab of Padegaon Sugarcane Research stations, Baramati
- 2.4 Sample location at NIASM Site
- 2.5 Field sketch of the lobate geometry of the compound pahoehoe flow
- 2.6 Photographs of lava features
- 2.7 Field photographs of water abstraction structures (dug wells) from the study area
- 2.8 Some representative lithological sections of dug wells from the study area
- 3.1 Primary mineral constituents of basalt in cross polarized light.
- 3.2 Secondary mineral constituents of basalt in cross polarized light
- 3.3 Mineral alteration and transformations
- 4.1 Total Alkali- Silica (TAS) diagram for basalt samples
- 4.2 Major oxide variation diagram
- 4.3 Trace element variation diagram
- 4.4 Spheroidal weathering of basalt
- 4.5 Crystal growth in cracks of basalt
- 4.6 Al_2O_3 vs. Weathering Index for basalt samples

- 5.1 Map showing the electrical conductivity zones along
- 5.2 Map showing the spatial variation in the Total Hardness values
- 5.3 Isochloride map
- 5.4 Map showing the distribution of nitrate in groundwater
- 5.5 Binary variation diagrams between E.C. and major cations and anions in groundwater
- 5.6 Variations in the Sodium Absorption Ratio
- 5.7 Modified USSL diagram for groundwater samples
- 5.8 Trilinear diagram (Piper 1994) used to classify chemical types of groundwater samples
- 6.1 Geophysical Surveys for groundwater exploration using Electrical Resistivity Method
- 6.2 Grid Map for Resistivity Survey showing 'Vertical Electrical Sounding' (VES) and 'Horizontal Profiling' (HP)
- 6.3 2-D subsurface images of Horizontal profiles 1-2
- 6.4 2-D subsurface images of Horizontal profiles 3-4-5
- 6.5 2-D subsurface images of Horizontal profiles 7-8
- 6.6 2-D subsurface images of Horizontal profiles 19-20
- 6.7 2-D subsurface images of Horizontal profiles 31-30-29-28-27
- 6.8 2-D subsurface images of Horizontal profiles 41-40-38
- 6.9 2-D subsurface images of Horizontal profiles 43-44-45
- 6.10 2-D subsurface images of Vertical profiles 5-6-13-14-22-32-41-42
- 6.11 2-D subsurface images of Vertical profiles 3-9-11-25-39
- 6.12 2-D subsurface images of Vertical profiles 10-17-18-26-35
- 6.13 2-D subsurface images of Vertical profiles 27-36-37-46

1. Introduction

Groundwater is a vital resource for communities and ecosystems in the various agro-climatic zones of Maharashtra State. Groundwater withdrawal for public supplies, agriculture, industry and other uses has increased manifold during the last decade. In many communities, groundwater is the primary or sole source of drinking-water supply and irrigation and therefore its development obviously depletes the amount of groundwater in aquifer storage and causes reductions in discharge to streams and lowers water level in ponds and lakes in the vicinity.

The National Institute of Abiotic Stress Management (NIASM) under administrative control of Indian Council of Agriculture Research (ICAR), Ministry of Agriculture, GoI, Malegaon, Baramati Taluka of Pune District is a newly established Research Institute with a geographical area of 150 acre which includes Institutional Buildings, Residential complexes, Livestocks and Research Farms etc. The site is part of the Karha River Basin which is a closed basin that originates in a hill range away from the Western Ghats and is seasonal, monsoon fed and drains into the Nira River Basin of the Upper Bhima River. The basin has been studied on various aspects like physical environment, geology, hydrogeology, geochemistry etc by many researchers viz. climate and impact on land use by Bhosale (1982), Gadgil et al. (1990) and Powar et al. (1984), Bhosale and Patil (1982); denudational history by Kale and Joshi (2002); soil morphology and mineralogy by Surana (1988); quaternary alluvial by Kale and Rajaguru (1987), Rajaguru et al. (1993), Kale and Dasgupta (2009); mineralogy and geochemistry of calcretes by Dessai and Warrier (1987); the occurrence of a volcanic ash bed in the alluvium by Kale et al. (1993) and Korisetar et al. (1983); the flow

demarcation and mineralogy of the basalts from the Purandhar area by Sowani and Peshwa (1966, 70) and Kanegaonkar and Powar (1978) and trace element distribution in basalts from the Dive Ghat area by Ghodke et al. (1984). Geological Survey of India has undertaken detailed mapping of the area and has classified the flows into the Dive Ghat Formation (Godbole et al., 1996, GSI, 1998). The detailed chemostratigraphy of the area was undertaken by Khadri et al. (1990) and the flows exposed in the area have been classified as those belonging to the Poladpur and Ambenali Formation of Wai Subgroup. More recently, Duraiswami et al (2008) also reported rubbly pahoehoe flows from the Dive Ghat section. Duraiswami (2009) also provided evidence for pulsed inflation in pahoehoe basalts from Morgaon.

The groundwater quality in the Karha Basin is important as several saline tracts and pockets of saline water are encountered in the basin (GSDA, 1992). Based on remote sensing techniques and ground truth verifications, Krishnamurthy et al. (2004) were able to delineate small fracture recharged fresh water pockets in the saline tract between Morgaon and Tardoli. Besides this subsurface modeling of salinity using the modified GLADIT score was attempted by Duraiswami et al. (2008). These studies have been undertaken on the regional scale and it will act as a ready reference to the NIASM watershed.

Study of the groundwater geochemistry is an important bearing on their elemental composition effecting the livestock, fisheries and fodders. The ill effects of various toxic elements (As, Hg, Se, Mo, Cd, Ni, Pd), their threshold concentration and uptake, mobility in livestock and human being, soil and plant systems are well known (Ghosh et.al 2006). Current emphasis on hydro-geochemistry is

related to the chemistry of trace elements controlling the movement, distribution and fate in plants and soils of native pools and anthropogenic addition of elements causing the stresses in different forms. It is therefore proposed to collect detailed geohydro-meteorological baseline data at the NIASM site so that its role vis-a-vis abiotic stress can be evaluated. The basic objectives of the publication is (i) to study thin sections of core and random rock samples for mineralogical make up and hydro-geochemistry of water samples as well as geochemistry of rock/soil samples at different interval of depth for locating the

abiotic stresses, (ii) to carryout geological, geophysical (electrical resistivity) and geohydrological surveys of the NIASM site for the delineation of potential/ suitable/ favorable zones for sinking of water abstraction structures (dug well / bore well) for water supply to farm land, plots and other utilities on the campus and (iii) aquifer performance test (APT) for determining aquifer characteristics and to ascertain the suitable sites for feasibility from the recharge point of view and construction of piezometers or piezometer nest for groundwater management.

2. The Study Area

The NIASM site under study is located between N 18°8'59.279" and 18°9'45.845" and E 74°29'30.38" and 74°30'38.299" and lies between Karha Basin of Bhima River in the north and Nira River Basin in the south. It lies in the Drought Prone Area of plateau region of western Maharashtra on a water divide with a smooth but slightly undulating topography within the limits of village Malegaon Khurd, Baramati Taluka of Pune district. The area is known for its frequent scarcity. The site is well connected by road

with major cities in the State and also by Central Rail Network to Pune via Daund Junction (Fig.2.1). The relief of the area gradually reduces from north to south (Fig.2.2). The side of the area is drained by two streams and generally exhibit dendritic drainage pattern especially in the lower order streams. A prominent percolation tank is built across the western stream while an earthen dam is built across the eastern stream.



Fig.2.1. Location of study area Malegaon in Pune District



Fig. 2.2: Location map of the NIASM site, Malegoan Khurd. Also shown are the locations of the water abstractions structures in the study area. Sample numbers indicated are those used for water quality studies

2.1 Climate

Climatic condition of Baramati has been synthesized based on the mean average of 20 years data which were provided by the Mahatma Phule Krishi Vidyapeeth, Rahuri from its Padegaon Sugarcane Research Station, Baramati for the period of 1990-2010, which are depicted below in Table 2.1 and in various figures (Figs. 2.3 a-h). As per the data the climate of the region is semi-arid dry. Based on the rational classification of climate (Potential evapo-transpiration and Moisture index), the study area experiences arid megathermal climate (Paranjpe, 2001). The total annual rainfall varies from 151.4 to 1124 mm with an average of 602.1 mm. The rainfall is scanty, irregular and relates to the southwest monsoon and it occurs during the months of June to November, smaller amounts of rain derived for the northeast monsoons during April and May contribute to the annual precipitation. The annual maximum temperature varies from 31.2 °C to 32.9 °C with an average of 32.1 °C whereas the annual minimum temperature

varies from 16.8 °C to 20 °C with an average of 17.9 °C (Fig.2.3b&c). The relative humidity varies from 88.3% to 96.4 % with an average annual relative humidity of 92.4 % in the morning whereas in the afternoon it varies from 43.8 % to 69.3 % with an average of 53.8 % (Fig. 2.3d&e). The sunshine hours in a given day varies from 8.2 to 6.7 with an average of 7.7 (Fig. 2.3f). The annual average wind velocity varies from 3.6 to 5 km/ hr with an average of 4.2 km/ hr for the last 12 years (Fig.2.3g). The annual daily evaporation varies from 4.7 to 8.0 mm with an average of 5.6 mm for last 10 years. Joshi (2005) studied the meteorological data obtained by GSDA at Chandgudewadi near Morgaon and according to him the maximum annual evaporation at Chandgudewadi is 17.5mm most of which takes place during the hot summer months of March to May when the average maximum daily temperature is about 33.7°C. Over the last 20 years Baramati received as little as 127 mm and at times greater than 1046 mm of rainfall in a year.

The annual rainfall for the last 20 years shows a general rising trend.

Table 2.1: Hydrometeorological data from Padegaon Sugarcane Research Station, Baramati.

Year	Rain-fall (mm)	Max Temp (°C)	Min Temp (°C)	Humidity at 7.30 hr (%)	Humidity at 14.30 hr (%)	Sun-shine hours	Evaporation (mm)	Wind Velocity (km/hr)
1990	678.8	31.2	17.5	91	49	7.3	5.5	--
1991	433.0	32.2	17.3	92	47	7.9	5.9	--
1992	458.3	32.3	16.8	90	45	8.2	6.1	--
1993	671.9	31.7	17.3	88	47	7.9	5.9	--
1994	286.2	31.3	17.5	93	50	7.6	5.1	--
1995	589.8	32.0	17.3	89	45	8.1	5.8	--
1996	904.5	32.3	17.6	90	44	8.1	5.6	--
1997	511.2	32.0	17.7	90	47	8.1	8.1	4.1
1998	916.8	32.3	18.3	93	52	7.7	5.2	5.0
1999	542.8	31.7	17.6	94	55	7.5	4.8	1.2
2000	537.2	32.3	17.5	92	52	8.0	5.4	4.5
2001	537.4	32.2	17.6	93	53	7.7	5.2	4.1
2002	426.5	32.9	18.2	92	56	7.8	5.6	4.6
2003	151.4	32.9	18.4	90	50	7.9	7.9	3.6
2004	563.8	32.3	18.0	92	58	7.8	5.8	1.7
2005	617.2	31.9	17.8	93	56	7.6	5.4	--
2006	643.2	31.9	18.4	95	58	7.6	5.1	--
2007	574.5	32.0	18.1	93	54	7.6	5.3	3.8
2008	570.0	32.1	17.9	94	61	7.5	5.2	4.0
2009	1124.7	32.3	19.1	95	63	7.4	5.3	4.0
2010	924.3	31.8	20.0	96	68	6.7	5.1	4.5

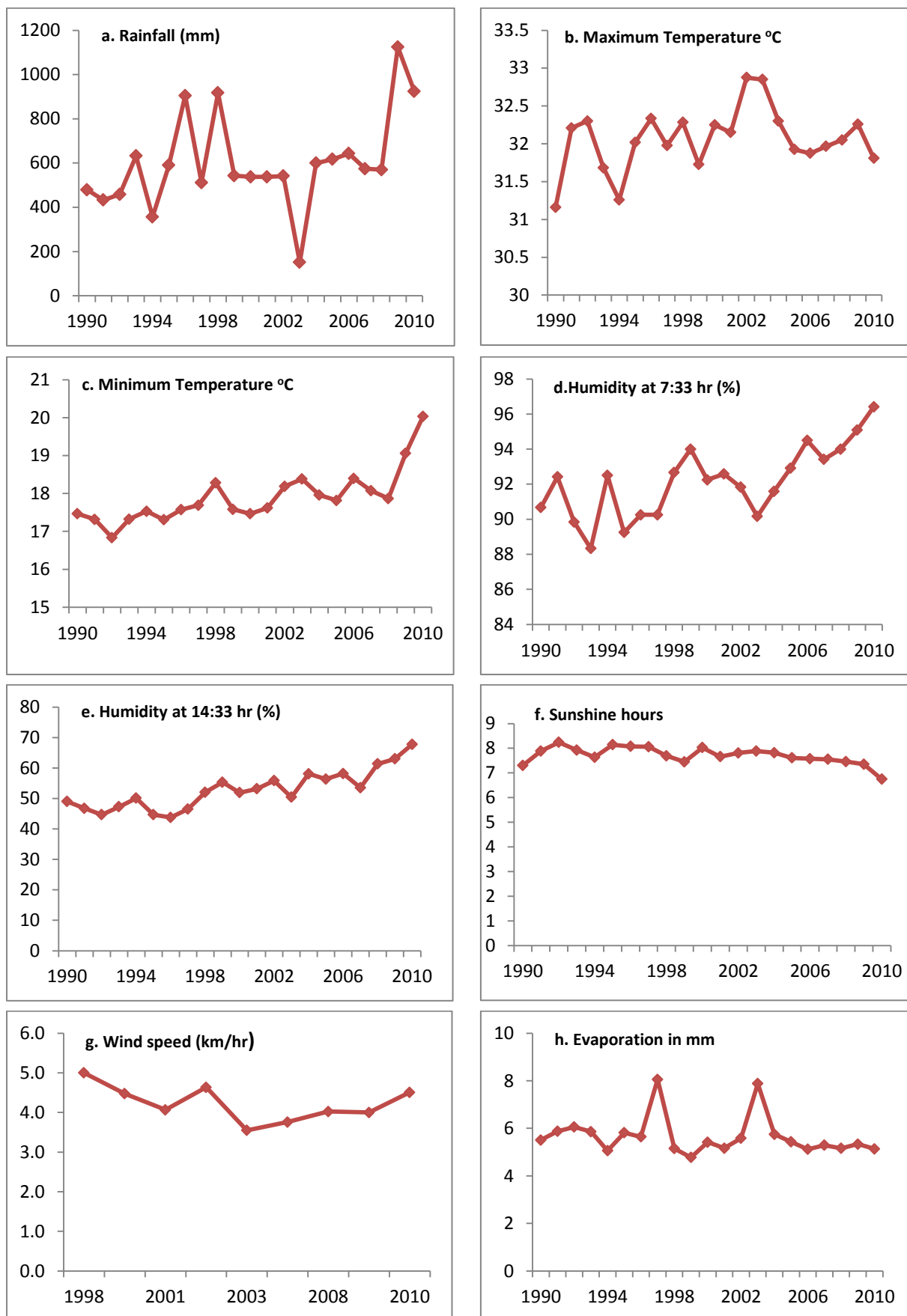


Fig. 2.3: Climatic conditions as recorded from hydro-meteorological lab of Padegaon Sugarcane Research stations, Baramati, showing variations in the rainfall (a), maximum and minimum temperature (b & c), humidity (%) at 7:33 & 14:33 hr (d & e), sunshine hours (f), wind speed in km/hr (g), and evaporation in mm (h)

2.2 Land Use/ Land Cover

The NIASM site consists of vast expanse of fallowland along the moderate basaltic slopes of a water divide (Fig. 2.2). In the fringe areas along the NIASM boundary, sparse vegetation, dominated by xeric shrubs, Babul (*Accacia* sp.) and Neem (*Azadirachta indica*) is present. In the adjacent stream, east and west of the NIASM site, kharif agriculture is generally practiced while perennial sugarcane cultivation is also practiced around the NIASM site by employing the lift irrigation practices. Towards the southwest of the site horticultural plants like pomegranate are grown.

2.3 Geology

The soils/rocks exposed in the study area range in age from Recent to Cretaceous-Eocene. The Recent rocks are represented by shallow alluvium and black cotton soil. The Quaternary is represented by consolidated sediments exposed in the downstream areas of the study. Two lava flows of varying thickness and morphology belonging to the Deccan Traps are exposed in the study area. The lowermost flow F1 is grey, fine-grained, jointed and simple. It is exposed only in the well sections in the study area as well at places where upper flow has been removed by denudation and weathering action. The upper flow F2 is pinkish, vesicular and belongs to the hummocky pahoehoe type. The flow is strongly compound and consists of lava toes, meter scale lobes and thick (~10m) sheet lobes. The vesicles in this flow are small (1-2 cm) and invariably filled with zeolites and other secondary minerals like calcite. The base of individual lava units are marked by pipe-amygdales. The upper flow F2 is extensively exposed in the NIASM site and in the adjacent well sections. An

elaborate geochemical (Beane et al., 1986) and lithostratigraphy (GSI, 1986, Godbole et al. 1996) exists for the Western Deccan Traps (Table 2.2). Detailed mapping in the adjacent areas has revealed the lower simple flow probably belongs to the Indrayani Formation (Godbole et al. 1996) equivalent to the Khandala Formations (Khadri et al. 1999) while the upper compound hummocky pahoehoe flow belongs to the Karla Formation (GSI, 1986, Godbole et al. 1996) or Bushe Formations (Duraiswami, 2009).

A rectangular pit (l:8m, b:2.5m, d:3m) is dug towards the south-central part of the NIASM site and is referred to as the main pit (MP) in this report (Fig. 2.4, Table 2.3). The pit exposes a weathering profile typical of compound pahoehoe flows (Bondre et al., 2004). An intricate geometry of lava lobes and toes is seen on the eastern face of the main pit (Fig. 2.5). Most of the lava toes and lobes (Fig. 2.6a) are completely vesicular and can be classified as s-type lobes of Wilmoth and Walker (1993). The southern face of the MP exposes three distinct lava lobes. The upper lobe is partially exposed and has developed a crude weathering profile. The middle lobe is intact and is completely exposed in cross section in the MP (Fig. 2.6b). The lobe is augen shaped and has a length of 1m and thickness of 0.5m. It consists of the typical 3-tiered internal structure of crust-core-basal zone of Aubele et al., (1988) but is characterized by the lack of pipe vesicles in the basal vesicular zones. Thus, this relatively large lava lobe also belongs to the s-type lobes. The crust of this lobe is highly vesicular and at places develops a crude vesicle banding. The vesicles are small towards the chilled margins of the lobes but become larger (up to 2 cm) towards the base of the crust. A large 40 cm central gas blister or cavity is seen towards the mid

Table 2.2: Established geochemical- and lithostratigraphy in the western Deccan Traps.

<i>Geochemical stratigraphy</i>			<i>Lithostratigraphy</i>						
Group	Sub-group	Formation	Super Group	Group	Sub Group	Formation			
D E C C A N	Wai	Desur	D E C C A N	S A H Y A D R I	Mahabaleshwar	Mahabaleshwar			
		Panhala				M4			
		Mahabaleshwar							
		Ambenali				Purandargad			
		Poladpur				Diveghat			
	Lonavala					Lonavala	Elephanta		
		Bushe					Karla		
		Kandhala					Indrayani		
	Kalsubai					T R A P	G R O U P	Kalsubai	M3
		Bhimashankar							Upper Ratangad
Thakurwadi			M2						
Neral			Lower Ratangad						
Igatpuri			M1						
Jawhar		Salher							
B A S A L T									

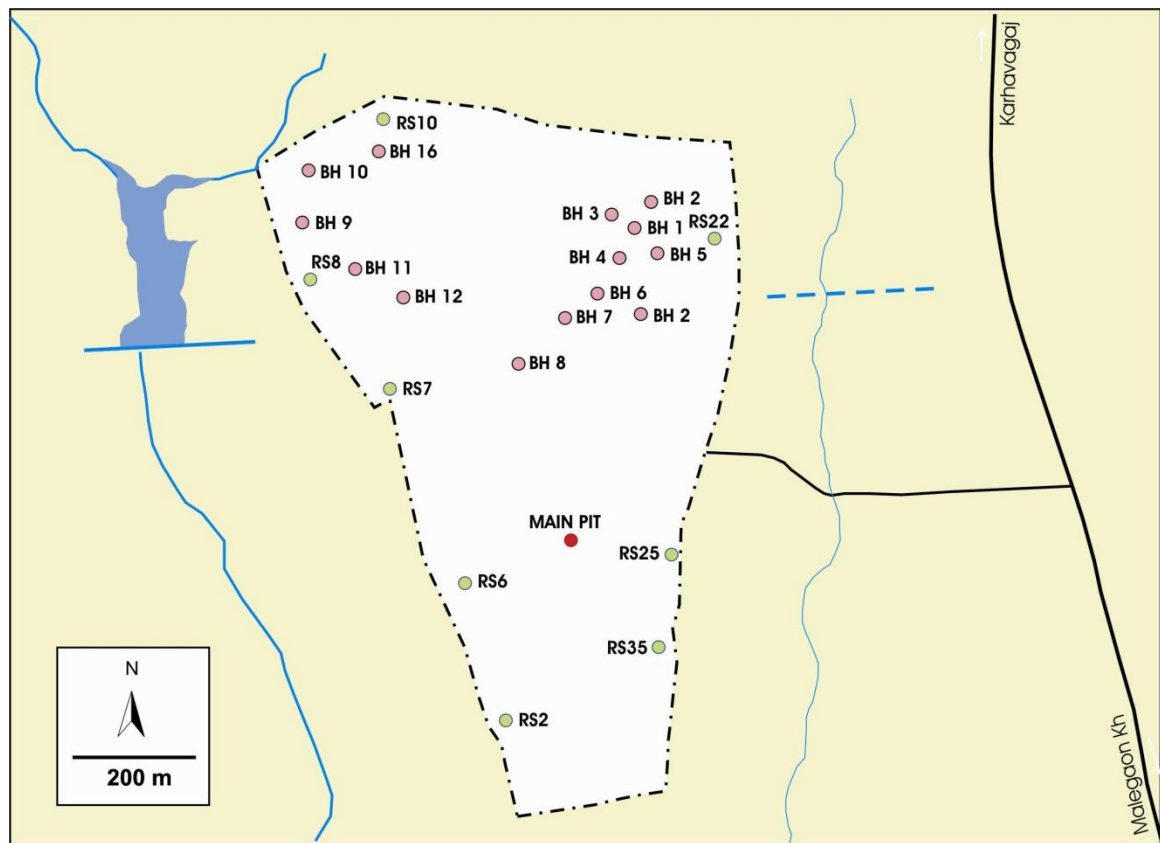


Fig.2.4: Sample location at NIASM Site. Master Pit (MP), Bore Hole Pit (BH 1-12 & 16) and Random Sample Pit (RS 2,6,7,8,10, 12,25 & 35)

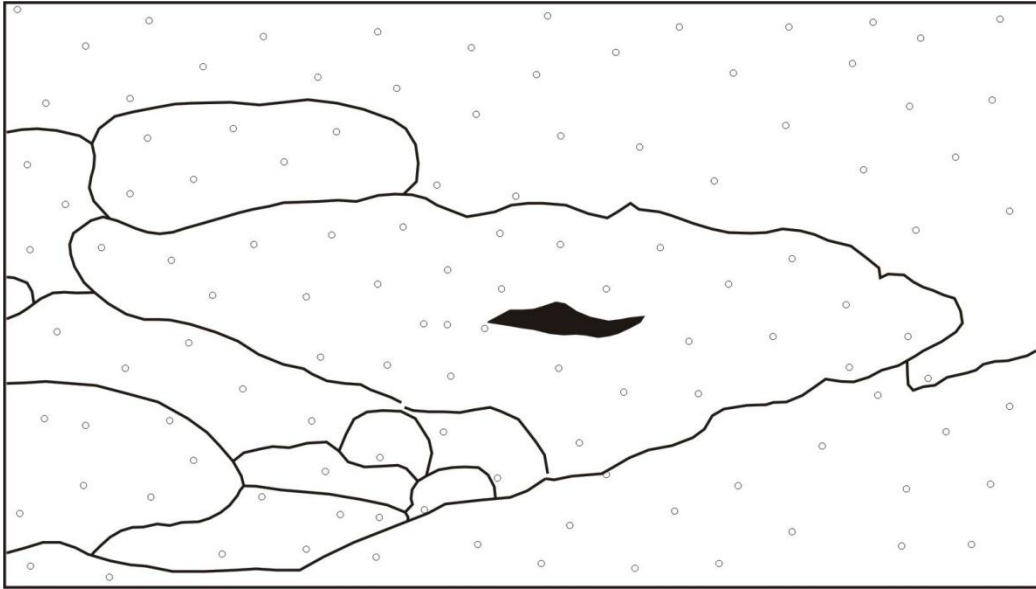


Fig.2.5: Field sketch of the lobate geometry of the compound pahoehoe flow exposed in the NIASM site.

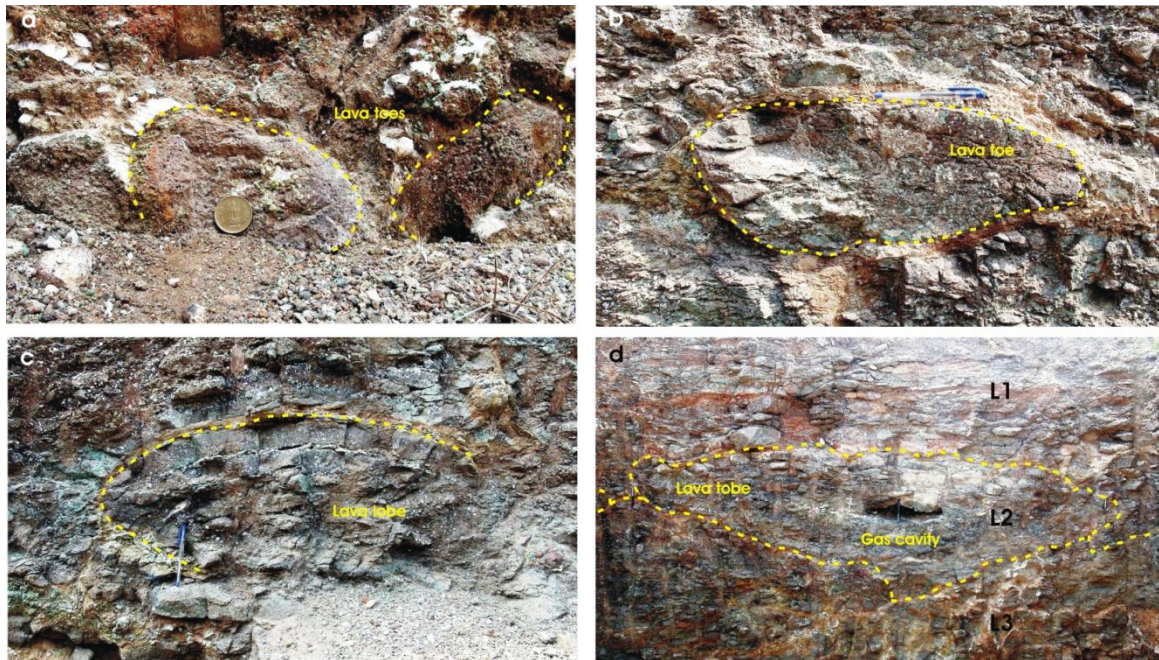


Fig. 2.6: Photographs of lava features from the Main Pit at NIASM site.

central part of the lobe. It is typically dome shaped (Fig. 2.6c) and is lined by zeolites. The western face of the MP exposes a chaotic assemblage of small lava toes (Fig. 2.6d) and lobes. The inter-lobe spaces are highly weathered and show beautiful zeolite mineralization. The MP was sampled at intervals for detailed petrological and geochemical investigations. The detailed lithologs of samples collected is [resented in Table 2.3. Besides this core drilling was conducted to limited depths on earlier dates at numerous locations on the NIASM site for

geotechnical investigations. The cores were inspected and logged and chips were harvested for detailed petrological and geochemical investigations (Table 2.4). Random samples (Table 2.5) were also collected from areas and are represented on the NIASM site (Fig. 2.4) so that weather patterns and inter borehole correlations could be established.

2.4 Hydrogeology

The shallow basaltic aquifer is the main aquifers in the study area. Dug wells and bore wells are the primary source of drinking water and irrigation in the area. The crust in compound flow is an important water-bearing horizon as these contain vesicles and large irregular voids. Besides this, the zone of secondary porosity is the main locales of groundwater. The nature of joints, their frequency and their interconnection determines the aquifer parameters of the flows (Duraiswami, 2000). Flow top breccias and red bole constitute an important aquiclude in the region.

The detailed inventory of the dug wells tapping the basaltic aquifers from the study area (Fig. 2.7) indicate that the well density in the study area varies from 2 per km² to as high as 5 per km². In general, the density of

wells is high along the stream courses. The depth of dug wells varies from 4 to 12 m and the depth to groundwater ranges from 2 to 10.5 m bgl. The lithological sections of select dug wells from the study area were measured in the field and are depicted in Fig. 2.8. There are wide variations in the summer and winter water levels in individual wells. Water level fluctuations in observation wells that tap the shallow, unconfined basaltic aquifers indicate saturation of aquifer during monsoon and desaturation during summer. The yields of the dug wells in basaltic aquifer in the study area vary from 2.60 to 165 kiloliters per day. The yields vary considerably depending on the amount of precipitation and season. Based on published literature (e.g. Joshi, 2005) the specific capacity of basalts varies from 51.05 to 801.71 lpm/m and the transmissivity varies from 34 to 258.48 m²/day. The percentage of storage coefficient varies from 0.46 to 0.128.

Table 2.3: Geological logs from main pit at NIASM site.

Sr. no.	Depth (cm)		Sample No	Description
	From	To		
1	0	17	MP1	Highly weathered basalts with few zeolite filled vesicles
2	17	27	MP2	Weathered basalt with fluffy white zeolite encrustation with few zeolite filled vesicles.
3	27	50	MP3	Fine grained, reddish bole (glassy rind of weathered pahoehoe lobe) with small white patches of calcrete
4	50	65	MP4	Light brown, moderately weathered basalt with 0.2 to 0.9 mm spherical vesicles partly filled with buff coloured zeolite and also one side with white patches of calcrete/zeolite (?)
5	65	70	MP5	Sample similar to MP3, probably lower rind of pahoehoe lobe, no calcrete deposition seen here unlike MP3 and sample slightly harder than MP3.
6	70	83	MP6	Grayish brown moderately weathered basalt with 0.22 to 0.5 mm white amygdales filled with zeolites.
7	83	156	MP7	Grayish moderately weathered basalt with < 2 mm spherical vesicles which contains greenish lining and zeolite mineralization.
8	156	231	MP8	Sample similar to MP7 except the presence of one 3 mm white amygdale and more weathered than MP7

Table 2.4: Geological logs from the different boreholes at NIASM site.

Sr. no.	Depth (m)		Sample No	Description
	From	To		
1	4.5	2.0	BH-1/28	Fresh, brownish, massive basalt with dixytaxitic texture, without vesicles.
6	0.2	1.0	BH-7/3	Brownish massive basalt.
7	4.0	5.0	BH 7/31	Red coloured, highly zeolitised massive basalt.
2	1.5	2.5	BH-9/1	Reddish brown, vesicular basalt with fine zeolites lining the vesicles.
3	4.0	4.5	BH-9/18	Reddish brown massive basalt devoid of vesicles.
4	4.5	5.0	BH-9/22	Reddish brown massive basalt with minute < 1 mm vesicles and some of them are filled with zeolites.
5	3.5	5.0	BH-10/19	Grayish black massive basalt with large stray vesicles filled by zeolites.

Table 2.5: Geological logs from various random locations at the NIASM site.

Sr. no.	Depth (m)		Sample No	Description
	From	To		
1	0.2	1.2	RS2	Reddish vesicular basalt, moderately weathered, few large (~10cm) elongated vesicles, partly filled with zeolites.
2	0.3	1.5	RS6	Reddish brown comparatively fresh basalt with numerous partly filled vesicles.
3	1.0	1.5	RS7	Comparatively fresh reddish grey, fine grained basalt representing massive part of the lava lobe with fine dixytaxitic texture.
4	0.8	1.4	RS8	Comparatively fresh reddish basalt with 0.2 mm to 0.5 mm vesicles lined creamish material, non zeolite bearing.
5	0.3	0.9	RS10	Moderately weathered fine grained basalt showing plain surfaces (joints) along which greenish encrustations of fine zeolite are deposited.
6	0.1	1.3	RS11	Comparatively fresh dense basalt with high vesicle density of spherical to irregular filled with zeolites
7	0.3	1.1	RS17	Comparatively fresh, grey, massive basalt devoid of zeolites but with minute irregular pores (dixytaxitic texture).
8	0.2	1.0	RS25	Sample similar to RS17, but comparatively more weathered.
9	0.1	1.3	RS26	Massive, dense, comparatively weathered basalt where dixytaxitic voids are filled with zeolites.
10	0.3	1.6	RS36	Reddish brown, moderately weathered basalt with small (~2 mm) vesicles filled by platy zeolites.



Fig. 2.7 Field photographs of water abstraction structures (dug wells) from the study area

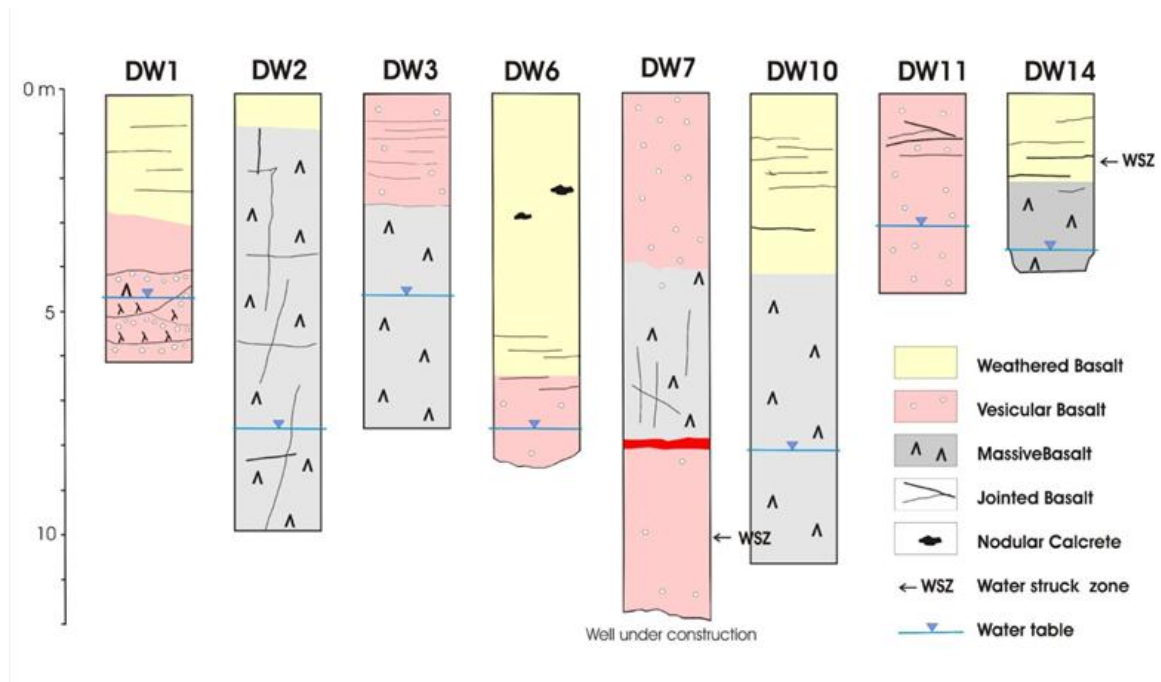


Fig 2.8: Some representative lithological sections of dug wells from the study area.

3. Petrography

Different rocks were collected from the master pit, random pit and bore logs in chronological order upto the depth of 5m from different locations at NIASM Site and are marked in Fig 2.4. Petrographic observation of thin sections were carried out for mineralogical composition of different types of basaltic rocks and their alteration and transformation at different depth to understand the nature and their water holding capacity for ground water recharge and well inventory. All these aspects have been dealt separately. Thin sections were prepared and optical properties of minerals were studied under the polarizing microscope (Nikon, Model No ECLIPSE E200POL) using NIS-Element F3.0 and Coral PHOTO-PAINT X3 software and minerals were identified following Kar (1977) and Read (1963).

3.1 Primary Mineral Constituents of Basalt

Study indicated the presence of two types of basalt i.e. vesicular and non-vesicular. Non-vesicular basalt are normally below the vesicular basalt and are exposed to the surface at northern side of the site where the vesicular basalts has been removed due to denudation/erosion and weathering. The detailed field characteristics of these two types of basalts and their associations, exposure and secondary mineralogical content are described by Maurya and Vittal (2010& 2011a, b). Thin section observations of these two types of basalt indicated a very clear and demarcating boundary in terms of their mineralogical constituents and alteration pattern. Vesicular basalt are mostly exposed on the surface and consists of coarse grained Ca-plagioclase feldspar (anorthite composition) dominantly of labradorite, pyroxene (augite) and olivine

minerals as shown in Figure 3.1 A-L. The primary textures shown by the basalts are micropophyritic, glomeroporphyritic, sub-ophitic and intersertal textures. The non-vesicular varieties show the development of dyxitaxitic textures. The plagioclase phenocryst grains (Figs. 3.1 M-V) are subhedral, few of them are very coarse grained, majority of the grains are medium to coarse with characteristic polysynthetic twinning. Grains show development of cracks and undulose extinction between crossed nicols suggesting strain effect. Ophitic and sub-ophitic textural relationship of plagioclase with augite is observed. The augite crystals occur as fine to medium sized anhedral crystals. The finer grained clinopyroxenes cluster around olivine grains frequently, they also exhibit cumulus texture in the thin section. The coarse grains show low order interference colours than medium and finer grains. Olivine occurs as medium grained anhedral crystals containing numerous cracks. Olivines are partly or completely pseudomorphed after iddingsite. The grains contain sets of fractures which exhibit rough parallelism. Between crossed nicols they show triangular isotropic facets developed. Brownish to yellowish devitrified glass occurs throughout the rock in a disseminated manner. Frequently glass contains microlites and inclusions of clinopyroxenes.

3.2 Secondary Mineral Constituents of Basalt

Thin section study of different rocks mostly of vesicular basalt was also studied for their secondary mineral constituents responsible for groundwater percolation and easily weatherability. Results indicated the growth and development of stilbite in the cavities/vesicles in the initial stage (Fig.3.2

A-D) and subsequently their development as fully crystalline minerals of different forms (Fig.3.2 E-M). Development of heulandite (Fig.3.2 N&O) and radiating crystals of scolecite (Fig.3.2 P) are also reported to be present. These figures indicated that vesicles are prone for any chemical reaction which may facilitate weathering. It has been observed from field study that if the vesicular rocks having more vesicles filled up with zeolite are more porous and prone to weathering.

3.3 Mineralogical Alteration, Transformation and Abiotic Edaphic Stresses

Mineralogical alteration and transformation using petrographic study of thin section is an important indicator in soils and rocks to delineate the type, nature and extent of abiotic edaphic stresses as well the water holding capacity of different rocks

distributed in the NIASM site. The effects of these stresses in different minerals (primary as well as secondary) from all type of rocks collected from random, master pit and bore hole are shown in figure 3.3 A-X. A perusal of figure 3.3 A-E shows the process of alteration and transformation of plagioclase and pyroxenes along the cleavage planes as well as the complete transformation of olivine (Fig. 3.3 F & I) and pyroxenes (Fig.3.3 G&H) to clay minerals. Gradual increase in alteration due to relative increase in the intensity of stresses has been observed in different pyroxene (Fig. 3.3 J-T) as well as in zeolite (Fig. 3.3 U-X) minerals. From the study of above figures it can be concluded that composition of rocks and mineral i.e. edaphic and atmospheric (water and CO₂) are the most important stressors controlling the alteration of rocks/minerals.

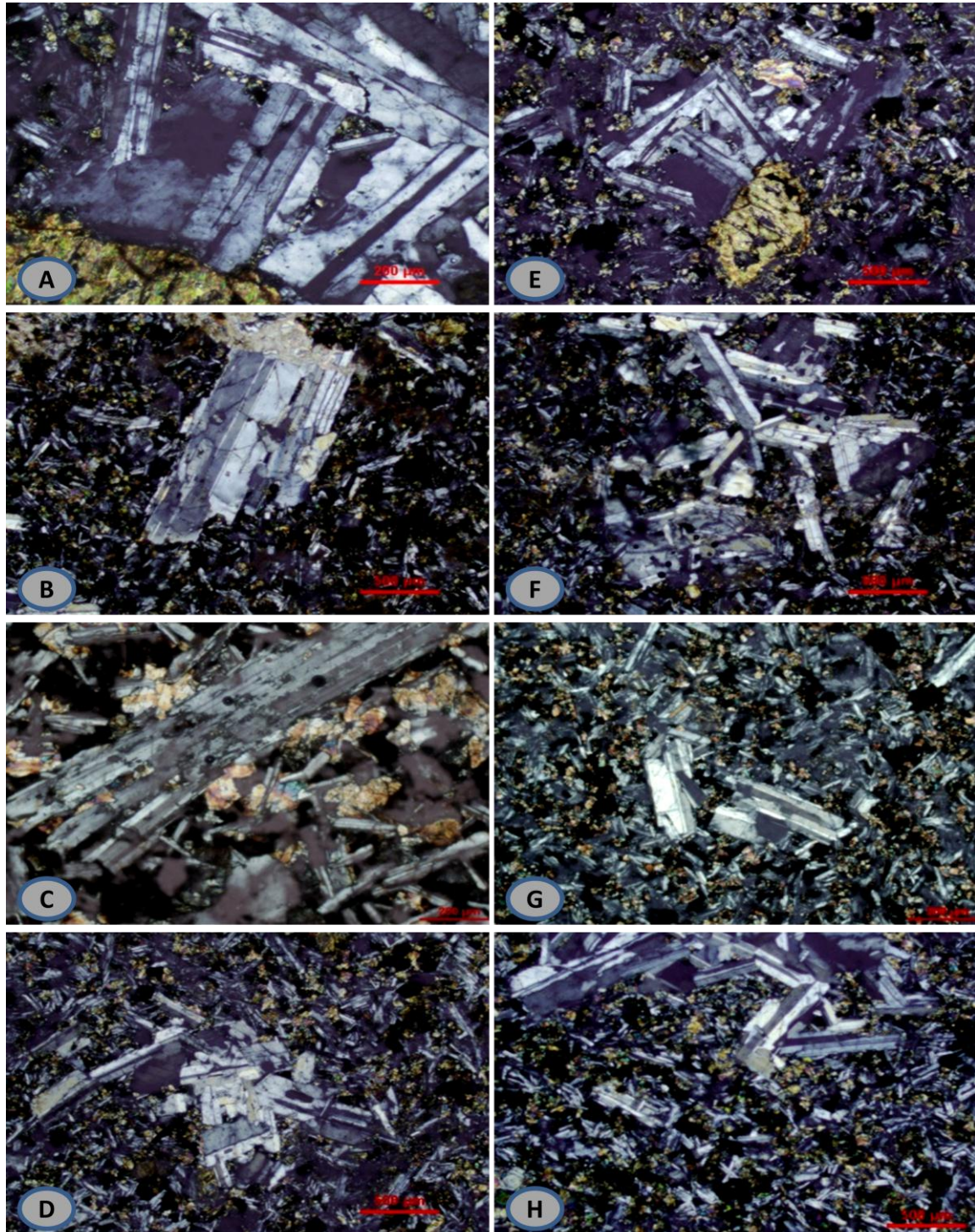


Fig.3.1 Primary mineral constituents of basalt in cross polarized light. Large crystals of plagioclase feldspar (labradorite) as phenocrysts showing Carlsbad twinning in A (RS 25-5), D (RS 25-8), E (RS 25-9), F (BH1/28-3) & H (BH2/8-1) and Albite twinning in B (BH1/28-2), C (RS 2-f) and G (RS 25-1) in the groundmass of fine grained plagioclase feldspar and pyroxene with porphyritic texture indicating two stage of magmatic eruption. Radiating crystals of labradorite can be observed in F.

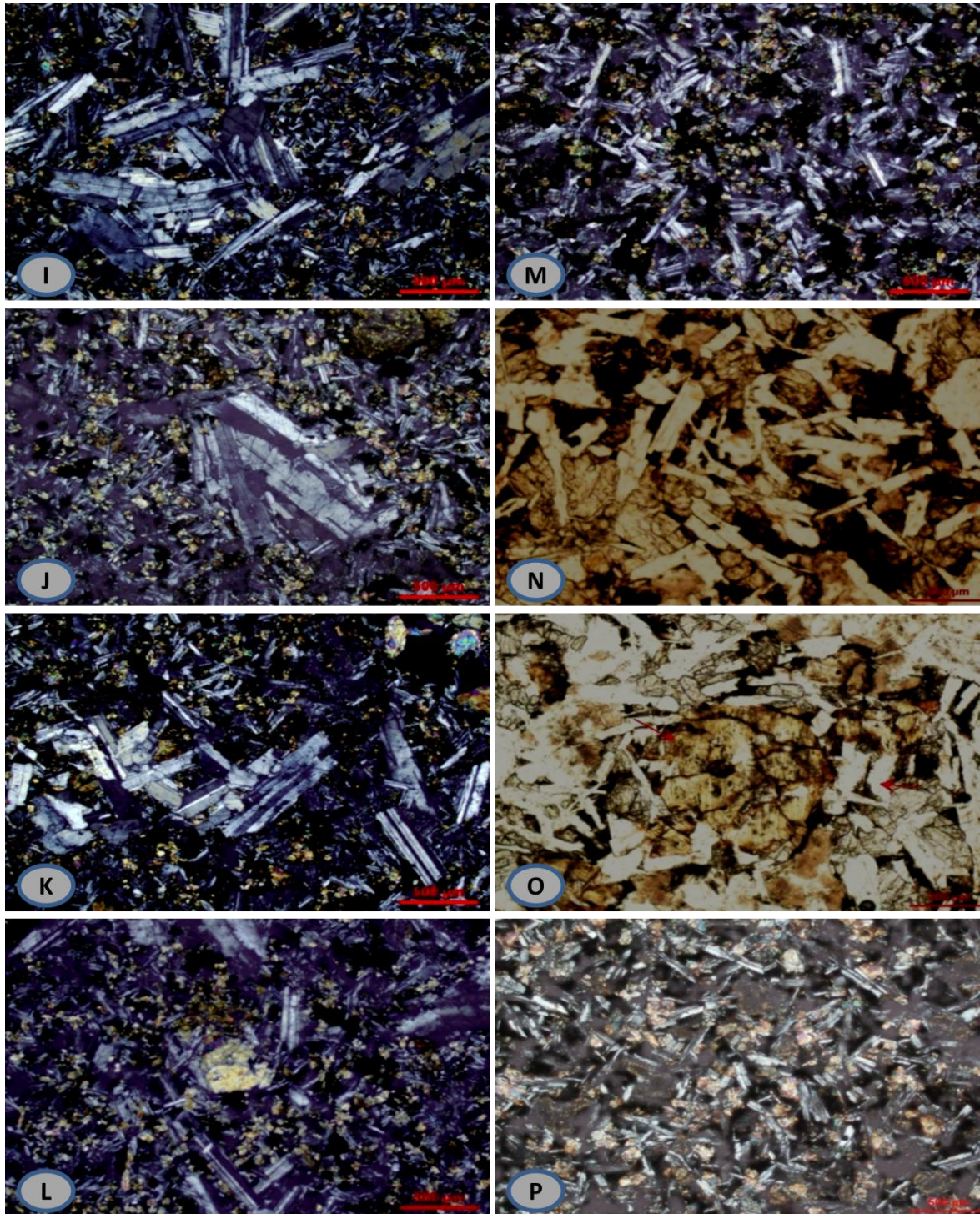


Fig. 3.1 contd. Primary mineral constituents of basalt in cross polarized light. Large crystals of plagioclase feldspar (labradorite) as phenocrysts showing Carlsbad and Albite twinning in figs. I (BH 4/2-3), J (BH 16/1-1), K (BH 16/1-2), L (BH 6/1-1) and M (BH 5/10-2) in the groundmass of fine grained plagioclase feldspar and pyroxene with porphyritic texture indicating two stage of magmatic eruption. Radiating crystals of labradorite can be observed in fig I. N (RS 2-2) is having even grained plagioclase feldspar (labradorite); O (RS 2-8) plagioclase feldspar with core of olivine; while fig. P (RS 2-a) with fine grained plagioclase feldspar and pyroxenes. Figure N, O & P indicate that cooling history of magma was same.

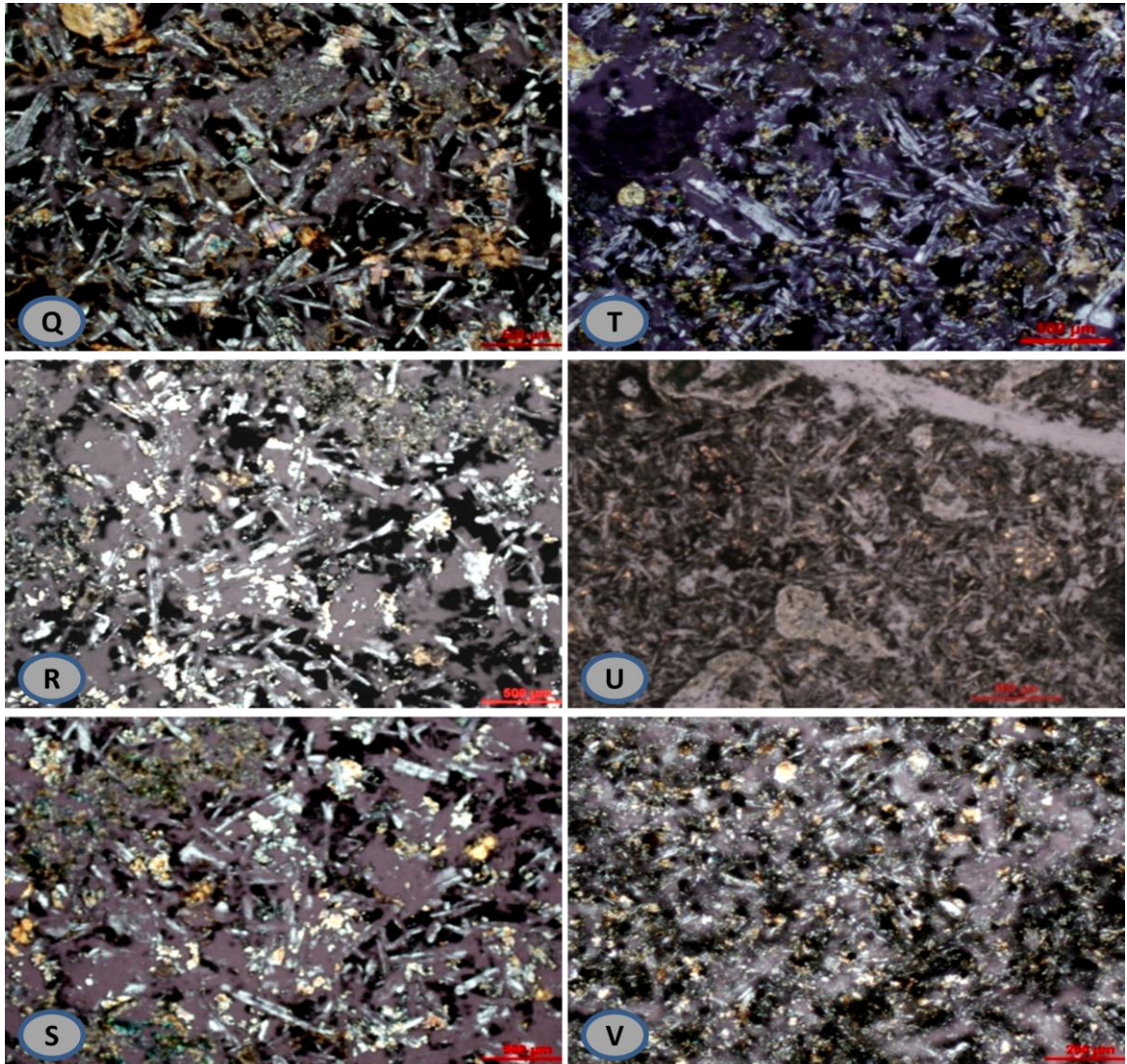


Fig. 3.1 contd. Primary mineral constituents of basalt in cross polarized light. Q (RS 8-11), R (RS 12-1), S (RS 12-3), T (RS 35-5), U (MP 2-11) & V (RS 10-5) are even and fine grained plagioclase feldspar (labradorite) in the matrix of pyroxene and olivine in nonvesicular basalt indicative of more rapid cooling

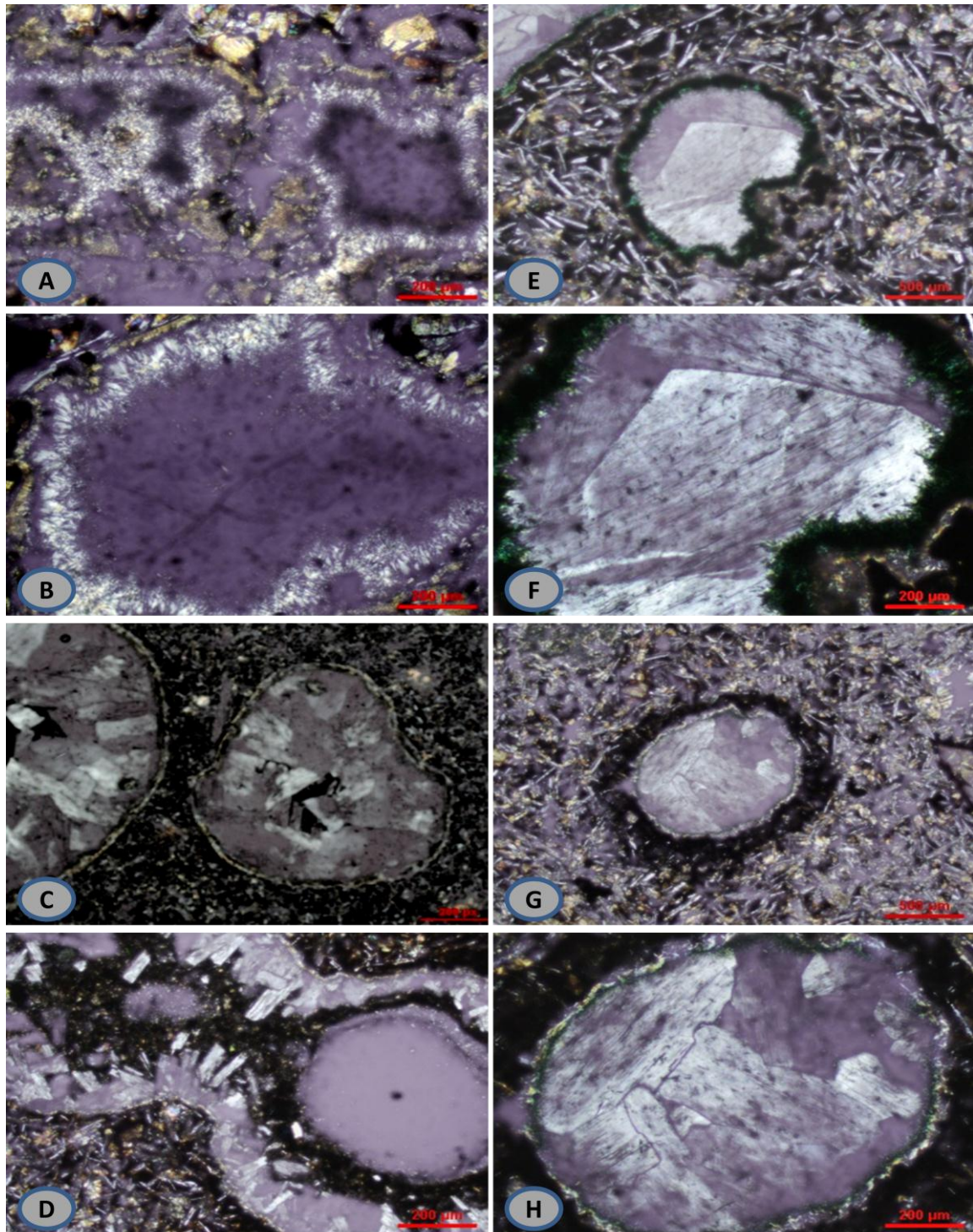


Fig. 3.2 Secondary mineral constituents of basalt. A (BH 10/9-3), B (BH 10/9-2), C (RS 10-6) and D (BH 7/31-1) indicate the growth /projection of stilbite in the cavities of amygdale (vesicular) basalt, while E (BH 6/35-2), F (BH 6/35-3), G (BH 11/10-3) and H (BH 11/10-4) showing perfect cleavage in stilbite crystal in the groundmass of fine grained plagioclase feldspar and pyroxene indicating two stage of magmatic eruption. These features are developed in vesicular basalt.

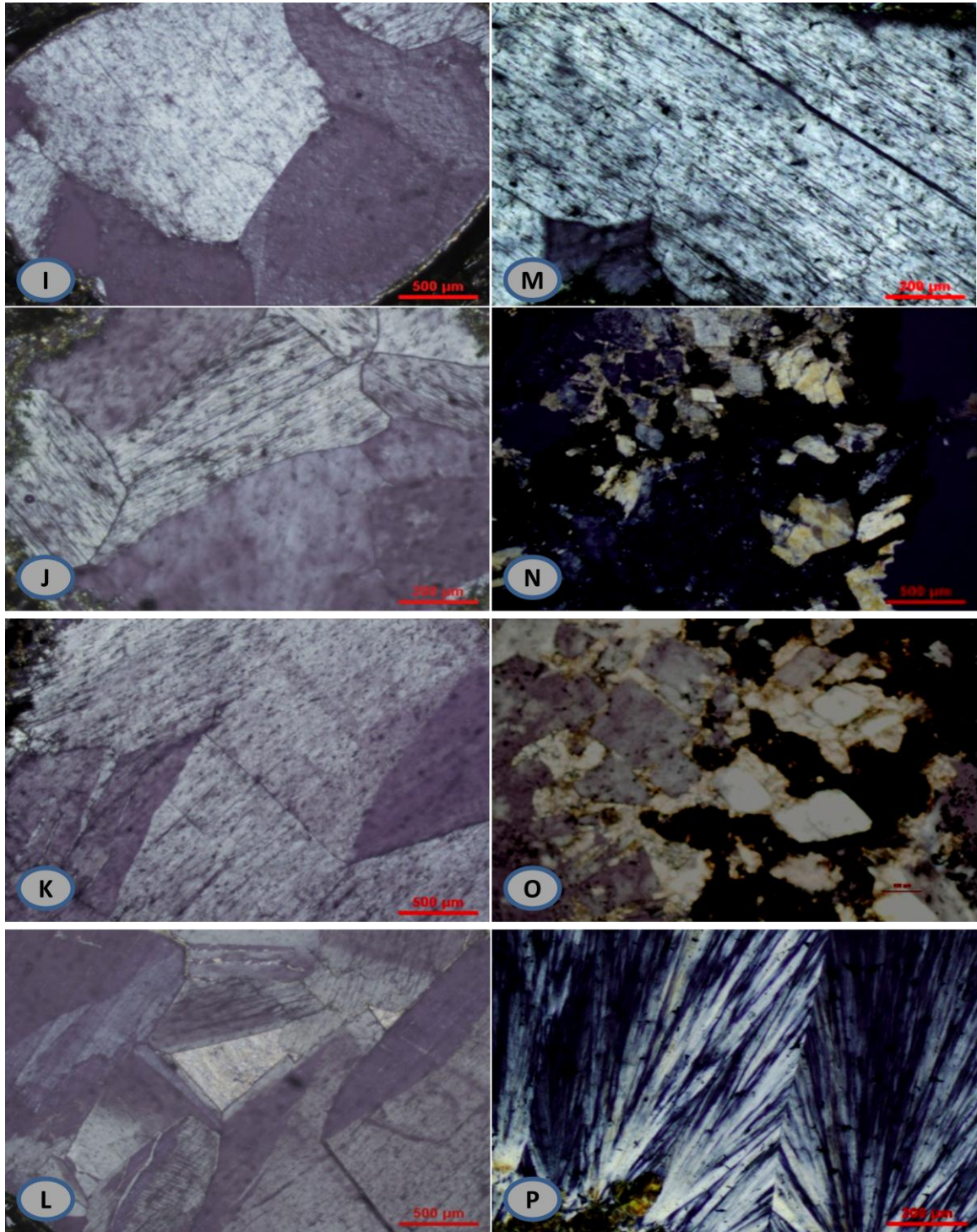


Fig.3.2 contd. Secondary minerals of basalt. I (MP 2-ac), J (MP 7-a), K (BH 8/2-2), L (BH 6/35-6) and M (BH 16/52-1) showing perfect cleavage in stilbite crystal from different samples of vesicular basalt; K and L also show cyclic twinning; N (MP 4-a) & O (MP 4-6) showing heulandite crystal with perfect cleavage and P (RS 2-ab) shows radiating scolecite crystals with twin plane from different samples of vesicular basalt at NIASM Site.

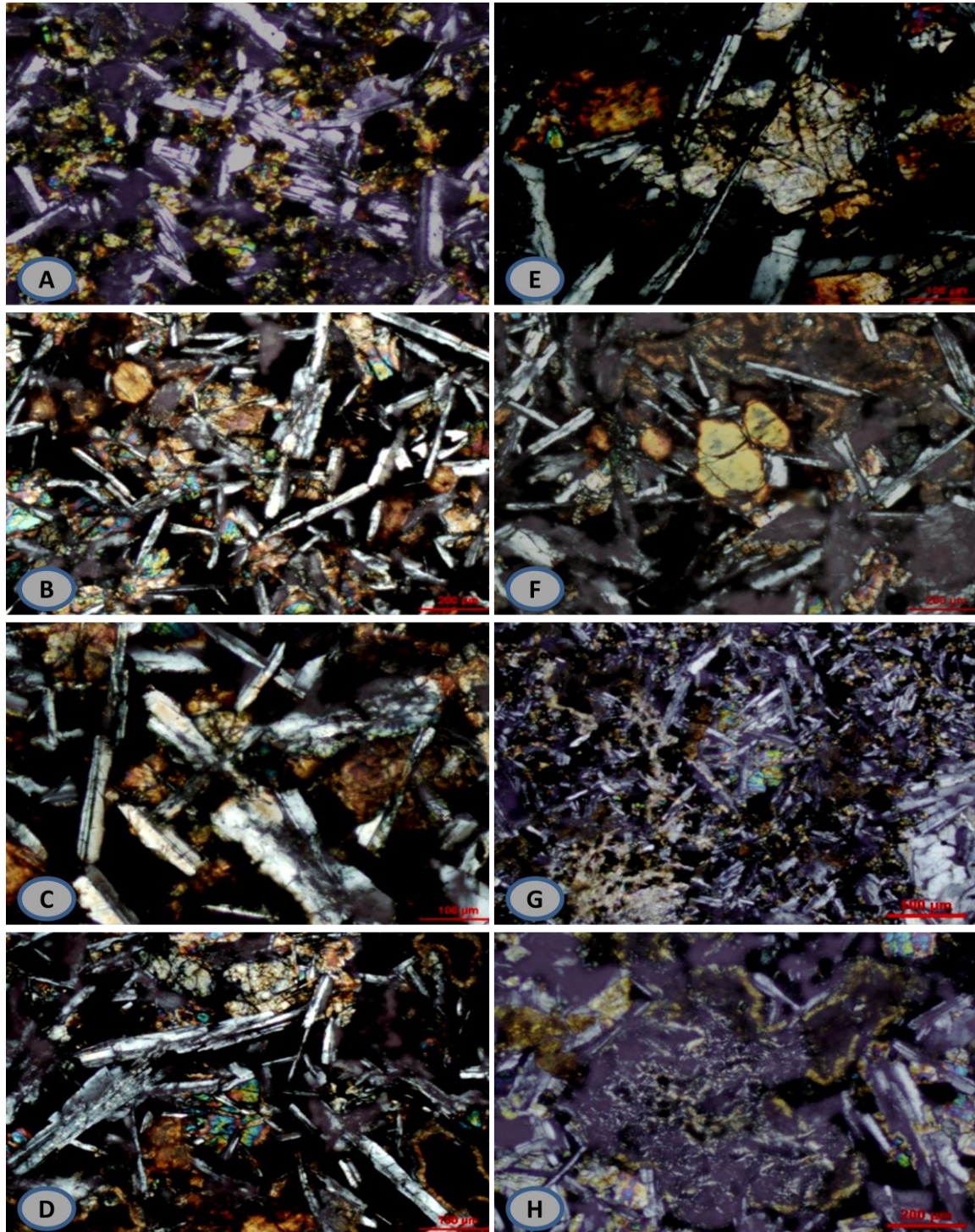


Fig.3.3 Mineral alteration and transformations. A (RS 25-3), B (RS 8-4), C (RS 8-5), D (RS 8-6) and E (RS 8-9) indicate plagioclase feldspar and pyroxenes have weathered and fragmented due to secondary action of water along the weak planes; F (RS 8-2) shows the complete transformation of olivine into clay mineral; G (BH 1/28-6) and H (BH 10/19-2) indicate the complete transformation of olivine and pyroxenes into clay minerals.

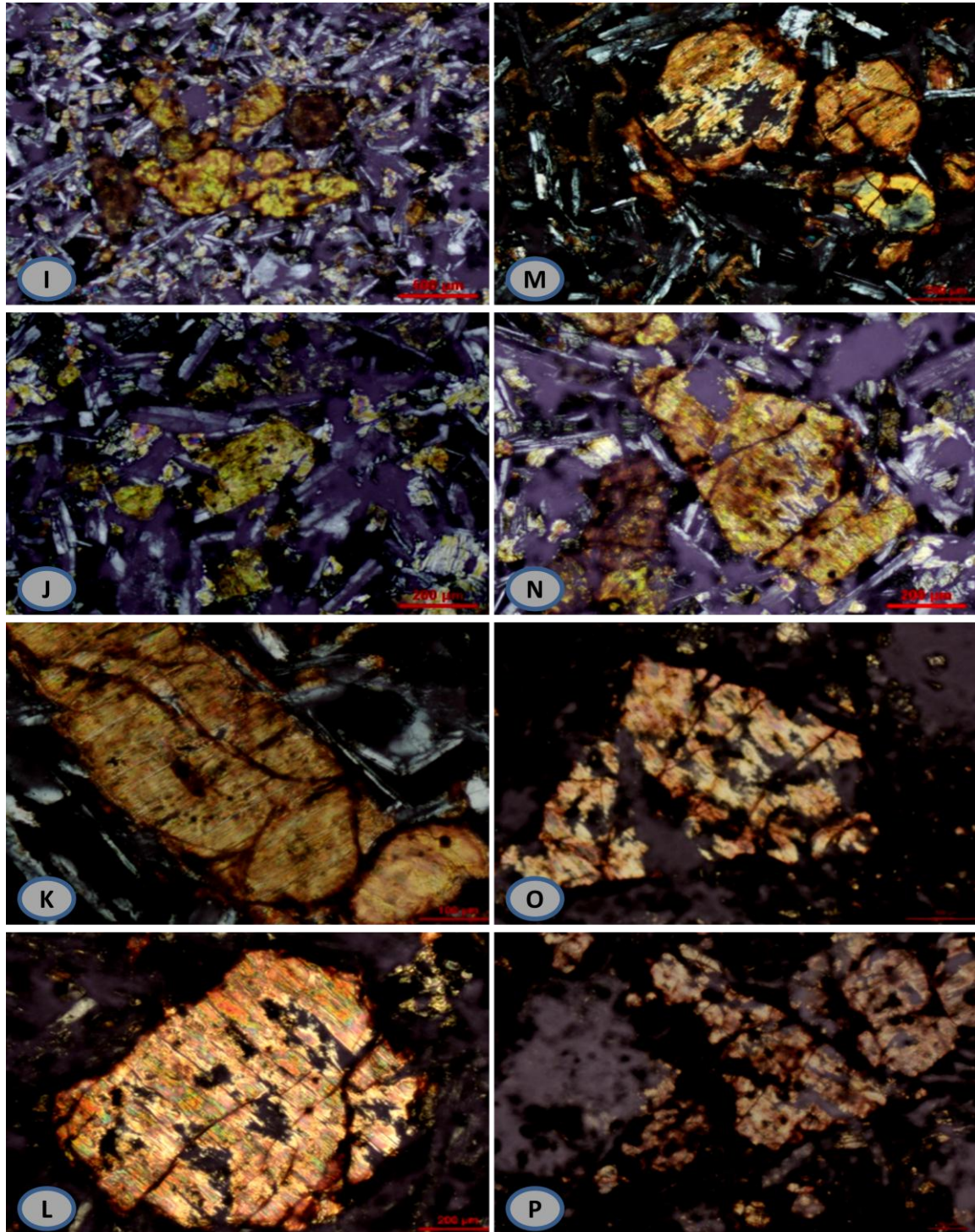


Fig.3.3 contd. Mineral alteration and transformations. Pyroxenes minerals are dissolved and broken along the cleavage planes due to the effects of chemical stresses in I (BH 9/18-1), J (BH 10/19-1), K (RS 8-10), L (RS 6-6), M (RS 8-1), N (BH 12/10-4), O (MP 6-2) and P (MP 6-1). These mineral properties are the signature of the rock with porous and effective water holding strata/horizon in the area.

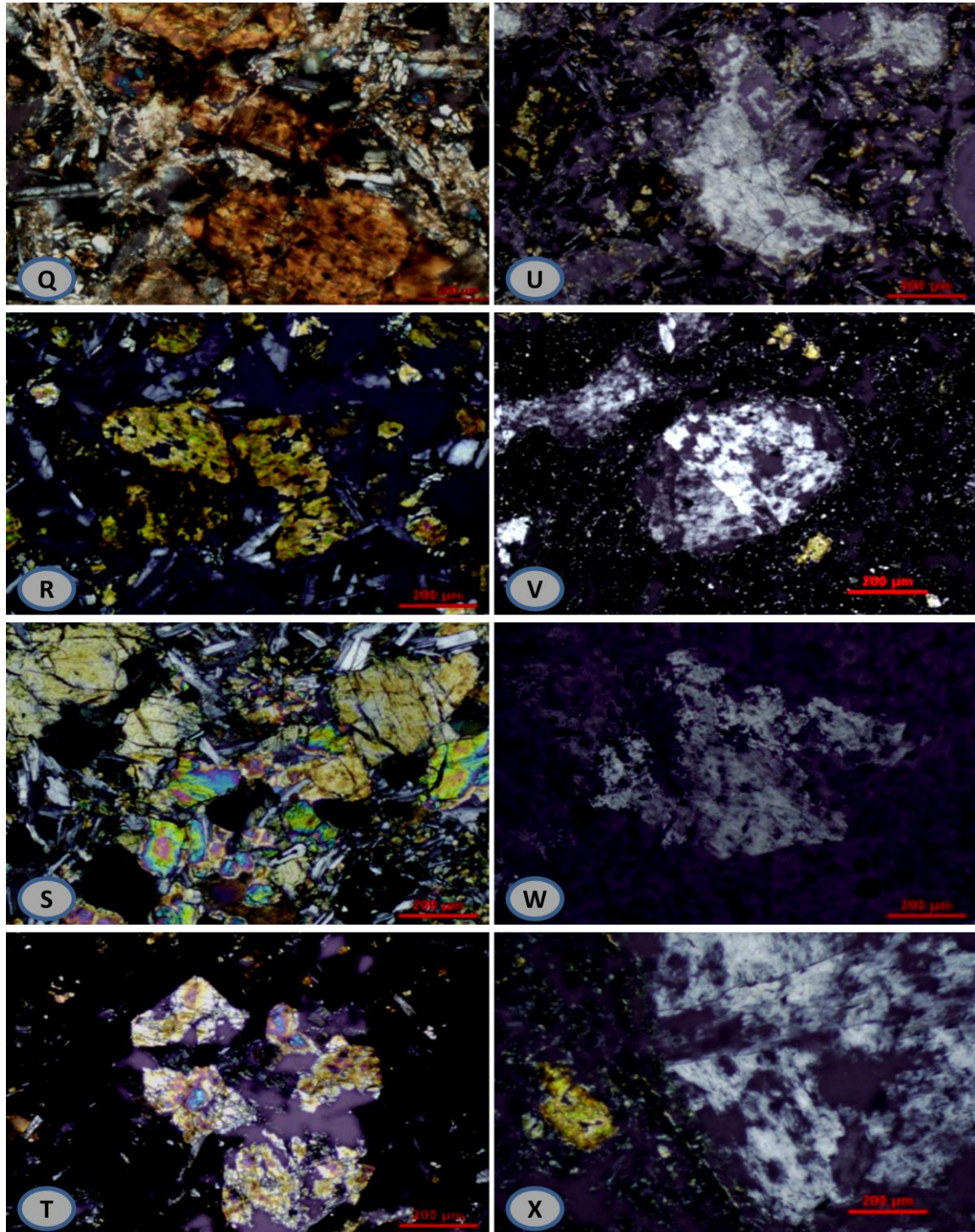


Fig.3.3 contd. Mineral alteration and transformations. Q (RS 7-6), R (BH 10/19-3), S (BH 2/8-8) and T (BH 3/22-3) indicate the dissolution of plagioclase feldspar, olivine and pyroxenes minerals and are changing into clay minerals while U (BH 8/23-1), V (RS 35-1), W (BH 3/22-1) and X (RS 35-2) shows the dissolution and etching effects along the boundary wall as well as effects of tectonic stress on zeolite (stilbite) minerals.

4. Rock Geochemistry and Weathering

Rock samples from surficial pits and boreholes were selected for geochemical analyses and were optimized on the basis of the representations in the basaltic weathering profile at NIASM project site. Despite this, it must be borne in mind that the multi-lobed compound geometry of the pahoehoe lava flow exposed at NIASM Project site, Malegaon Khurd has considerable control on weathering and mobility of major and trace element. Eight representative samples each from the main pit and the boreholes and ten representative samples from random surficial locations from NIASM site were selected for major oxide and trace element analyses. Small chips of each sample (~150 gm) were broken by a steel hammer, rinsed several times with ultra-pure water and crushed with an agate mortar and pestle and pelletized into pellets using 4 grams of sample powder mixed with 0.7 grams of wax at 10 tons/in² pressure using a hydraulic press. Samples for both major and trace elements were analyzed after calibrating internal standards using SPECTRO ED-XRF at the Department of Geology, University of Pune, Pune. The standard deviation for all major oxides is less than 0.5, except for SiO₂ and Na₂O where it is around 1. The analytical results of both major oxide and trace element data are presented in Table 4.1-4.6.

The sum total of all the major oxide analyses vary from 73.23 to 99.92 indicating that the samples selected for analyses show variable degrees of weathering and range from highly weathered samples to fresh rock. The LIO was not determined for these samples and the analyses were used on an anhydrous basis in the SINCLAS programme (Verma et al., 2002) to recalculate major oxides and normalise the geochemical analyses to 100. The programme also gives a rock name following the Total Alkali Silica (TAS)

diagram and also fixes the Fe₂O₃:FeO ratio for the given rock name and then calculates the norm. Total iron was split into ferrous and ferric oxides on the basis of well established criteria (Middlemost, 1989). In the measured iron-oxidation ratio option, all iron was considered as Fe₂O_{3(T)} the Middlemost option (Middlemost, 1989) was used, which proposed a fixed ratio of Fe₂O₃ to FeO that depended on the rock type (classification). Following this recommendation, the SINCLAS program adjusts the Fe₂O₃:FeO ratio according to the rock type, readjusts the complete chemical data and classifies the sample. The major oxide and normative mineralogy obtained were used to classify the rock.

4.1 Geochemical Variations in Major Oxide Content

In general, most samples analysed are sub-alkaline, tholeiite (hypersthene normative) basalts. Besides this, most fresh samples are olivine normative with the normative olivine content varying from 3.28 to 6.48. This geochemical observation corroborates with the fact that the petrography of unaltered basalts contain modal olivine. Other samples analysed contain variable amount of normative quartz (0.42 to 12.91). Normative quartz is recorded in moderately to highly weathered samples, the proportion of normative quartz increases with increase in the degree of weathering. Based on the normative mineralogy and plotting silica (SiO₂) vs. total alkalis (Na₂O+K₂O) content in the TAS diagram (Fig. 4.1) the present samples were classified into sub-alkaline basalts, basaltic andesites and andesite. In fact all samples analysed in the present study are basalts. The basalts showing up as basaltic andesites and andesite are invariably vesicular basalts with variable zeolite mineralization or highly weathered vesicular basalts where highly mobile oxides have been leached relative to silica.

Table 4.1: Major oxide geochemistry and CIPW norms of samples from main pit of NIASM site.

Sample	MP 1	MP 2	MP 3	MP 4	MP 5	MP 6	MP 7	MP 8
Rock type	B, subal	B, subal	B, subal	B, subal	A	B, subal	BA	B, subal
SiO ₂	44.25	43.44	35.94	44.48	42.34	44.81	43.26	45.13
TiO ₂	2.21	1.92	0.46	2.28	0.58	2.04	1.90	2.55
Al ₂ O ₃	8.94	9.56	11.11	8.47	12.58	9.64	9.32	7.95
Fe ₂ O _{3(T)}	12.06	11.89	3.85	13.88	5.14	12.54	11.28	15.00
MnO	0.17	0.13	0.04	0.17	0.05	0.16	0.12	0.15
MgO	4.59	3.69	1.66	3.65	3.49	4.95	5.21	6.12
CaO	12.95	10.46	19.92	10.32	8.19	10.75	7.99	7.07
Na ₂ O	1.67	2.76	0.17	3.14	1.28	2.34	2.96	3.50
K ₂ O	0.37	0.58	0.05	0.27	0.31	0.37	0.46	0.45
P ₂ O ₅	0.16	0.25	0.03	0.28	0.03	0.20	0.20	0.29
Total	87.37	84.68	73.23	86.94	73.99	87.80	82.70	88.21
SiO ₂ adj	51.25	51.92	49.30	51.87	57.53	51.66	52.88	51.91
TiO ₂ adj	2.56	2.30	0.63	2.66	0.79	2.35	2.32	2.93
Al ₂ O ₃ adj	10.35	11.43	15.24	9.88	17.09	11.11	11.39	9.15
Fe ₂ O ₃ adj	2.13	2.17	0.81	2.47	1.67	2.21	2.93	2.63
FeOadj	10.65	10.84	4.03	12.34	4.78	11.03	9.77	13.16
MnOadj	0.20	0.16	0.06	0.20	0.07	0.18	0.15	0.17
MgOadj	5.32	4.41	2.28	4.26	4.74	5.71	6.37	7.04
CaOadj	15.00	12.50	27.32	12.03	11.13	12.39	9.77	8.13
Na ₂ Oadj	1.93	3.30	0.23	3.66	1.74	2.70	3.62	4.03
K ₂ Oadj	0.43	0.69	0.07	0.32	0.42	0.43	0.56	0.52
P ₂ O ₅ adj	0.19	0.30	0.04	0.33	0.04	0.23	0.24	0.33
Q	4.33	0.79	3.72	0.96	15.92	2.44	1.78	-
Or	2.53	4.10	0.40	1.86	2.49	2.52	3.32	3.06
Ab	16.37	27.92	1.97	30.98	14.72	22.83	30.62	34.07
An	18.31	14.32	40.33	9.58	37.59	16.96	13.18	5.35
Di	45.49	38.21	51.11	40.31	14.07	35.66	27.60	27.14
Hy	4.60	6.47	-	6.93	11.21	11.41	14.27	16.50
Ol	-	-	-	-	-	-	-	3.73
Mt	3.09	3.14	1.17	3.58	2.43	3.20	4.25	3.81
Il	4.86	4.36	1.20	5.05	1.50	4.47	4.41	5.57
Ap	0.43	0.69	0.10	0.76	0.10	0.53	0.57	0.77
Mg#	47.08	42.04	50.20	38.07	63.88	47.99	53.75	48.82
FeO _(T) //MgO	2.36	2.90	2.09	3.42	1.33	2.28	1.95	2.21
Salic	41.53	47.12	46.43	43.38	70.71	44.74	48.90	42.48
Femic	36.28	31.67	14.60	32.60	24.77	37.71	39.59	44.13
CI	71.05	54.45	66.72	48.24	63.53	61.08	54.82	44.26
DI	23.22	32.80	6.10	33.80	33.12	27.79	35.71	37.13
SI	25.98	20.60	30.73	18.47	35.51	25.87	27.39	25.72
AR	1.21	1.40	1.01	1.44	1.17	1.31	1.49	1.71
WI	3610	3945	3167	3890	2537	3719	3780	4050

B, subal- Basalt, subalkaline; BA- Basaltic andesite; A- Andesite.

Table 4.2: Major oxide geochemistry and CIPW norms of samples from the boreholes at the NIASM site.

Sample	BH1/80	BH7/3	BH7/13	BH9/1	BH9/2	BH9/18	BH10/9	BH10/19
Rock type	B, subal	B, subal	BA	BA	BA	B, subal	B, subal	B, subal
SiO ₂	47.23	46.90	48.38	47.50	46.72	45.67	45.79	46.85
TiO ₂	2.61	2.65	2.04	2.12	1.96	2.39	2.23	2.32
Al ₂ O ₃	12.20	12.19	10.65	10.74	10.10	11.85	12.43	12.50
Fe ₂ O ₃ (τ)	12.74	12.64	12.54	12.20	11.78	13.60	13.11	13.13
MnO	0.16	0.20	0.18	0.17	0.17	0.30	0.20	0.20
MgO	5.52	5.05	4.58	4.04	4.77	5.62	5.65	4.79
CaO	12.12	13.00	11.21	9.99	9.02	12.89	11.85	11.11
Na ₂ O	2.89	2.78	2.52	2.41	3.04	2.50	2.54	2.76
K ₂ O	0.40	0.22	0.48	0.48	0.66	0.15	0.22	0.29
P ₂ O ₅	0.22	0.24	0.21	0.19	0.19	0.19	0.21	0.21
Total	92.54	88.13	86.24	93.79	99.92	91.99	94.23	94.16
SiO ₂ adj	49.71	49.47	52.70	53.44	53.41	48.58	49.18	50.35
TiO ₂ adj	2.75	2.80	2.22	2.39	2.24	2.54	2.40	2.49
Al ₂ O ₃ adj	12.84	12.86	11.60	12.08	11.55	12.61	13.35	13.43
Fe ₂ O ₃ adj	2.05	2.03	2.90	2.92	2.86	2.21	2.15	2.15
FeOadj	10.23	10.17	9.68	9.73	9.54	11.03	10.74	10.76
MnOadj	0.17	0.21	0.20	0.19	0.19	0.32	0.22	0.22
MgOadj	5.81	5.33	4.99	4.55	5.45	5.98	6.07	5.15
CaOadj	12.76	13.71	12.21	11.24	10.31	13.71	12.73	11.94
Na ₂ Oadj	3.04	2.93	2.75	2.71	3.48	2.66	2.73	2.97
K ₂ Oadj	0.42	0.23	0.52	0.54	0.75	0.16	0.24	0.31
P ₂ O ₅ adj	0.23	0.25	0.23	0.21	0.22	0.20	0.23	0.23
Q	-	-	5.20	7.53	3.10	-	-	0.42
Or	2.49	1.37	3.09	3.19	4.46	0.95	1.40	1.84
Ab	25.74	24.81	23.23	22.95	29.41	22.50	23.08	25.10
An	20.14	21.24	17.79	19.20	13.68	21.99	23.48	22.42
Di	34.31	37.30	34.13	29.14	29.70	36.99	31.53	29.34
Hy	3.61	3.24	7.60	8.73	10.76	2.60	7.93	12.50
Ol	4.99	3.20	-	-	-	6.48	4.40	-
Mt	2.97	2.95	4.21	4.23	4.15	3.20	3.11	3.12
Il	5.22	5.31	4.22	4.53	4.25	4.83	4.55	4.74
Ap	0.54	0.59	0.53	0.50	0.50	0.47	0.52	0.52
Mg#	50.32	48.29	47.88	45.45	50.47	49.13	50.19	46.03
FeO(τ)/MgO	2.08	2.25	2.46	2.72	2.22	2.18	2.09	2.47
Salic	48.37	47.42	49.30	52.88	50.64	45.43	47.96	49.78
Femic	36.12	34.98	34.52	32.72	36.05	36.91	37.22	35.25
CI	65.70	67.71	60.36	55.04	54.14	68.70	65.65	58.70
DI	28.23	26.18	31.52	33.67	36.96	23.45	24.48	27.36
SI	26.97	25.74	23.94	22.24	24.69	27.13	27.69	24.13
AR	1.31	1.27	1.32	1.32	1.48	1.24	1.26	1.30
WI	4316	4183	3934	3637	4084	4014	3948	3929

Table 4.3: Major oxide geochemistry and CIPW norms of random samples from the NIASM site.

Sample	RS 2	RS 6	RS 7	RS 8	RS 10	RS 11	RS 17	RS 25	RS 26	RS 35
Rock type	B, subal	B, subal	B, subal	B, subal	BA	B, subal	B, subal	B, subal	B, subal	BA
SiO ₂	45.83	45.39	42.02	45.38	48.33	42.42	45.54	49.13	45.26	48.56
TiO ₂	2.40	2.22	2.15	2.22	1.92	2.22	2.21	2.75	2.28	1.88
Al ₂ O ₃	11.97	11.81	11.23	11.51	10.60	11.69	11.54	13.27	10.64	10.55
Fe ₂ O _{3(T)}	13.39	12.20	12.47	13.03	10.71	12.33	13.20	13.32	12.68	11.32
MnO	0.17	0.15	0.15	0.17	0.17	0.17	0.20	0.20	0.17	0.13
MgO	5.07	3.91	5.72	5.73	3.77	4.07	7.02	5.27	4.99	5.17
CaO	11.85	11.37	11.40	11.83	8.77	11.20	11.40	12.41	9.54	9.34
Na ₂ O	2.41	1.88	1.77	2.24	2.05	1.69	2.13	3.11	2.50	2.20
K ₂ O	0.19	0.20	0.21	0.22	0.64	0.26	0.32	0.17	0.71	0.51
P ₂ O ₅	0.22	0.17	0.20	0.21	0.17	0.19	0.23	0.29	0.22	0.18
Total	93.50	89.30	87.32	92.54	85.13	86.24	93.79	99.92	88.99	86.84
SiO ₂ adj	49.62	51.43	48.71	49.63	56.01	49.79	49.14	49.73	51.48	54.59
TiO ₂ adj	2.60	2.52	2.49	2.43	2.23	2.61	2.39	2.78	2.59	2.11
Al ₂ O ₃ adj	12.96	13.38	13.02	12.59	12.29	13.72	12.45	13.43	12.10	11.86
Fe ₂ O ₃ adj	2.21	2.11	2.21	2.17	2.64	2.21	2.17	2.06	2.20	2.71
FeOadj	11.06	10.54	11.02	10.87	8.80	11.04	10.86	10.28	11.00	9.02
MnOadj	0.18	0.17	0.17	0.19	0.20	0.20	0.22	0.20	0.19	0.15
MgOadj	5.49	4.43	6.63	6.27	4.37	4.78	7.58	5.34	5.68	5.81
CaOadj	12.83	12.88	13.22	12.94	10.16	13.15	12.30	12.56	10.85	10.50
Na ₂ Oadj	2.61	2.13	2.05	2.45	2.38	1.98	2.30	3.15	2.84	2.47
K ₂ Oadj	0.21	0.23	0.24	0.24	0.74	0.31	0.35	0.17	0.81	0.57
P ₂ O ₅ adj	0.24	0.19	0.23	0.23	0.20	0.22	0.25	0.29	0.25	0.20
Q	0.47	6.09	-	0.09	12.91	3.62	-	-	1.67	9.10
Or	1.22	1.34	1.44	1.42	4.39	1.80	2.04	1.02	4.78	3.39
Ab	22.08	18.02	17.36	20.73	20.11	16.79	19.45	26.64	24.07	20.93
An	23.04	26.28	25.59	22.64	20.66	27.63	22.65	22.01	17.87	19.57
Di	32.38	30.32	31.69	33.05	23.54	30.10	30.16	31.73	28.43	25.59
Hy	12.12	9.68	15.28	13.77	9.89	11.40	14.14	7.17	14.50	13.01
Ol	-	-	0.17	-	-	-	3.32	2.49	-	-
Mt	3.21	3.06	3.20	3.15	3.82	3.20	3.15	2.98	3.19	3.92
Il	4.94	4.78	4.73	4.61	4.23	4.95	4.53	5.29	4.93	4.02
Ap	0.55	0.45	0.54	0.53	0.46	0.52	0.57	0.68	0.58	0.47
Mg#	46.95	42.83	51.74	50.69	46.96	43.55	55.42	48.05	47.91	53.47
FeO(T)/MgO	2.38	2.81	1.96	2.05	2.56	2.73	1.69	2.27	2.29	1.97
Salic	46.81	51.73	44.39	44.88	58.06	49.84	44.13	49.67	48.38	52.99
Femic	37.08	32.03	41.26	39.80	30.64	34.14	43.14	35.07	37.65	36.29
CI	63.42	60.61	69.93	67.04	51.55	62.70	68.86	62.75	55.32	57.82
DI	23.76	25.45	18.80	22.24	37.40	22.21	21.48	27.65	30.51	33.42
SI	25.45	22.80	29.93	28.49	23.09	23.52	32.58	25.41	25.20	28.24
AR	1.25	1.20	1.19	1.24	1.32	1.19	1.24	1.29	1.38	1.32
WI	3785	3293	3444	3783	3355	3226	3882	4272	3914	3574

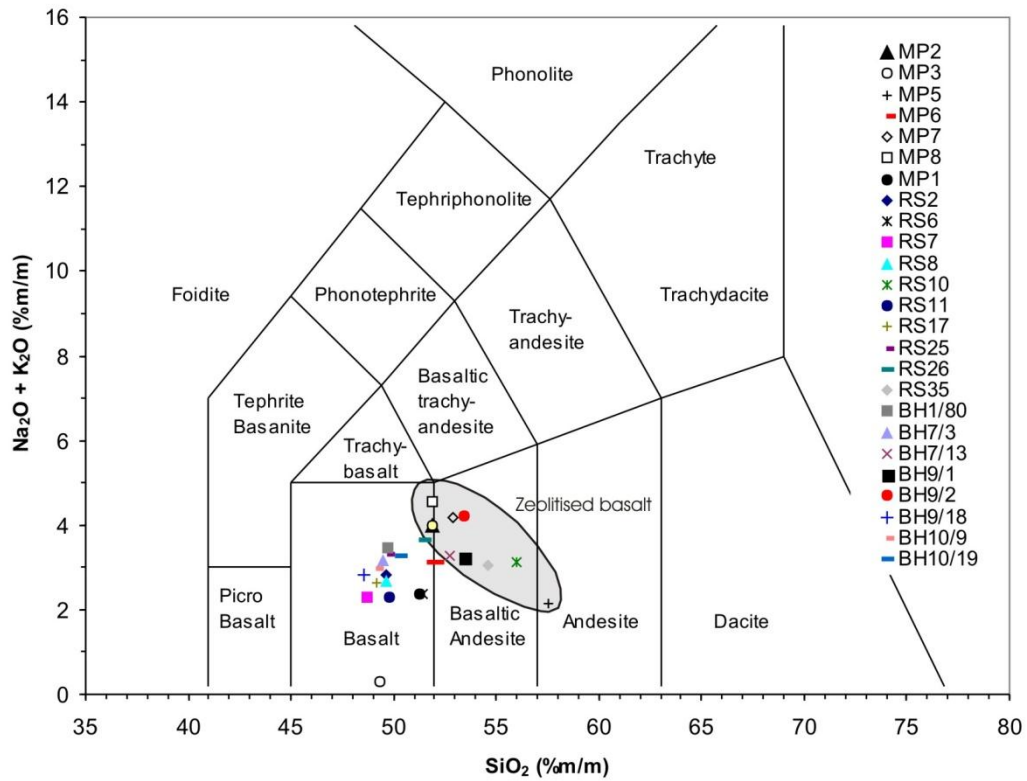


Fig. 4.1: Total Alkali- Silica (TAS) diagram for basalt samples from the NIASM

Although a total of 26 samples were analysed in the present study, the samples from the Main Pit (MP) were used to depict the geochemical variation across a weathering profile of compound pahoehoe as the lobate geometry of the pahoehoe units were better understood in the Main Pit. Major oxide variation diagram (Fig. 4.2) of samples from main pit indicated silica (SiO_2) content varies from 49.30 wt.% to as high as 57.53 wt.% in the present study. The TiO_2 content varies from 0.63 to 2.93 wt.% and as such belong to the low Ti-basalts of the Deccan Traps. Alumina (Al_2O_3) content varies from 9.88 to 15.24 wt.% with an exceptionally high content of 17.09 wt.% for sample MP5. MgO content in the samples varies from 2.28 to 6.63 wt.% while CaO from 8.13 to 15.0 wt.% (Table 4.1). High CaO could be related either to high modal plagioclase content in the basalt or the presence of secondary mineralization of calcite or common alteration product calcite. The alkalis (Na_2O , K_2O) show variable content depending on the affects of alteration and degree of weathering the individual samples had undergone. The

Na_2O content varies from 1.74 to 4.03 wt.% while K_2O varies from 0.04 to 0.33 wt.%. The Mg# of the subalkaline basalt varies from 38.07 to 55.42 and indicates moderately evolved magmas. Higher Mg# (53.75 to 63.88) is recorded in the basaltic andesites and andesite sample which reflect a pseudo increase due to secondary mineralization or relative enrichment in the samples analysed (Table 4.2, 4.3). The normative mineralogy was used to calculate Colour Index (CI) of the samples that varies from 54.14 to 71.05. The Alkalinity Index (AI) varies from 1.01 to 1.71. From the Fig.4.2 it appears that there is an anomalous concentration of different major oxides at 50 cm and 70 cm depth due to presence of the thin clay horizons related to weathering of glassy rind of a single 20 cm thick pahoehoe toe.

In general, there is a perceptible increase in the alumina and magnesia contents at the upper interface of the toe (at 50 cm) while there is a perceptible decline in the TiO_2 and FeO at the same interface (Fig. 4.2). Similar oxide pattern is also pronounced at the lower

interface at 70 cm (Fig. 4.2). From the major oxide variation diagram it is clear that oxides such as silica and alumina which are relatively immobile during weathering and leaching tend to accumulate towards the upper parts of the weathering horizons. In contrast the oxide such as titania and iron (FeO) tend to be mobile in an oxidizing environment and get leached towards the lower parts of the weathering profile. The unique lobate geometry of the lava flow however does not weather uniformly as individual lobes and their sub-units tend to weather independently, especially in the initial stages of weathering. This results in a rather jagged oxide variation diagram which is predominantly a function of the lobe geometry and the porosity and permeability of the lobe sub-units. This is reflected in the Main Pit at the NIASM site where three distinct lobes are exposed. The oxide variations can be better explained by taking

the examples of the relatively mobile elements like titania and iron. The upper lobe is partially exposed at the Main Pit of the NIASM site and is exposed to the hydrometeorological elements that break down mineral constituents like plagioclase, augite, olivine and glass to release iron and titania. Being mobile these tend to get leached and move downwards. At 50 cm of the profile, the glassy upper rind tends to be unstable in the weathering regime and has weathered to a great extent there by rendering a rapid decline in the oxide values (Fig. 4.2). Similar type of situation exists at the 70 cm mark where the lower glassy rind occurs. The intermittent sample at 65 cm represents the vesicular core of the lava toe that has nearly the original oxide content due to relatively less weathering thereby giving a pseudo positive anomaly in the profile. Lobe 3 in the Main Pit occurs below 70 cm and is exposed incompletely

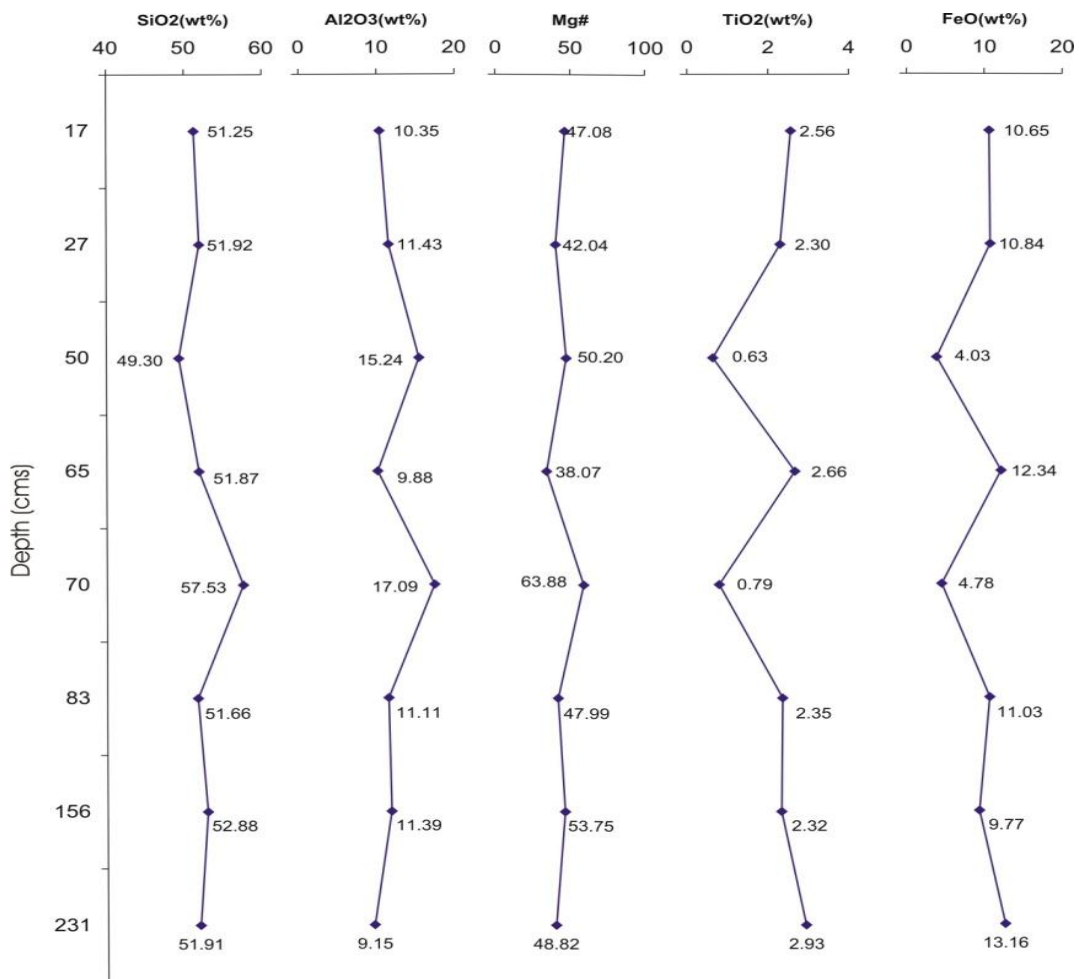


Fig. 4.2: Major oxide variation diagram with depth in main pit samples from the NIASM site. #Mg in counts

until 2.30 m bgl. In this lobe a reversal of the weathering pattern is seen where in the degree of weathering is highest at 70 cm (at the red bole glassy horizon) up to 2.31 m where the original unweathered basalt is exposed. The steady increase in the oxide percentage from the weathered glassy rind to the host rock is also reflected in the major oxide pattern of this lobe. Also one can notice the difference in the nature of weathering in the upper and lower lobe. Hence, in weathering regimes of the compound pahoehoe the lobe geometry will dictate the weathering pattern which is in stark contrast to the weathering pattern seen in the simple flows or conventional soil profiles in basalts.

4.2 Geochemical Variations in Trace Element content and their role in the Abiotic Stresses

The analytical results of trace element analyses are presented in Tables 4.4 to 4.6 and variations diagram representative to main pit are shown in Fig. 4.3. There is a general variability in the trace element content of the samples analysed and this is a reflection of host basalt geochemistry and its weathering products. The biogeochemistry of the significant trace elements is discussed here so as to give a brief account of its role in the abiotic stress at NIASM site, Malegaon.

Vanadium (V) content in the samples analysed varies from 100 to 464 ppm and as such is within the normal range in the weathering profiles of Deccan Traps. In fact, the vanadium bearing blue zeolite - cavensite and phillipsite are common to basalt cavities in and around Pune. It is common in numerous plants and is biomagnified in organic matter, lignites and coals. Vanadium enters the food chain through soil, vegetation and herbivorous animals and is a frequent micronutrient in terrestrial animals. The cycle of vanadium initiates with the weathering of the basalt under a relatively high redox potential. It is generally adsorbed on to clays and is released

into the hydrosphere only by humic solutions. Highly alkaline surface waters and groundwater with calcite in the oxidizing weathering profile could precipitate small quantities of Pb, Cu, Zn or U vanadates. The presence of Vanadium in the weathering mantle of the NIASM site indicates that the flora (crops, fodder) and fauna (poultry, cattle) to be raised on the experimental plots may not be stressed due to Vanadium deficiency.

Cobalt (Co) and nickel (Ni) are widely distributed in the biosphere and in the present study their concentrations varies from 14 to 58 ppm and 77 to 146 ppm respectively. In the natural environment cobalt and nickel geochemically resemble iron (Fe). In basalts, the Co and Ni behave similarly and generally reside in minerals such as olivine and augite which are main constituents of basalts in the study area. In the weathering profile, Co remains in solution as bicarbonate or colloidal hydroxides of magnesium (wad), in contrast, Ni tends to accumulate in the insoluble weathering residue. Cobalt appears to be essential to the digestive bacterial processes in the rumen of cattle. Deficiency of Cobalt in soils and subsequently in cattle fodder is the established cause of 'bush sicknesses in grazing animals (Rankama and Sahama, 1949). The presence of these trace elements in the weathering regime at NIASM site indicates that these elements may not cause significant abiotic stress.

Basalts in general are relatively enriched in copper (Cu) and values vary between 149 to 200 ppm. In the present study its concentrations vary from 119 to 441 ppm. Cu^{2+} has a similar ionic radius as Fe^{2+} and as such Cu replaces ferrous iron in mineral structure, especially when sulphur is absent. In basalts Cu is therefore present as minor sulphides or occurs in olivines and pyroxenes and is released in the weathering profile in oxidizing environments by the breakup of sulphides and silicates.

Table 4.4: Trace element concentrations (ppm) of samples from main pit of NIASM site.

Sample	MP1	MP2	MP3	MP4	MP5	MP6	MP7	MP8
Rock type	B, subal	B, subal	B, subal	B, subal	A	B, subal	BA	B, subal
V ppm	319	279	122	353	100	298	322	343
Cr	247	194	15.8	233	16.8	241	228	288
Co	47.2	30.4	19.6	41.2	23.3	29.7	30.7	58.1
Ni	114	96.9	144	105	227	105	97.1	125
Cu	172	145	441	247	577	128	145	142
Zn	90.4	90.5	47.3	92.7	63.1	97.4	76.5	104.5
Ga	19	10.1	43.5	9.1	30.6	16.6	16.5	20.6
Rb	15.9	13.1	4	6.2	23.1	17.5	22.3	24.9
Sr	374	541	77.9	280	1456	705	400	218
Y	25.2	25.3	6.6	34.3	4.4	26.5	30.5	39.9
Zr	119	123	58.9	142	72.4	127	121	160
Nb	8.0	7.0	8.5	8.8	5.6	5.8	5.5	10.4
Mo	6.2	4.3	2.6	5.5	1	4.0	4.0	6.0
Sn	14.2	16.7	13.1	15.9	12.7	12.5	14.8	12.6
Ba	241	420	51.0	118	360	134.2	191	103
Pb	3.4	1.9	4.1	1.0	5.2	2.7	2.5	5.0

Table 4.5: Trace element concentrations (ppm) of samples from the boreholes at the NIASM site.

Sample	BH1/80	BH7/3	BH7/13	BH9/1	BH9/2	BH9/18	BH10/9	BH10/19
Rock type	B, subal	B, subal	BA	BA	BA	B, subal	B, subal	B, subal
V ppm	464	416	317	312	315	378	363	386
Cr	203	213	256	179	187	221	234	185
Co	35.6	41.2	36.9	42.8	26.3	41.0	34.1	32.6
Ni	96.7	103.7	114.9	86.0	86.7	113.9	113.9	88.0
Cu	182	198	201	158	171	184	119	190
Zn	98.3	99.2	91.8	98.4	92.0	102.1	100.2	98.5
Ga	17.6	27.8	14.3	18.5	21.9	18.5	18.8	17.2
Rb	9.6	3.3	16.3	14.7	27.4	5.1	9.5	11.1
Sr	230	228	350	561	306	204	218	276
Y	32.3	31.3	27.9	25.6	26.7	28.9	27.5	27.5
Zr	149	149	125	132	127	135	132	140
Nb	8.0	8.5	6.5	7.0	6.8	8.3	7.0	6.9
Mo	5.5	4.9	4.8	3.8	3.8	5.2	5.0	5.4
Sn	14.7	11.0	12.4	11.4	12.4	16.5	8.6	16.7
Ba	70.3	79.5	171	214	133	86.7	64.3	103
Pb	2.7	2.8	2.0	1.0	2.9	2.1	2.2	2.5

Table 4.6: Trace element concentrations (ppm) of random samples from the NIASM site.

Sample	RS2	RS6	RS7	RS8	RS10	RS11	RS17	RS25	RS26	RS35
Rock type	B, subal	B, subal	B, subal	B, subal	BA	B, subal	B, subal	B, subal	B, subal	BA
V ppm	364	329	342	344	275	352	370	467	335	274
Cr	196	203	214	264	163	181	307	216	218	223
Co	31.3	35.7	35.9	41.5	14.2	28.4	45	31.4	44.1	35.5
Ni	94.1	77.1	120	113	77.4	77.9	146	100	94.2	104
Cu	192	175	165	162	132	170	153	181	181	167
Zn	105	91.0	92.9	107	84.7	94.5	102	104	106	86.2
Ga	22.4	20.4	21.7	22.7	14.6	20.0	22.2	24.3	19	18.5
Rb	5.4	8.1	9.9	12.4	28.1	15.2	19.3	2.2	35	19
Sr	251	319	172	191	383	187	192	234	551	169
Y	28	24.3	26	27.2	20.9	27.2	25.4	31.8	27.5	20.7
Zr	138	135	129	134	118	132	127	157	128	114
Nb	8.2	6.6	7.2	7.1	8.2	6.2	6.8	10.9	6.6	7.0
Mo	7.0	7.1	6.7	6.3	5.5	5.2	8.5	5.6	7.4	6.9
Sn	14.1	17	15.9	17.3	11.5	19	15.6	18.2	10.2	16.8
Ba	73.7	76.7	35	57.8	153	36.5	42.1	85.1	152	95.5
Pb	1.0	2.1	2.8	2.4	2.5	2.6	2.2	1.6	1.9	2.2

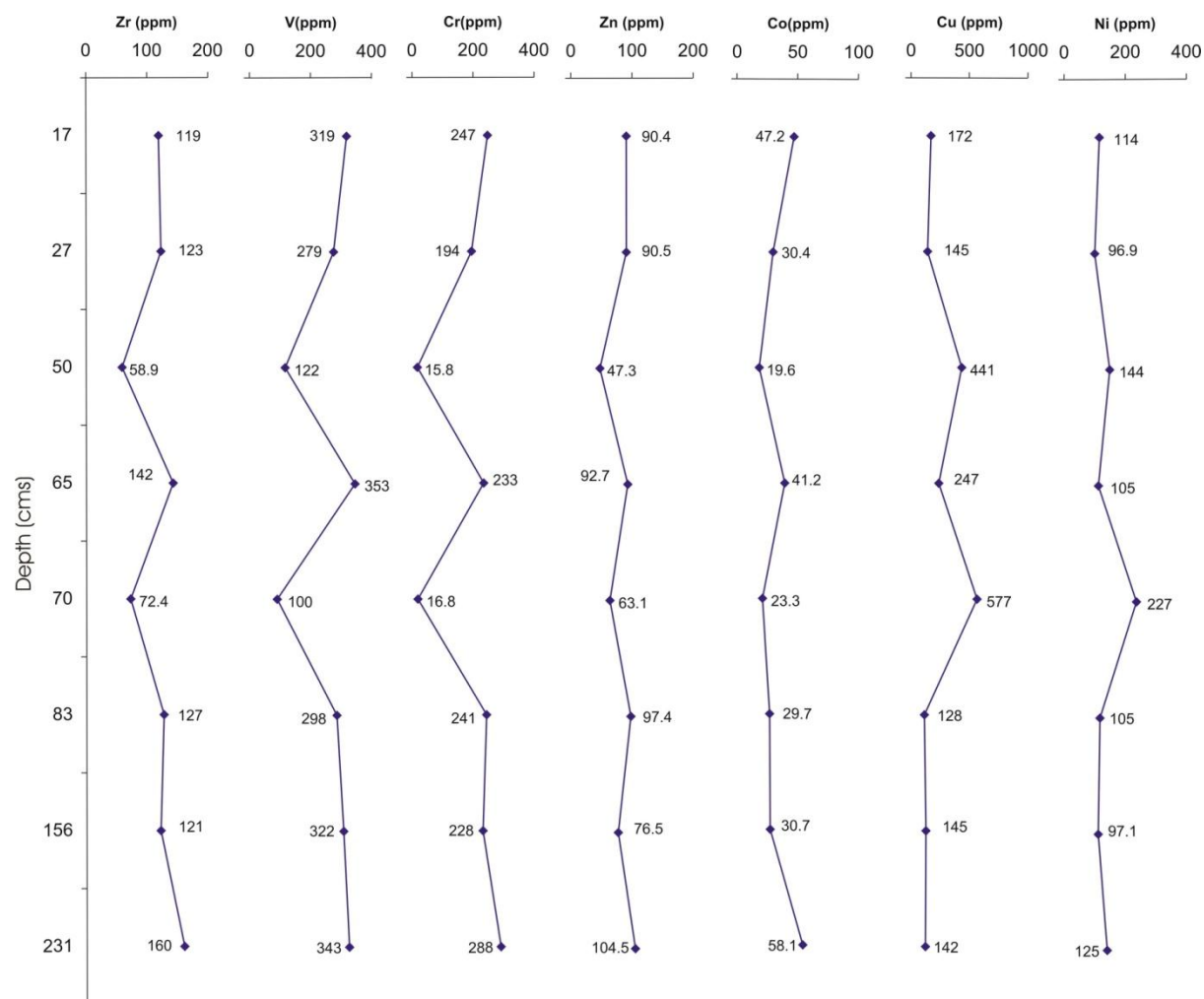


Fig.4.3: Trace element variation diagram with depth in Main Pit samples from the NIASM site.

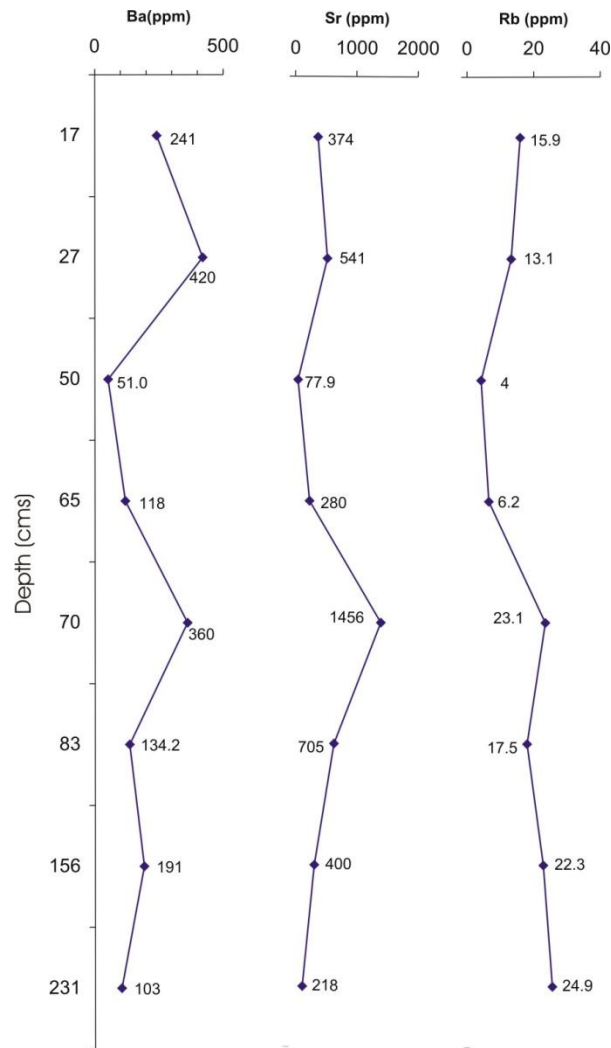


Fig.4.3 contd.: Trace element variation diagram with depth in Main Pit samples from the NIASM site.

Cu is biophile and is invariably found as a micronutrient in the biosphere and its small quantities stimulate plant growth but higher concentrations are known to be toxic in nature (Rankama and Sahama, 1949). Plants such as *Viscaria alpine*, *Melandrium oloieum*, etc. are considered as geobotanical indicators of Cu-mineralisation and are frequently found in gossans. Copper is considered an essential micro-nutrient to plants and its presence in the weathering profile in a considerable range at the NIASM site is encouraging.

Zinc (Zn) is relatively abundant in basalts and during weathering it readily converts to sulphates and chlorides that dissolve in water and consequently Zn-salts is abundant in streams and ground waters from where these are absorbed into the biosphere. It is

an essential element in plants and animals and in low concentrations Zn stimulates healthy growth in plants and animals. However, like Cu, it is toxic in high concentrations. In the samples analysed, Zn concentrations varies from 47 to 107 ppm indicating that the crops cultivated on the NIASM soils would not face zinc deficiency and stresses due to Zn.

In the upper lithosphere Molybdenum (Mo) is oxyphile and it tends to get concentrated more in acidic igneous rocks than basic igneous rocks like basalts. Mo is essential for the growth of some fungi and is probably essential in the fixation of nitrogen by soil micro-organism. It is common in organic matter as in humus, coal ashes and in petroliferous hydrocarbons. Weathering of minerals bearing Mo (olivine- in basalt?)

commonly forms small quantities of hydrated oxides like molybdenite (MoO_3 or $\text{FeO}/3\text{MoO}_3 \cdot 8\text{H}_2\text{O}$) in the soil profile. Molybdenum is also known to accumulate in bituminous, sapropelic and Mn-rich oxidate sediments. However, high Ca in weathering profiles or groundwater could precipitate Mo in calcretes or carbonates. According to Scerbina (1939), Mo is also known to replace iron in the environment ($\text{Fe}^{2+} + \text{Mo}^{6+} \rightleftharpoons \text{Fe}^{3+} + \text{Mo}^{5+}$). In the samples analysed Mo varies from 1 to 8.5 ppm. In the present study it is generally seen that the subalkaline basalts have a general higher Mo concentrations as compared to the basaltic andesite samples. Increase in the organic matter of soil developed on the NIASM site could lead to greater concentration of Mo in the soil profile.

The trace element concentrations of samples from the Main Pit were also plotted as a function of depth (Fig. 4.3). It is observed that there are two prominent trace element anomalies at 50 and 70 cm depth and is similar to the major oxides variation pattern in the Main Pit. The first anomaly is seen at 50 cm depth which is marked by the sudden lowering in the concentrations of trace elements like Zr, V, Cr, Zn, and Co in response to the highly weathered nature of the horizon (red bole). Thereafter is a sharp increase in these trace elements due to the moderately weathered nature of the rock sample analysed that represents the lava toe core. A further lowering of the trace element concentrations is seen at a depth of 70 cm bgl and corresponds to the highly weathered nature of the horizon similar to the upper red bole horizon. It is followed by a gradual increase in the trace element concentrations from 70 cm bgl to 231 cm bgl corresponding to the weathering profile in Lobe 3. This pattern is similar to the major oxide variation in lobe 3 of the Main Pit.

The trace element concentration patterns of Cu and Ni appear to have a distinctly opposite signature when compared to trace elements like Zr, V, Cr, Zn, and Co (Fig.

4.3). There are significantly higher concentrations of these elements at depths of 50 cm bgl and 70 cm bgl where the weathering regime in the form of red bole is present. Such anomalous accumulations could suggest that the clays provide suitable sites for their adsorption or that considerable enrichment of these elements takes place due to deposition of soluble salts in an oxidizing environment. There is a wide variation in the trace element patterns of elements such as Ba, Sr and Rb (Fig. 4.3). They are invariably higher concentration in the upper and lower parts of the Main Pit at NIASM site. This could be the effect either due to the fact that the initial concentrations of these minerals may vary in the 3 lava lobes exposed in the Main Pit due to modal variations in the plagioclase content which primarily hosts these trace elements or due to the variable mobility of these elements in response to differential weathering across the Main Pit profile. There is a significant decrease in the concentrations of these element at 50 cm bgl and may be related to the highly weathered nature of the horizon. Since these elements are highly mobile during weathering they just leached out from these upper horizons under the influence of percolating water during monsoon. The increase of Ba, Sr and Rb at 70 cm bgl could indicate precipitation of these elements at the upper contact of Lobe 3. The behavior of these elements needs further study as other factors such as crystallization of zeolites and other secondary minerals could also influence the trace element distribution in the weathering regime of compound pahoehoe.

4.3 Weathering of Basalts

Basalts are fine-grained, mafic (dark coloured) volcanic rocks and usually made up of olivine, a high temperature mineral that occurs in two types i.e. forsterite $\text{Mg}_2[\text{SiO}_4]$ and fayalite $\text{Fe}_2(\text{Co, Ni})[\text{SiO}_4]$, pyroxene is another mafic mineral and is usually represented by augite (Ca,Na)

(Mg, Fe²⁺, Fe³⁺, Al) (Mn, Ti, Cr) [(Si, Al)₂O₆] and lath shaped plagioclase feldspar usually of anorthite Ca[Si₃AlO₈] variety, opagues and glass are common in basalts and occur in rocks from the present study, as shown in various thin sections in chapter 3. Skeletal crystals of titanomagnetite represent the opagues and brown devitrified patches of glass are also present in some of the studied slides. Geochemically, basalts contain 42 to 52 wt.% silica (SiO₂) and total alkali's (Na₂O + K₂O) between 2 to 6 wt.%.

The *in situ* process of physical or chemical alteration of basalts at or near the surface of the earth is called weathering which is powered by an exogenic energy supply i.e. solar energy. The depth of weathering in basalts is therefore restricted to the depth to which the exogenic processes can operate which is generally up to 10m in basaltic terrain. The weathering processes are influenced by factors such as climate, topography, biologic activity, host rock and time. Basalts generally weather along joints, wherever, there are three sets of joints, spheroidal weathering is common (Fig. 4.4). Weathering produces a typical pale coloured product, commonly referred to as 'morum' which is usually devoid of humus and consist of decomposed mineral matter and clays. The ultimate product of weathering of basalt is the formation of agriculturally fertile 'black cotton soil' which covers vast

tracts of the Deccan Trap country. Weathering of basalts can be divided into three sub-types viz. physical, chemical and biological. Physical weathering of basalts occurs as mechanical disintegration along the joints and fractures and it is the most important processes by which basalts broken down. In highly jointed basalts, physical weathering has produced variable amount of scree on hill slopes. The physical weathering seen in basalts can be produced due to:

1. Differential expansion with pressure release (Fig.4.4)
2. Thermal expansion and contraction
3. Growth of crystal in cracks and pores (Fig.4.5)
4. Organic activity

Chemical weathering of basalts occur as rock decomposition. Having formed in an environment of high temperature, the minerals in basalts at the surface of the earth tend to weather by exothermic chemical reactions like oxidation, hydration, hydrolysis, carbonation, base-exchange, etc. Chemical weathering in basalts results in increase in volume, formation of lower density minerals, formation of more mobile material, formation of more stable minerals and formation of smaller particle size.

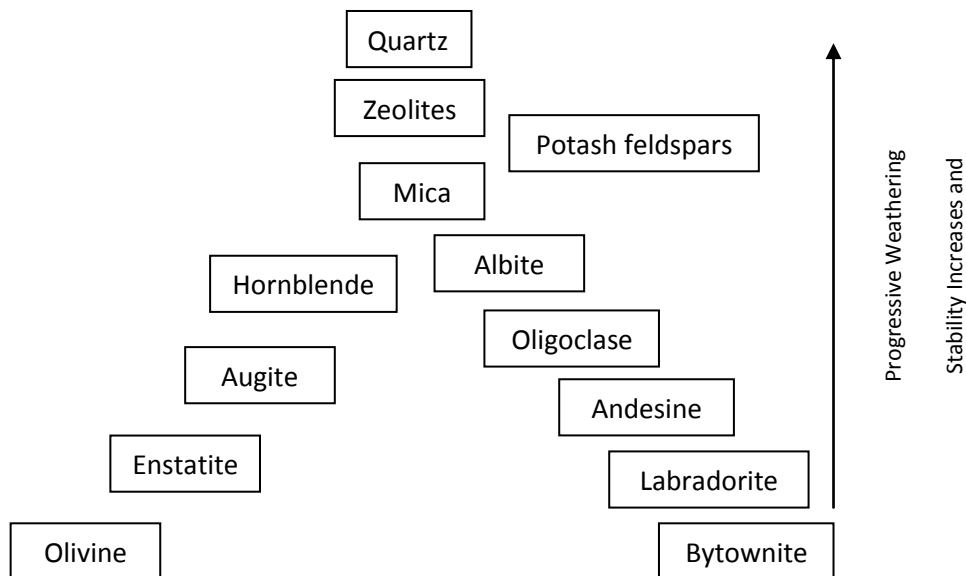


Fig.4.4 Spheroidal weathering of basalt at NIASM site



Fig.4.5 Crystal growth in cracks of basalt at NIASM site

The principle of mineral stability is to be understood to appreciate fully the persistence of certain minerals in nature. Goldich (1938) has proposed a general order of the more stable minerals, which is inverse to Bowen's Reaction series



In weathering of basalts, the following pattern of weathering susceptibility is seen:

Glass ~ olivine > plagioclase > pyroxene > opaque minerals

Percentage loss of major element is as follows:

Calcium (Ca)	85	Silica (Si)	45
Magnesium (Mg)	80	Manganese (Mn)	40
Sodium (Na)	70	Aluminium (Al)	05

During weathering of basalts, there is a rapid early loss of Ca, Mg, K, Na, Rb, Sr, REE and Ba that is related to alteration of glass to smectite, formation of iddingsite and weathering of plagioclase. In matured weathered profiles there is a low and uniform leaching of Si, Mn, P, Cu and Zn.

In highly matured weathering profile Ti, V, Cr, Fe, Ni, Zr, and Nb are essentially immobile and tend to accumulate in soils or weathering products (Eagleton et al., 1987). Weathering of basalts thus produces soluble substances that dissolve in water.

The bulk major oxides from samples can be used to calculate chemical weathering indices to quantify weathering in weathering profiles. The assumption is that in homogeneous parent rocks weathering indices change systematically with depth. The Weathering Index of Parker (WIP) is the most appropriate for application to weathering profile on heterogeneous and homogeneous parent rocks as it involves only the highly mobile alkali and alkaline earth elements and allows for aluminum mobility (Price and Velbel, 2003). The

Weathering Index (Parker, 1970) was calculated in the present study using the original uncorrected analyses and is presented in Tables 4.1 to 4.3. The Weathering Index for the samples varies from 2537 for the highly altered andesite sample to 4316 for fresh basalt. When Al_2O_3 (relatively less mobile oxide during weathering) was plotted against the calculated Weathering Index for samples from the Main Pit at NIASM site, it was found that alumina content increased with increasing degree of weathering (Fig. 4.6).

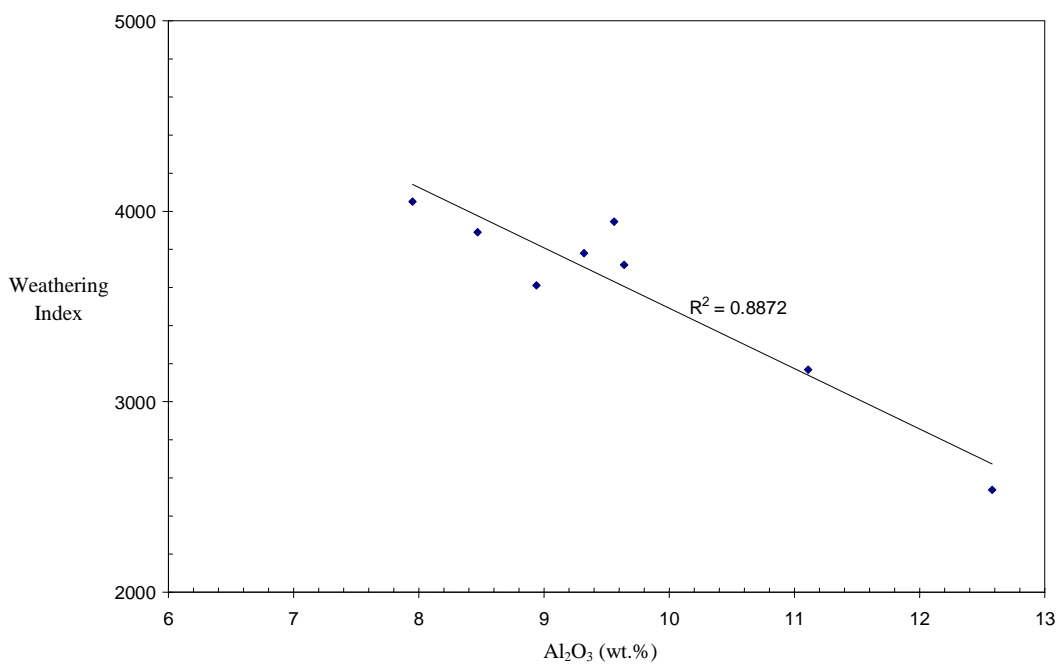


Fig. 4.6: Al_2O_3 vs. Weathering Index for basalt samples from the NIASM site.

5. Groundwater quality

Fifteen water abstraction structures along the two streams adjacent to the NIASM site were selected for studying the geochemistry of the groundwater as shown in Fig. 2.2 of Chapter 2. In all, 13 groundwater samples (11 samples from dug wells, 2 from dug-cum-bore wells (NW3), 1 sample representing canal water plus groundwater (NW9) and 1 sample from canal water (NW15) were collected in 1-liter polyethylene bottles and the chemical characteristics of the groundwater samples were determined according to the prescribed procedure (APHA, AWWA and WPCF, 1981). The results are compiled and presented for the Post monsoon season (Table 5.1).

5.1 Groundwater Characteristics

The groundwater from the study area is alkaline in nature (pH: 7.6 to 8.6). Their electrical conductivity ranges from 470 to 2400 micromhos/cm. Based on the electrical conductivity the samples from the present study fall within 3 categories viz. 1 sample (NW9) representing medium (C2 - 250 to 750 micromhos/cm), 11 samples representing high (C3- 750 to 2250 micromhos/cm) and 2 samples representing very high (> 2250 micromhos/cm) salinity. The canal water (NW7) analysed in the present study has an electrical conductivity of 256 micromhos/cm. Sample NW9 represents a mixed sample between groundwater and canal water and therefore has lower electrical conductivity value of 470 micromhos/cm. It is therefore concluded that most groundwater from the NIASM watershed have high electrical conductivities and it is very high in the northeastern parts (Fig. 5.1). The total dissolved solids (TDS) of the groundwater vary from 649 to 1111 mg/L.

The Total Hardness is an important parameter of groundwater quality, especially

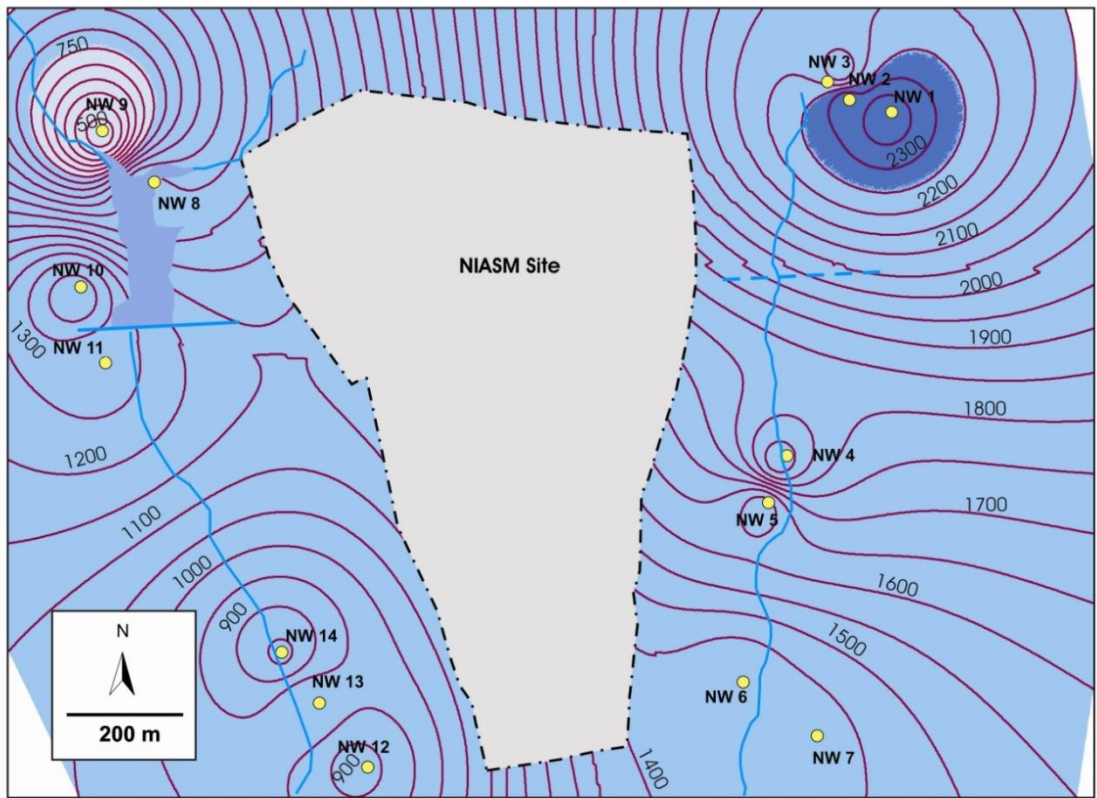
when the water is to be used for domestic purposes. The Total hardness is mainly due to Ca and Mg and originates in areas where topsoil is thick and lime rich formations are present. In basalts, the weathering of plagioclase releases abundant Ca along with Mg, which is also additionally released by weathering of augite and olivine. The Total Hardness for groundwater samples from the present study varies from 70 to 240 mg/L. Thus, almost all the groundwater samples from the NIASM watershed have Total Hardness below the prescribed drinking water limit of 600 mg/L. In the NIASM watershed high (>200 mg/L) Total Hardness is seen in the northeast part (Fig. 5.2). The excess of Total Hardness in the groundwater may cause scale deposition in distribution system, excessive soap consumption, scum formation and lead to health hazards such as urolithiasis, nervous system defects, etc.

Calcium is one of the most abundant cations in the groundwater from the area. The calcium concentration in the study area ranges from 82 to 175 mg/L. The abundance of calcium can be related to weathering of plagioclase and augite in the basalts. The Magnesium (Mg) concentration in the groundwater from the study area is subordinate to Calcium and has limited range from 2.56 to 2.95 mg/L. These values are far below the permissible limit of 100 mg/L for Magnesium by the Bureau of Indian Standards (1990). Another major cation in the groundwater from the study area is Sodium (Na) and its concentrations range from 39 to 128 mg/L - well below the prescribed limit of 200 mg/L set by World Health Organisation (WHO). The higher concentration of sodium vis-à-vis calcium may also be partly accounted for by the precipitation of calcite in the semi-arid dry climate.

Table 5.1: Geochemical analysis of groundwater from the NIASM watershed. All values are in mg/L except where mentioned.

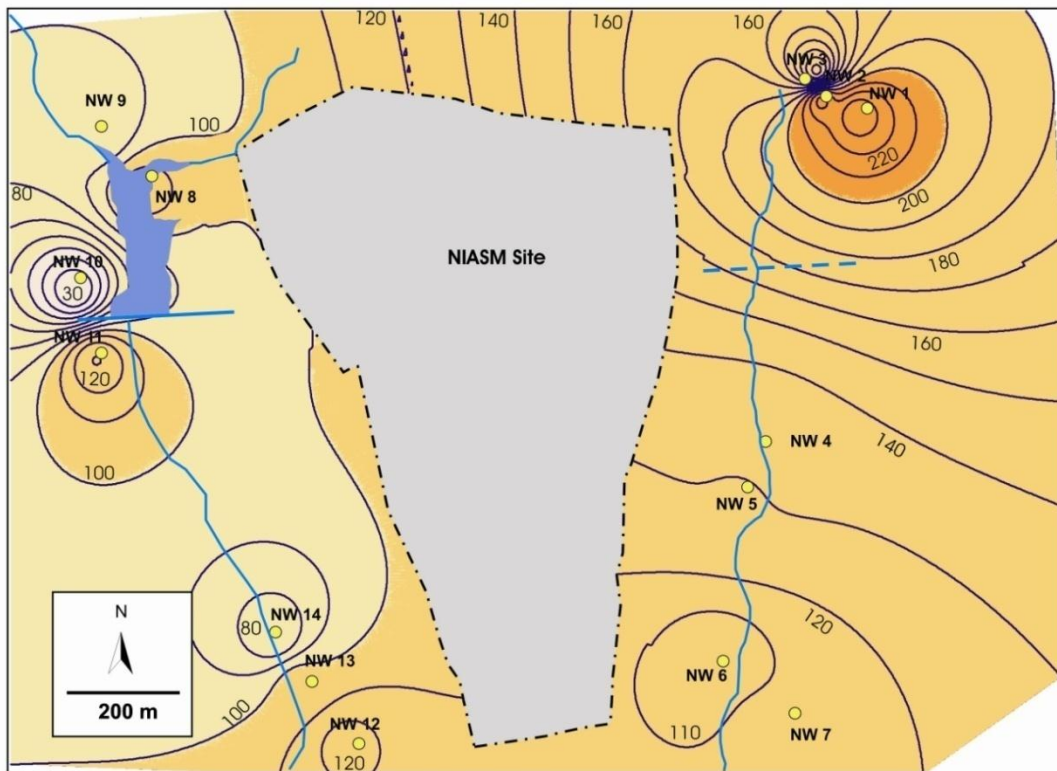
Number	NW1	NW2	NW3	NW4	NW5	NW6	NW7	NW8	NW9	NW10	NW11	NW12	NW13	NW14	NW15	
Use	Irrigation	Irrigation	Irrigation	Irrigation	Irrigation	Irrigation	Irrigation	Irrigation	Irrigation	Irrigation	Domestic	Horticulture	Horticulture	Horticulture	Irrigation	
Source	DW	DW	DW-BW	DW	DW	DW	DW	DW	DW+CW	DW	DW	DW	DW	DW-BW	CW	
Temp (°C)	27	27.5	27.5	28.5	28.5	29	29	28	28	27	27	28	28	28	28	
pH	7.6	7.6	7.9	7.8	7.8	7.8	8.0	8.3	7.9	8.6	8.2	8.3	8.1	8.1	8.2	
E.C. $\mu\text{s}/\text{cm}^2$	2400	2340	2110	1930	1570	1410	1410	1030	470	1390	1270	880	1000	840	256	
Density* g/cm^3	0.99717	0.99696	0.99692	0.99691	0.99659	0.99647	0.99648	0.99674	0.99655	0.99704	0.99708	0.9967	0.99673	0.99671	0.99638	
Dissolved solids*	892.5	801.07	747.23	1110.9	687.15	721.94	727.84	689.84	445.07	715.84	766.26	632.34	672.23	649.1	211.87	
Total Hardness	240	234	106	136	128.44	130.46	124.44	106.35	70.242	102.3	112.33	100.33	116.38	80.264	20.073	
Ca	175.2	125.8	124.6	188.4	87.61	103.2	102.6	95.7	82.3	103.5	110.1	102.3	104.1	99.45	42.8	
Mg	2.95	2.95	2.93	2.94	2.88	2.87	2.86	2.75	2.56	2.84	2.75	2.69	2.69	2.65	2.12	
Na	121.6	128.3	91.46	124.3	104.6	116.6	113.2	103.3	39.17	106.8	121.7	86.3	81.6	87.27	17.4	
K	0.58	0.44	0.36	0.14	0.05	0.47	0.09	0.73	0.00	0.19	0.27	0.29	0.07	0.00	0.67	
Alkalinity	285	245	225	520	260	260	280	310	215	275	315	285	320	330	78.5	
CO₃	--	--	--	--	--	--	--	--	--	--	--	--	--	--	--	
HCO₃	285	245	225	520	260	260	280	310	215	275	315	285	320	330	78.5	
Cl	227.3	220.1	225	196	151.9	160.5	147.7	96.56	28.4	150.4	144.8	75.26	80.94	46.86	11.36	
SO₄	70.57	70.45	70.72	70.49	70.68	70.62	70.89	72.19	72.9	71.28	71.6	72.54	72.32	72.77	58.48	
NO₃-N	9.33	8.08	7.16	8.62	9.37	7.72	10.53	8.61	3.21	5.88	9.33	7.96	10.51	10.1	0.54	
Salinity Hazard	Very High	Very High	High	High	High	High	High	High	High	High	High	High	High	High	High	Medium
SAR	2.50	3.09	2.21	2.46	3.00	3.09	3.01	2.84	1.16	2.83	3.13	2.30	2.16	2.36	704x10 ⁻³	
Exch. Sodium ratio	0.589	0.856	0.616	0.561	0.987	0.942	0.919	0.898	0.395	0.86	0.925	0.705	0.655	0.733	0.328	
Magnesium Hazard	2.7	3.72	3.73	2.51	5.14	4.38	4.39	4.52	4.88	4.33	3.96	4.16	4.09	4.21	7.55	
Res. Sodium Carbonate	0	0	0	0	0	0	0	0	0	0	0	0	0	0	0	
Water Type	Ca-Cl	Ca-Cl	Ca-Cl	Ca-HCO ₃	Ca-HCO ₄	Ca-Cl	Ca-HCO ₃	Ca-HCO ₃								

*calculated



C.I. - 50

Fig. 5.1: Map showing the electrical conductivity zones along the NIASM watershed. Note the highly saline areas with electrical conductivity > 2250 micromhos/cm.



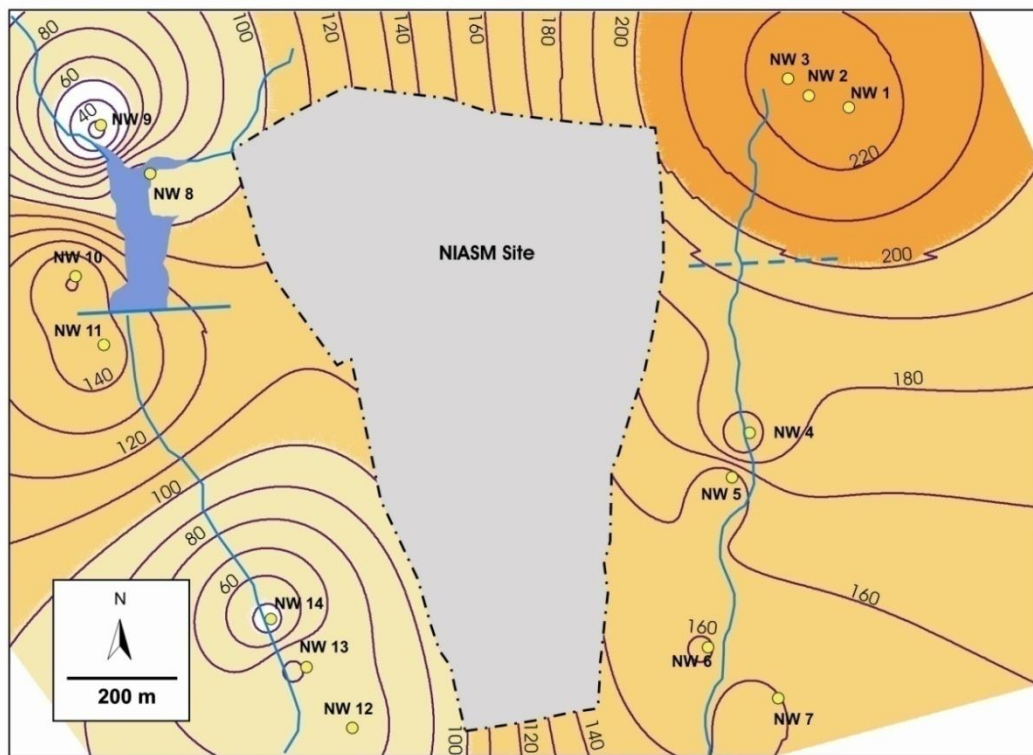
C.I. - 10

Fig. 5.2: Map showing the spatial variation in the Total Hardness values along the NIASM watershed.

The chloride (Cl) content at NIASM watershed is variable (28 to 227 mg/L) in the groundwater. High chloride of > 200 mg/L is associated with three wells to the northeast of the site (Fig. 5.3) and can be attributed to several factors such as domestic sewage, effluents and excessive irrigation with poor drainage. However, in the NIASM watershed the high EC-Cl water appears to be genetically associated with the highly saline waters from Karhavagaj (Duraismami et al., 2008b).

Nitrate concentrations in the groundwater ranges from 3.2 to 10.5 mg/L. Such low concentrations of nitrates (NO₃) in groundwater are in stark contrast to similar

irrigated areas of upland Maharashtra (Pawar and Nikumbh, 2000). Interesting picture emerges from the present dataset which indicate two dugwells i.e. NW13 and NW14 record slightly higher nitrate in the groundwater (Fig. 5.4) attributable to the application of nitrogenous fertilisers to the horticultural plants. In general the sulphate (SO₄) concentrations in the groundwater from the present study have similar values and ranges from 70.45 to 72.9 mg/L. The percentage of carbonate is between 0 to 12 mg/L. The sodium absorption ratio (SAR) of the groundwater samples ranges from 0.10 to 8.98.



C.I. - 10

Fig. 5.3: Isochloride map of the NIASM watershed. High chloride of > 200 mg/L is associated with three wells to the northeast of NIASM site.

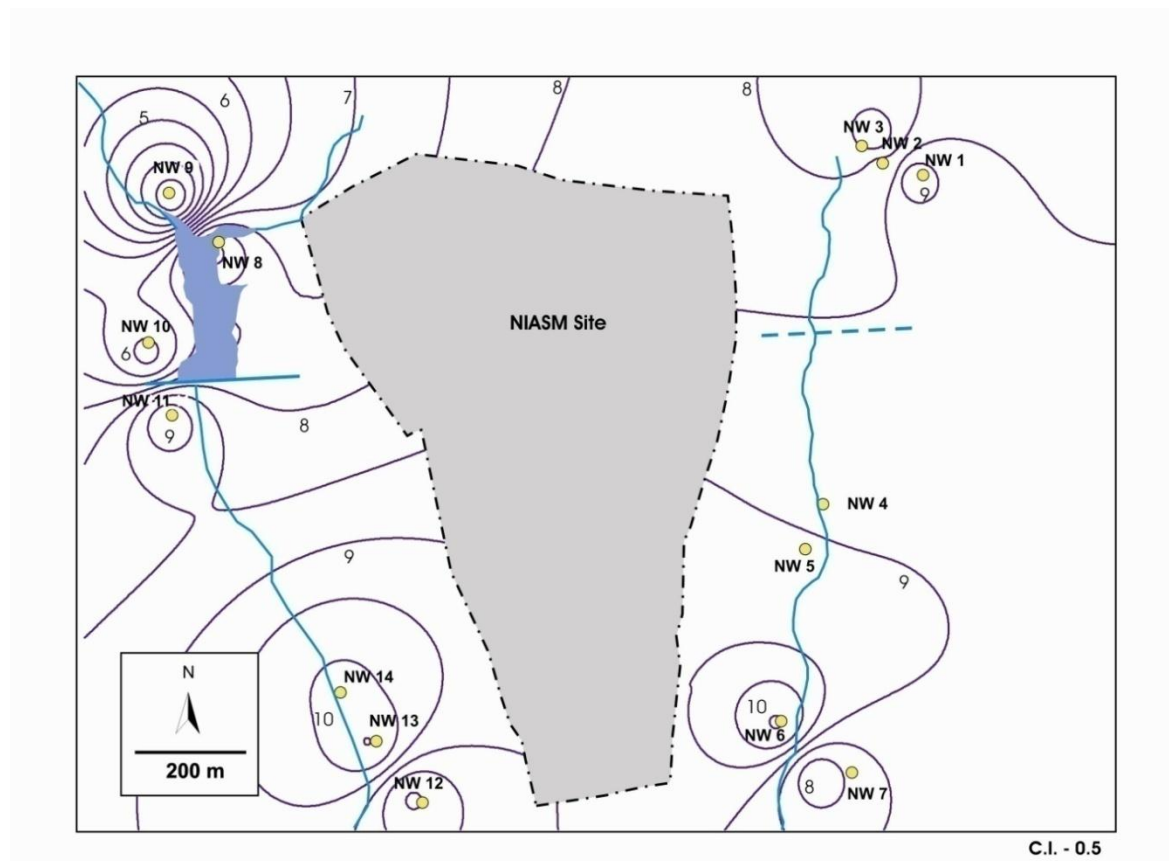


Fig. 5.4: Map showing the distribution of nitrate in groundwater from the NIASM watershed.

The geochemical data generated was used in binary diagrams (Fig. 5.5) to understand the genesis and process involved. The Electrical conductivity of waters from the NIASM site shows a positive correlation with major cations $\text{Ca} + \text{Mg}$ ($R^2 = 0.63$, Fig. 5.5a) and $\text{Na} + \text{K}$ ($R^2 = 0.61$, Fig. 5.5b). This indicates a strong lithological control on the major oxide cations of the groundwaters. A strong positive correlation is also seen between E.C. and Cl ($R^2 = 0.96$, Fig. 6.5c) while the correlation between E.C. and HCO_3 is weak ($R^2 = 0.12$, Fig. 5.5d) indicating that the amount of chloride in the groundwater controls the Electrical Conductivity of the groundwaters from the

NIASM Site. When $\text{NO}_3\text{-N}$ concentration from the groundwaters were also plotted against E.C. the samples showed considerable scatter with a weak correlation ($R^2 = 0.19$, not shown in the diagram). Such variation in the $\text{NO}_3\text{-N}$ concentration from the groundwaters reflects the role of physical process such as evaporation and /or anthropogenic additions to the groundwater. The SO_4 concentration showed no distinct correlation with E.C. ($R^2 = 0.07$, not shown in the diagram) indicating that its concentration did not contribute to the conductivity of groundwaters from the NIASM site.

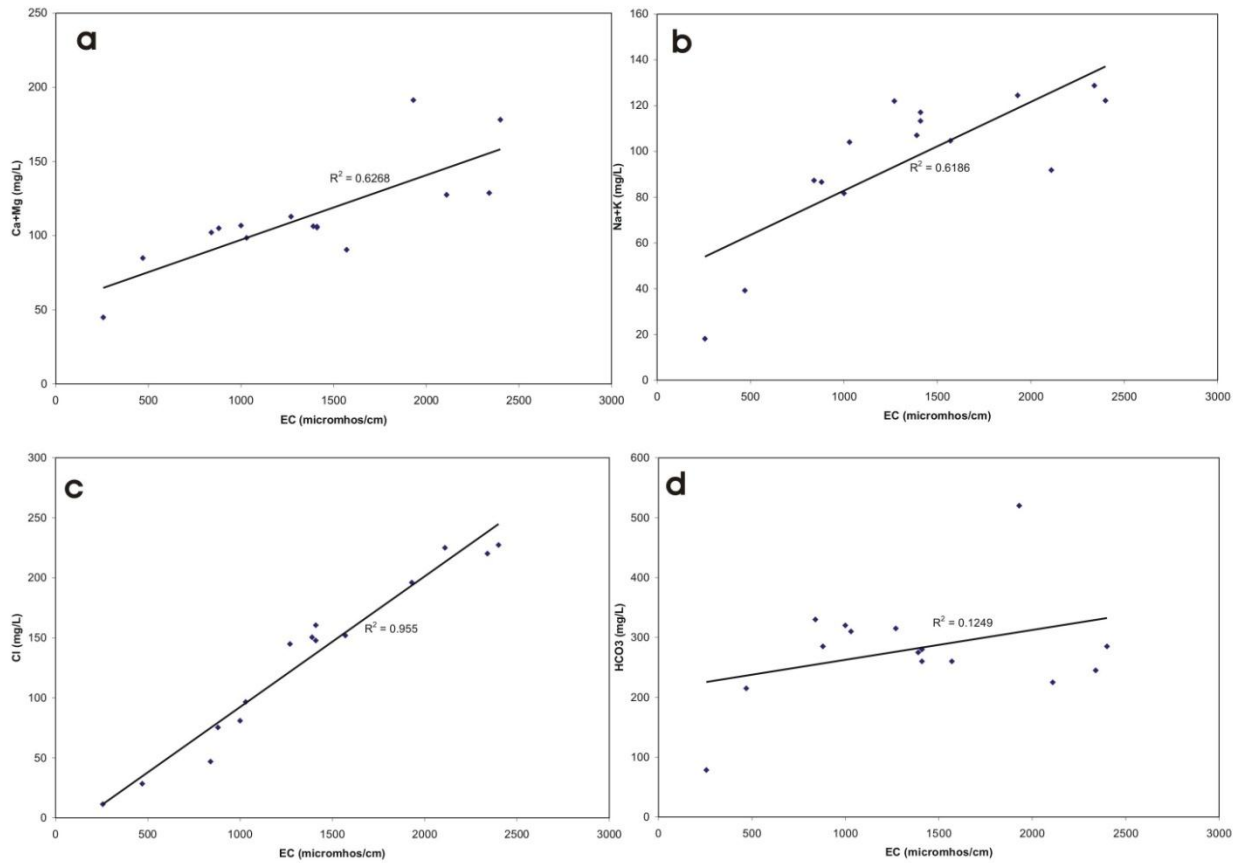


Fig. 5.5: Binary variation diagrams between E.C. and major cations and anions in groundwater from the NIASM watershed.

5.2 Evaluation of Groundwater for Irrigation

Rain fed agriculture is the prime occupation in the area around the NIASM site. Groundwater along with surface water lifted from canals is the prime source of irrigation waters in and around the NIASM site. The groundwater analysis was used to classify the water into categories suitable for irrigation purpose. The following parameters are evaluated.

5.2.1 Salinity

High electrical conductivity indicates high salt concentration in irrigation waters that ultimately leads to the formation of saline soils. High salinity interferes with the absorption of water and nutrients by plants from the soils by reversal of osmotic gradients (Saleh et al., 1999). Richards (1954) has classified irrigation waters into four groups based on the electrical conductivity values and based on this classification scheme the groundwater from

the study area fair (11 samples) to bad (3 samples) for irrigation.

5.2.2 Sodium Adsorption Ratio (SAR)

Sodium generally replaces calcium in soils irrigated by saline groundwater through the process of base-exchange. High Na in the soils reduces the permeability of soils owing to dispersion of clay particles. The effect of Na on soil is known as sodium hazard or alkali hazard and is described as the sodium absorption ratio (SAR). SAR is calculated by using the formula $[Na+/\sqrt{(Ca^{2+}+Mg^{2+}/2)}]$ and is a useful parameter to evaluate the degree to which irrigation waters tend to enter into cation exchange in soils. The SAR of groundwater samples from the NIASM watershed range from 1.2 to 3.09 and their distribution pattern are shown in Fig. 5.5. In the stream east of the NIASM site it is seen that the SAR values generally increase downstream which is as expected in a moderately drained, agriculturally dominated landuse-landcover. In contrast, it is seen that the SAR values reduces

downstream along the stream west of the NIASM site. High values of SAR are seen in the northwestern part of the study area in and around the MI tank. From the distribution of SAR values from the present study it can be concluded that SAR values increase in the areas where there is water logging due to surfacial obstruction of the natural drainage system or where groundwater are relatively shallow or with sluggish flow due to low hydraulic gradient.

SAR values are generally plotted against E.C. in the USSL diagrams (Fig. 5.6) and it

shows that two samples each plot in the C2S1 (Low SAR-Medium EC) and C4S1 (Low SAR- Very High EC) category while the remaining samples plot in the C3S1 (Low SAR-High EC) category. The use of groundwater from dug wells NW1 and NW2 that plot in the C4S1 (Low SAR- Very High EC) category should be discouraged for agriculture. Based on the SAR values, the groundwater for irrigation purposes are classified as generally 'good'.

Table 5.2: Classification of groundwater quality in DPR, Maharashtra for irrigation purpose (after Richards, 1954).

Water Class	Salinity Hazard			Alkali Hazard		
	E.C. ($\mu\text{S}/\text{cm}$)	Number of samples	Percentage	SAR (epm)	Number of samples	Percentage
Excellent	Up to 250	--	--	Up to 10	15	100
Good	250-750	02	13.3	10-18	--	--
Medium/Fair	750-2250	11	73.3	18-26	--	--
Poor/Bad	>2250	02	13.3	>26	--	--

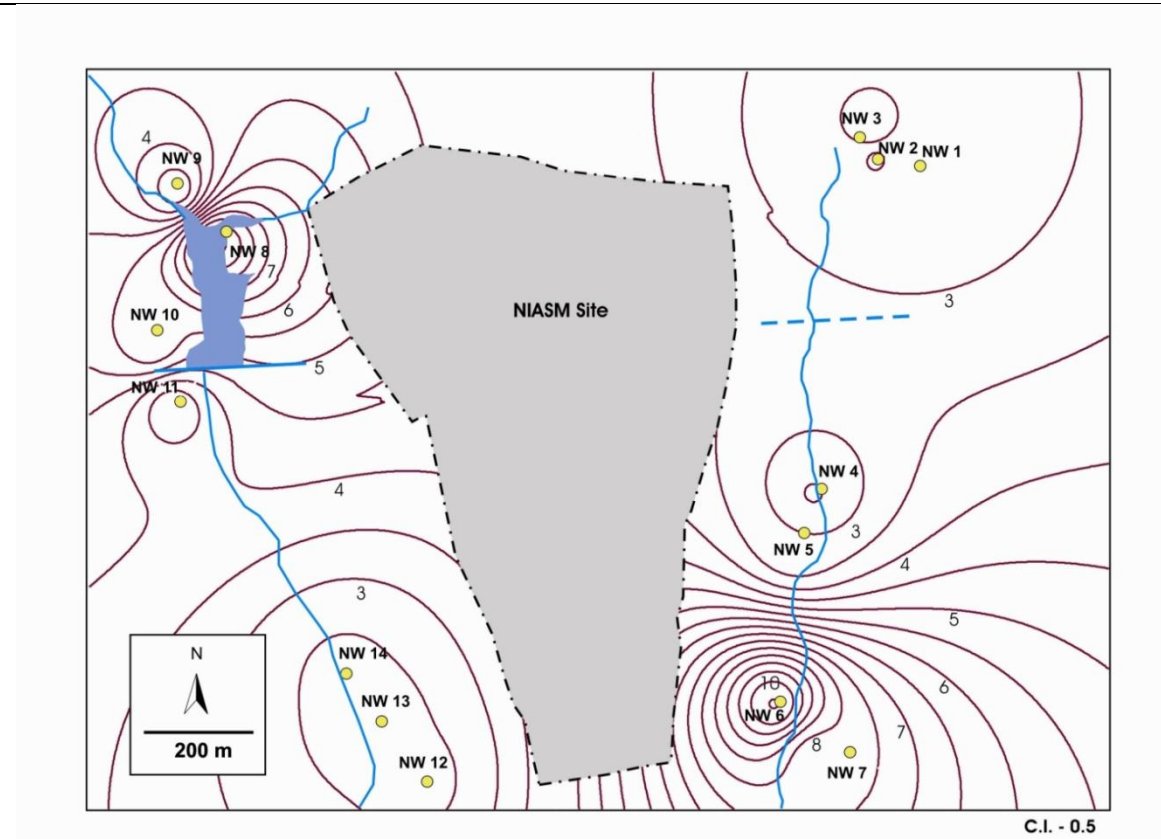


Fig. 5.5: Variations in the Sodium Absorption Ratio for the NIASM watershed.

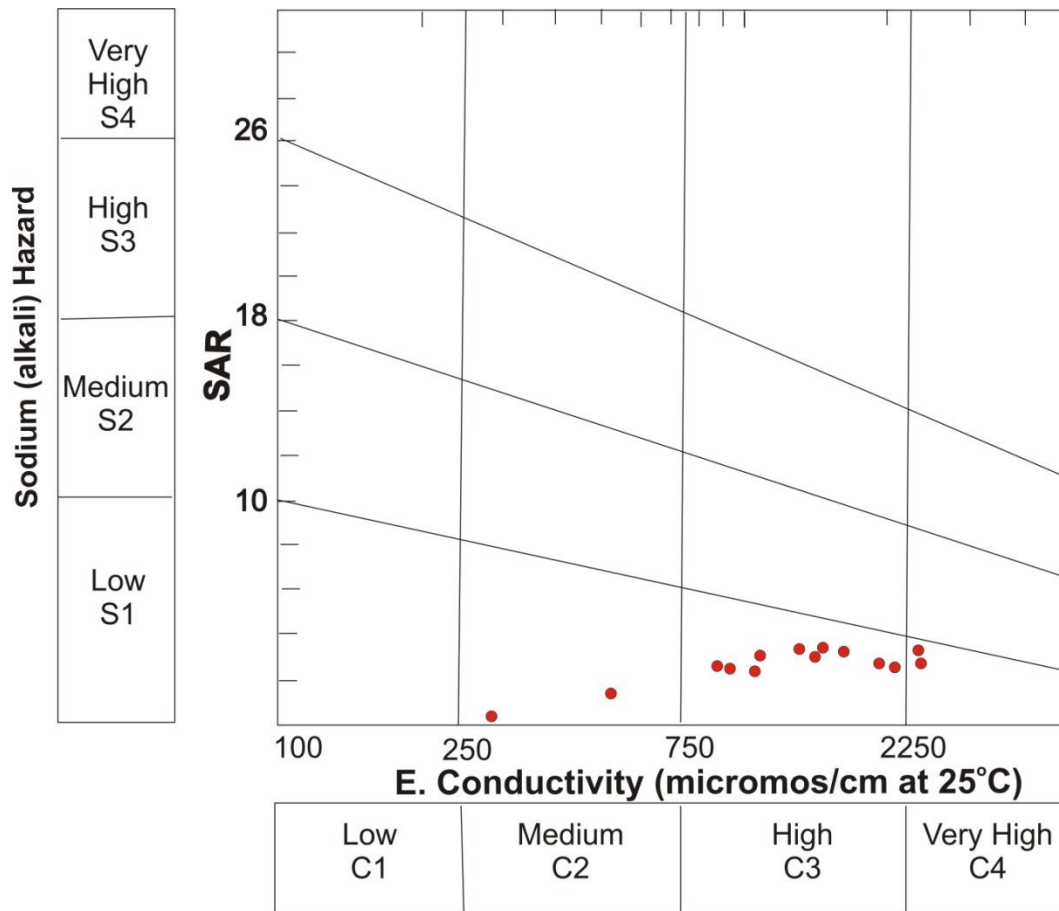


Fig. 5.6: Modified USSL diagram for groundwater samples from the NIASM watershed.

5.2.3 Residual Sodium Carbonate (RSC)

RSC is calculated using the formula $RSC = (CO_3 + HCO_3) - (Ca + Mg)$, where all ionic concentrations are expressed in milliequivalents per liter. RSC values are especially useful when the groundwater contain low levels of salinity. Hence, agriculture experts generally consider RSC superior to SAR. Groundwater containing high CO_3 and HCO_3 tend to precipitate Ca and Mg carbonates in the soils when used for irrigation. Precipitation of Ca and Mg in the soils increases the concentration of Na in the soil and results in lower soil permeability affecting crop growth and crop yields adversely. Depending upon the RSC values the groundwater can be classified into three categories i.e. good (<1.25 meq/L), medium (1.25 to 2.50 meq/L) and poor (>2.5 meq/L). In the study area, most groundwater samples

show RSC values less than zero and are considered to represent good quality water.

5.3 Groundwater Facies

The hydrochemical facies as described by Piper (1994) can be used to denote the diagnostic chemical characteristics of water in hydrogeological system. Hydrogeochemical facies generally reflects the geochemical processes that are operative in the larger host rock-water framework and is a good indicator of the pace and flow of the groundwater in response to hydraulic gradient and geohydrological framework. The major cations and anions from the pre-monsoon groundwater samples were plotted in the Pipers Trilinear diagram in order to understand the spatio-temporal variation in the hydrogeochemical facies. The data generated in the present study is shown in Figure 5.7.

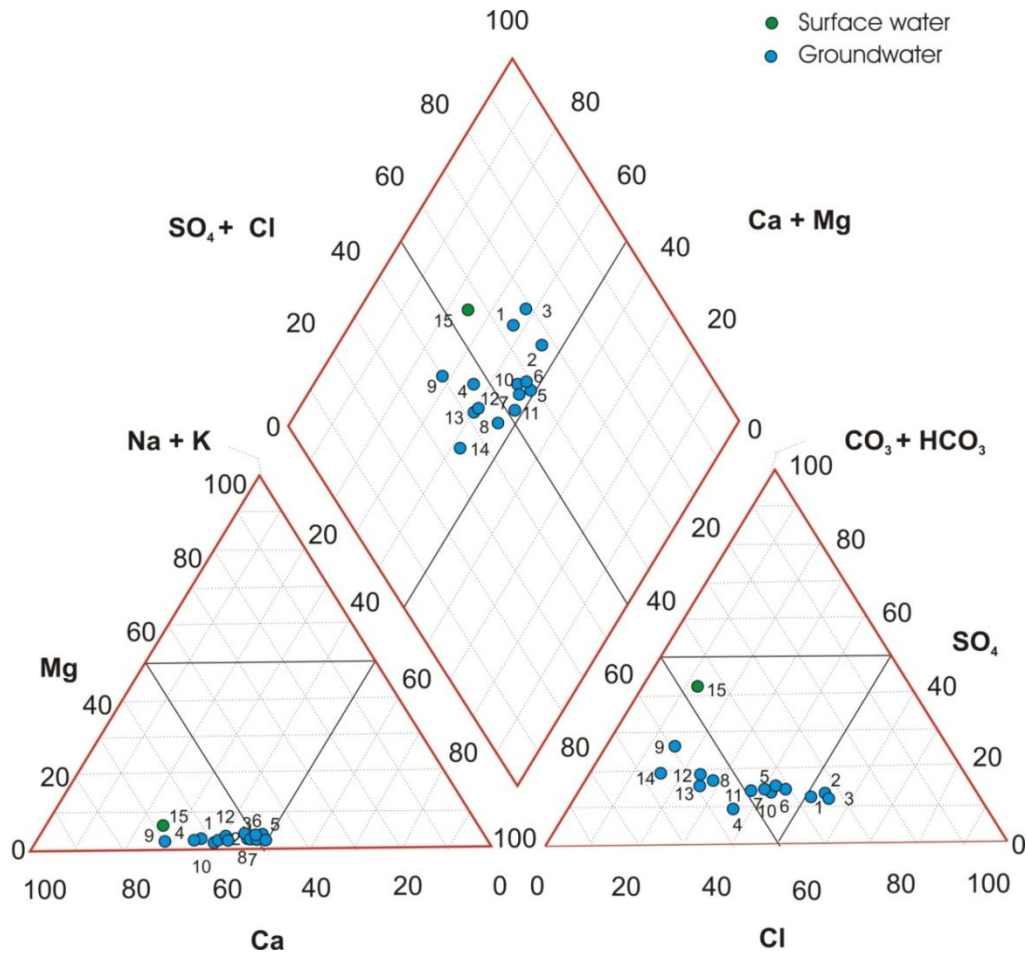


Fig. 5.7: Trilinear diagram (Piper 1994) used to classify chemical types of groundwater samples from the NIASM watershed.

Most groundwater from the study area belong to the $Ca + Mg > Na + K$; $HCO_3 + CO_3 > Cl + SO_4$ facies. Weathering regimes (recharge zones) of jointed basaltic aquifers in the DPR generally show this hydrogeochemical facies. However, some groundwater belong to the $Ca + Mg > Na + K$; $Cl + SO_4 > HCO_3 + CO_3$ facies are also present. Besides variation in the chloride and sulphate ions in some samples most

variations in the groundwater reflect values that are well within the range from the Deccan Trap groundwater province. This indicates that the basalt provenance for the major cations is reflected in the chemistry of the groundwater. The discrepancies in the major cations can also be accounted for by taking into consideration process such as evaporation and precipitation in the semi-arid dry climate.

6. Geophysical Surveys

6.1 Electrical Resistivity Method (ERM)

Geophysical Surveys for groundwater exploration were carried out using Electrical Resistivity Method (ERM) for the delineation of potential/ suitable/ favorable zones for sinking of water abstraction structures (dug well / bore well) for water supply to farm land, plots and other utilities on the NIASM campus. In this method resistance to the flow of an electric current through the subsurface materials is measured at intervals on the ground surface. The resistivity is usually defined as the resistance between opposite phases of a unit cube of the material. Each material has its own resistivity depending upon the water content, compaction and composition. This method is routinely used for:

1. Determining the sub-surface strata classification
2. Determination of hard rock foundation
3. Estimation of overburden thickness and hard rock quantities and
4. Determination of the suitability of the area for quarrying and excavation

A variety of electrode arrangements have been used to measure the earth resistivity

and depending upon the electrode arrangement they are grouped into three classes.

1. Arrangements in which the potential differences between two widely spaced measuring electrodes are recorded.
2. Arrangements in which a potential gradient or electric field intensity is measured using closely spaced pair of measuring electrodes.
3. Arrangements in which the curvature of the potential function is measured using a closely spaced current electrode pair as well as a closely spaced measuring electrode pair.

Any one of these arrays may be used to study variations in resistivity with depth or in lateral condition. In studying the variation of resistivity with depth, as in the case of a layered medium the spacing between the various electrodes is gradually increased. With larger spacing, the effect of material at depth on the measurements becomes more pronounced as has been done in the present study.

The test is conducted by driving four metal spikes to serve as electrodes in to the ground along a straight line at equal distances as shown below (Fig.6.1).



Fig. 6.1. Geophysical Surveys for groundwater exploration using Electrical Resistivity Method at NIASM Site

A direct voltage is imposed between the two outer potentiometer electrodes and the potential drop is measured between the inner electrodes. To interpret the resistivity data for knowing the nature and distribution of the subsurface formations, it is necessary to make preliminary trial on known formations. The potential 'V' thus obtained divided by the current 'I' applied gives the resistance 'R' of the ground. The product of the resistance and the spacing factor, which is depending upon the disposition of the electrodes, is the resistivity of the ground.

In studying the lateral as well as vertical variations, various electrode configurations are adopted and the array is moved as a

whole along a traverse line. The first type of measurement is called as 'Vertical Electrical Sounding' (VES) and the second one is 'Horizontal Profiling' (HP). M/S Sanjeevani Consultancy, Chakan, Pune, undertook the electrical resistivity surveys (ERS) on the NIASM site. Both VES and HP were conducted at 46 different locations (Table 6.1) along 18 horizontal and 28 vertical profiles at the (Fig. 6.2). Care was taken to accommodate the lateral and horizontal variations in the terrain geometry. The L sections generated on the basis of values of electrical resistivity for the site have been used to depict 2-D subsurface images of the strata (Fig.6.3-6.13).

Table 6.1. Latitude and longitude of Electrical Resistivity Survey observation points at NIASM Site.

VES No.	N	E	VES No.	N	E
1	N 18°09'05.9"	E 74°30'01.5"	24	N 18°09'22.7"	E 74°30'02.4"
2	N 18°09'05.6"	E 74°30'06.8"	25	N 18°09'23.0"	E 74°30'06.0"
3	N 18°09'07.9"	E 74°30'06.8"	26	N 18°09'22.9"	E 74°30'10.4"
4	N 18°09'07.3"	E 74°30'02.1"	27	N 18°09'25.0"	E 74°30'11.4"
5	N 18°09'08.9"	E 74°29'57.4"	28	N 18°09'29.0"	E 74°30'06.8"
6	N 18°09'10.6"	E 74°29'57.1"	29	N 18°09'29.5"	E 74°30'02.4"
7	N 18°09'10.4"	E 74°30'02.0"	30	N 18°09'28.5"	E 74°29'55.4"
8	N 18°09'10.5"	E 74°30'05.1"	31	N 18°09'25.1"	E 74°29'51.7"
9	N 18°09'10.2"	E 74°30'08.4"	32	N 18°09'29.5"	E 74°29'48.9"
10	N 18°09'13.0"	E 74°30'08.9"	33	N 18°09'30.8"	E 74°29'54.8"
11	N 18°09'13.9"	E 74°30'05.2"	34	N 18°09'31.4"	E 74°30'00.9"
12	N 18°09'14.1"	E 74°30'01.9"	35	N 18°09'31.8"	E 74°30'06.5"
13	N 18°09'14.9"	E 74°29'55.7"	36	N 18°09'29.3"	E 74°30'12.4"
14	N 18°09'16.3"	E 74°29'55.4"	37	N 18°09'33.4"	E 74°30'12.1"
15	N 18°09'17.0"	E 74°30'02.4"	38	N 18°09'34.1"	E 74°30'05.3"
16	N 18°09'16.8"	E 74°30'05.3"	39	N 18°09'34.3"	E 74°30'00.9"
17	N 18°09'16.6"	E 74°30'09.4"	40	N 18°09'34.5"	E 74°29'55.9"
18	N 18°09'20.2"	E 74°30'10.2"	41	N 18°09'31.9"	E 74°29'48.1"
19	N 18°09'20.1"	E 74°30'06.9"	42	N 18°09'35.3"	E 74°29'47.1"
20	N 18°09'19.3"	E 74°30'02.4"	43	N 18°09'38.3"	E 74°29'55.6"
21	N 18°09'17.1"	E 74°29'55.3"	44	N 18°09'38.1"	E 74°29'59.5"
22	N 18°09'22.8"	E 74°29'53.9"	45	N 18°09'36.7"	E 74°30'09.1"
23	N 18°09'22.5"	E 74°29'57.7"	46	N 18°09'36.2"	E 74°30'11.9"

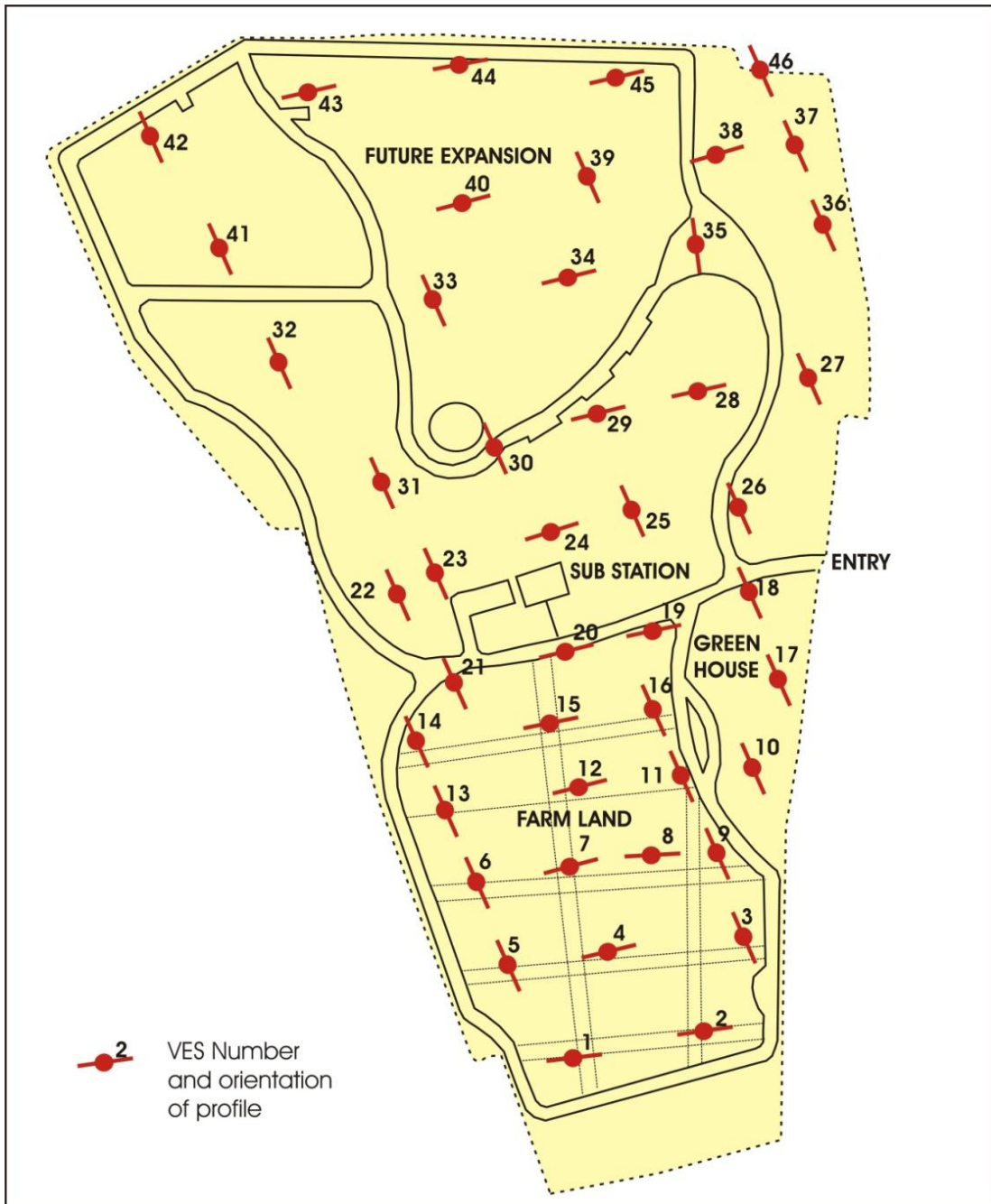


Fig. 6.2. Grid Map for Resistivity Survey showing 'Vertical Electrical Sounding' (VES) and 'Horizontal Profiling' (HP) at NIASM Site.

Longitudinal profiles showing 2-D subsurface images.

The blue and black colour indicates soil + weathered + fractured rock while the other colours indicate moderately fractured and hard rock

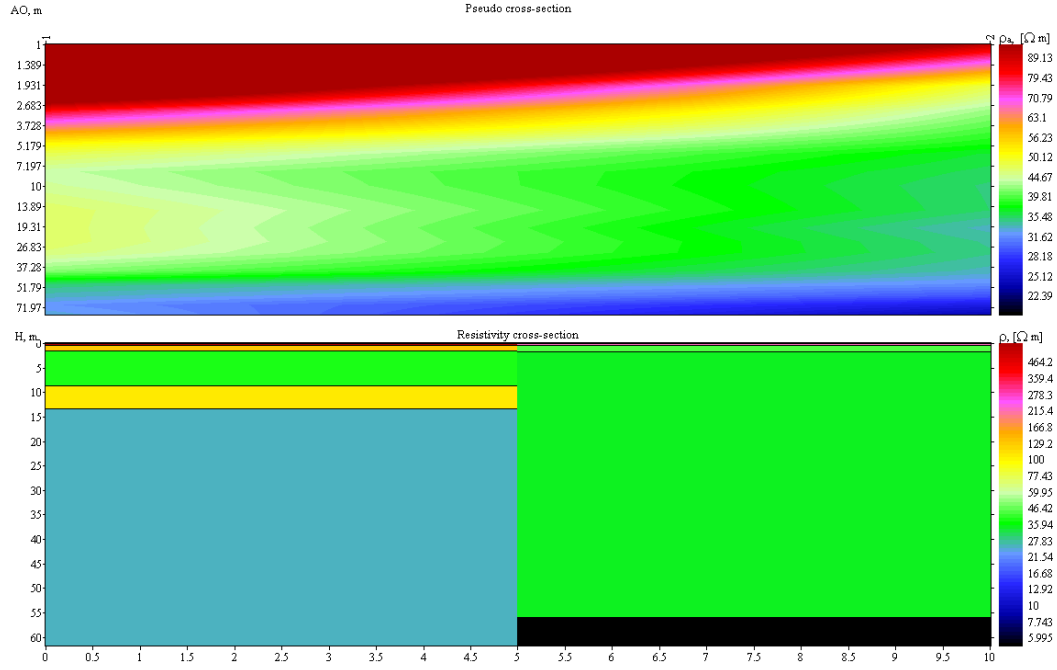


Fig.7.3. 2-D subsurface images of Horizontal profiles 1-2

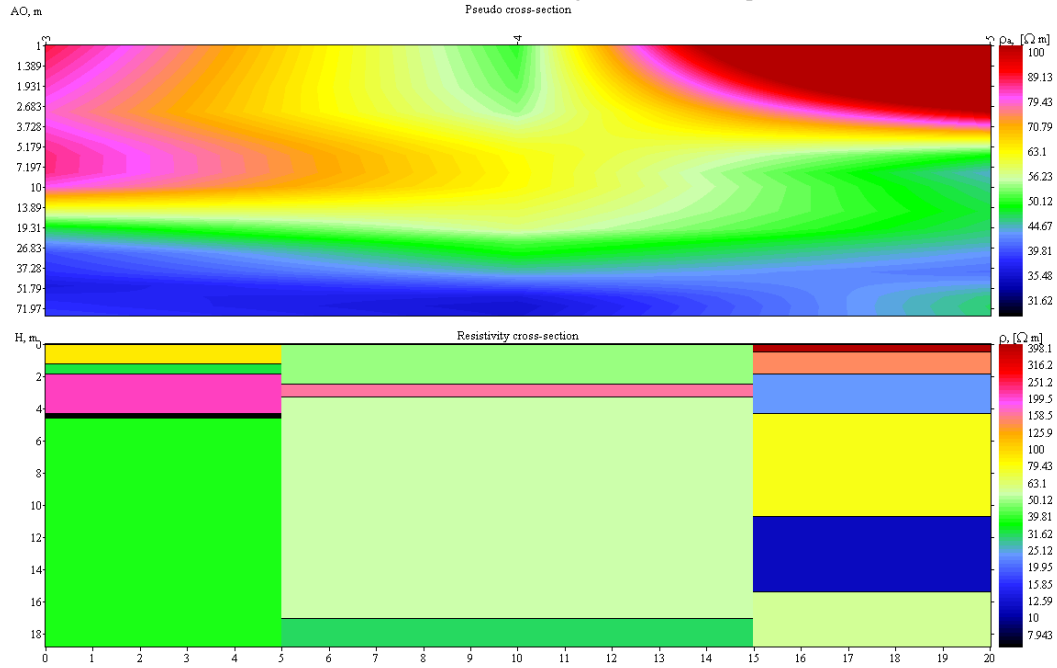


Fig.6.4. 2-D subsurface images of Horizontal profiles 3-4-5

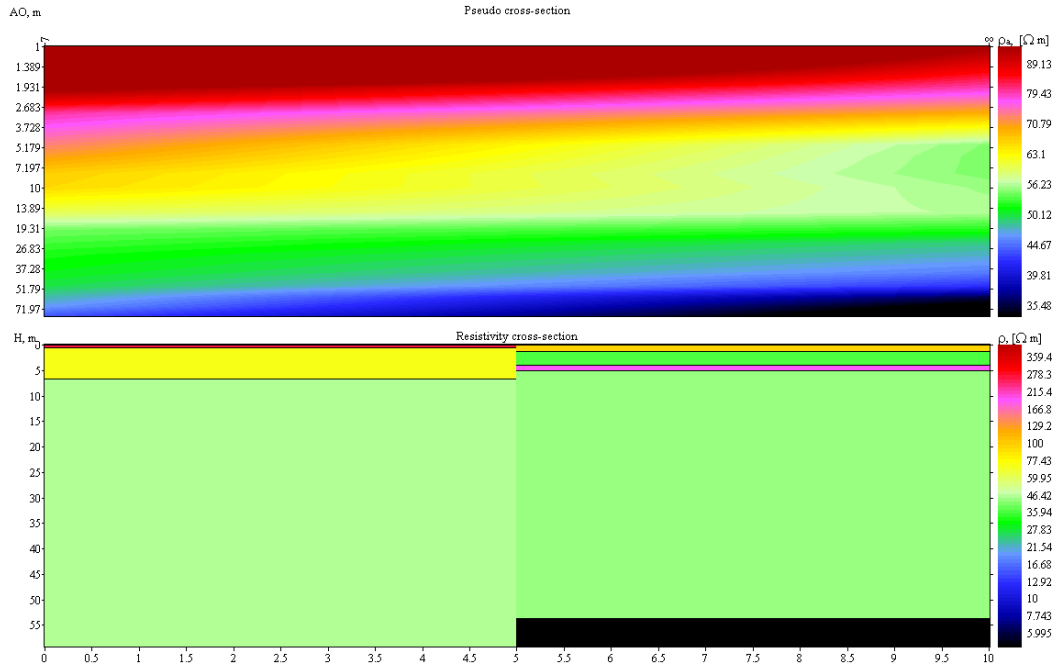


Fig.6.5. 2-D subsurface images of Horizontal profiles 7-8

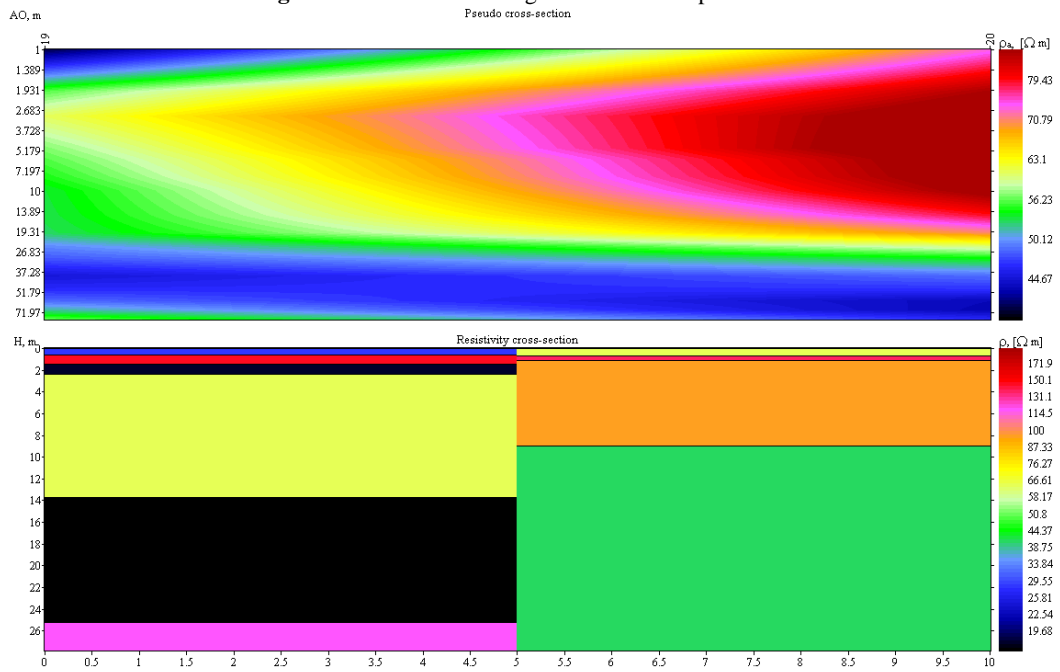


Fig.6.6. 2-D subsurface images of Horizontal profiles 19-20

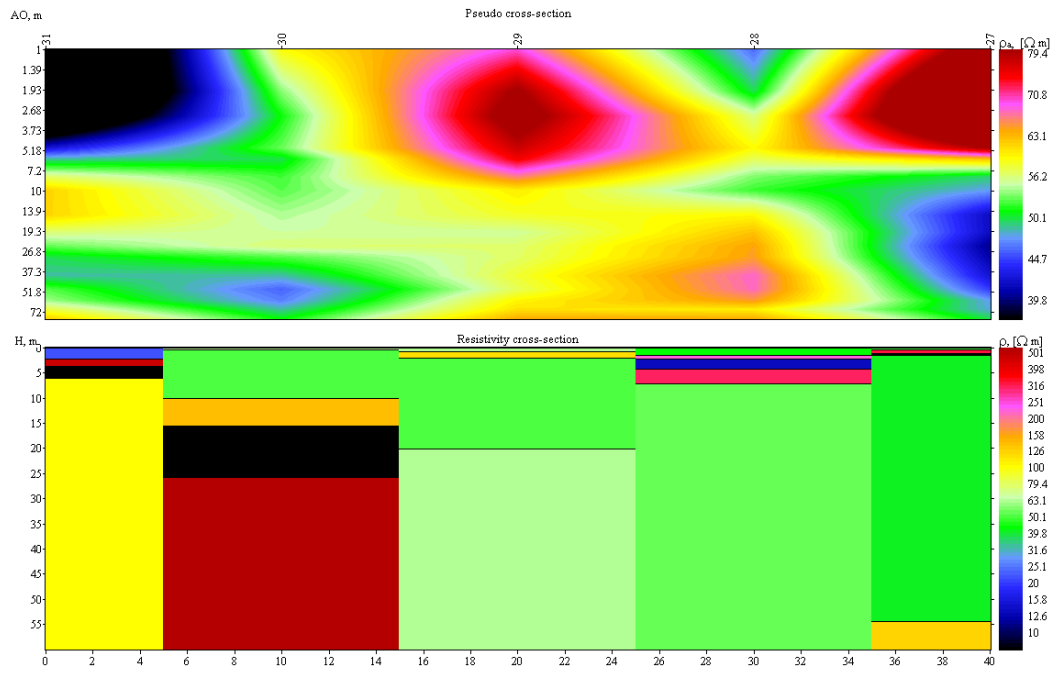


Fig.6.7. 2-D subsurface images of Horizontal profiles 31-30-29-28-27

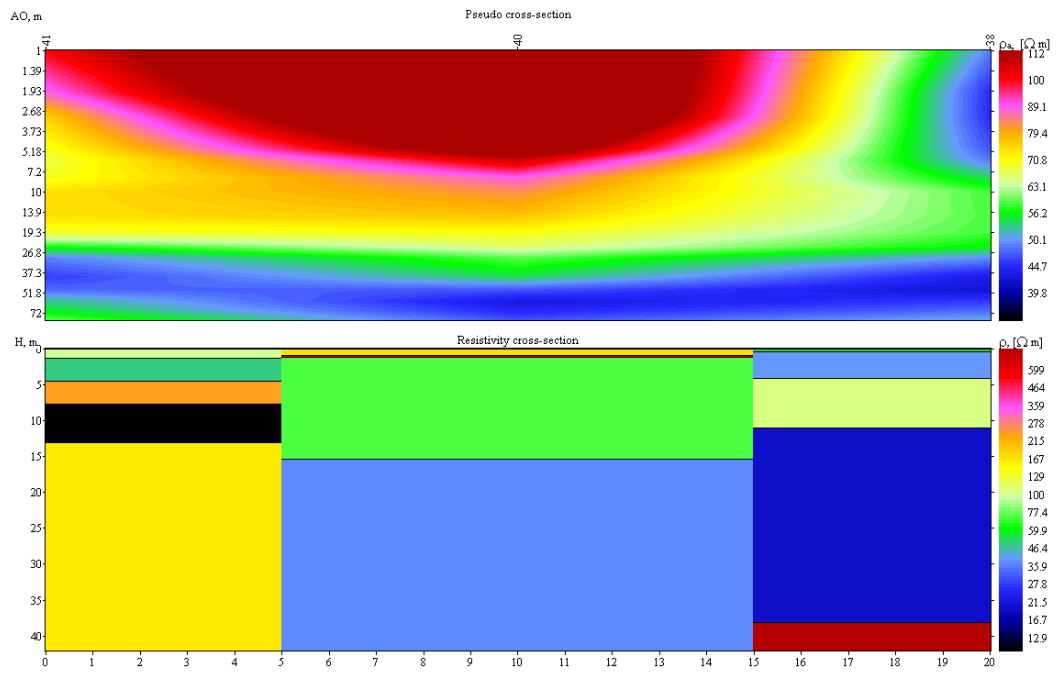


Fig.6.8. 2-D subsurface images of Horizontal profiles 41-40-38

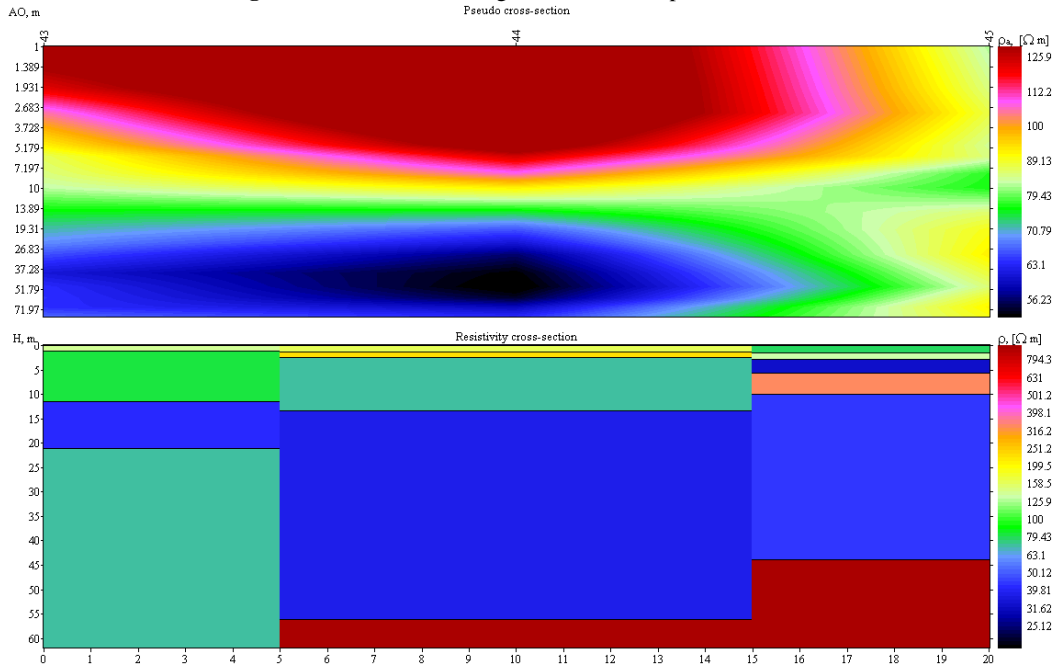


Fig. 6.9. 2-D subsurface images of Horizontal profiles 43-44-45.

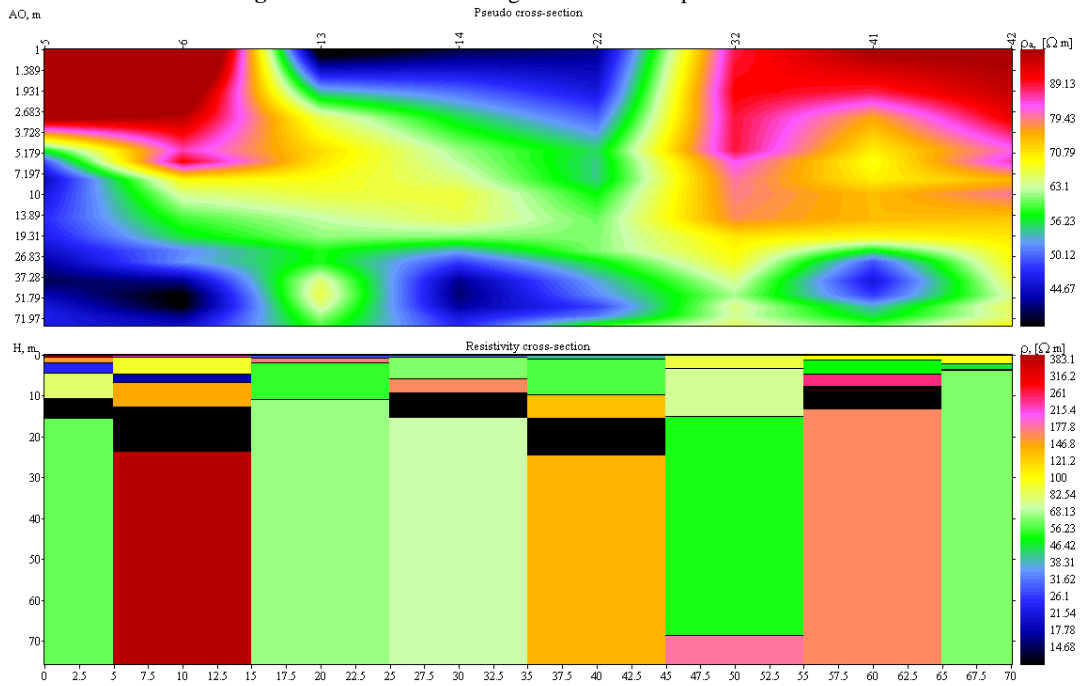


Fig. 6.10. 2-D subsurface images of Vertical profiles 5-6-13-14-22-32-41-42.

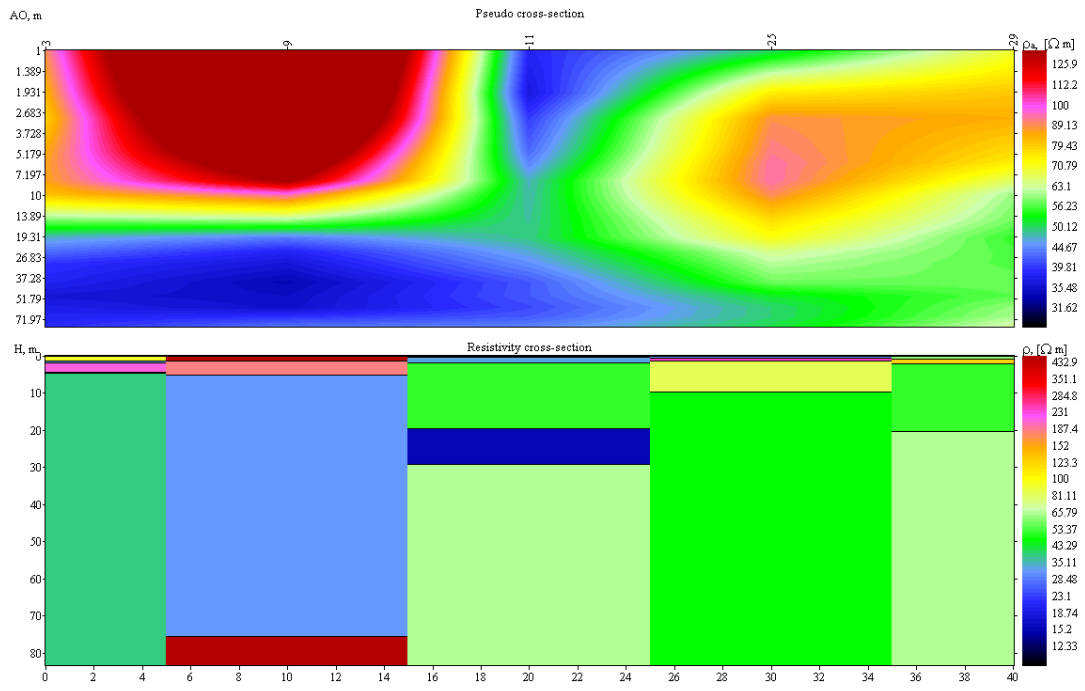


Fig. 6.11. 2-D subsurface images of Vertical profiles 3-9-11-25-39

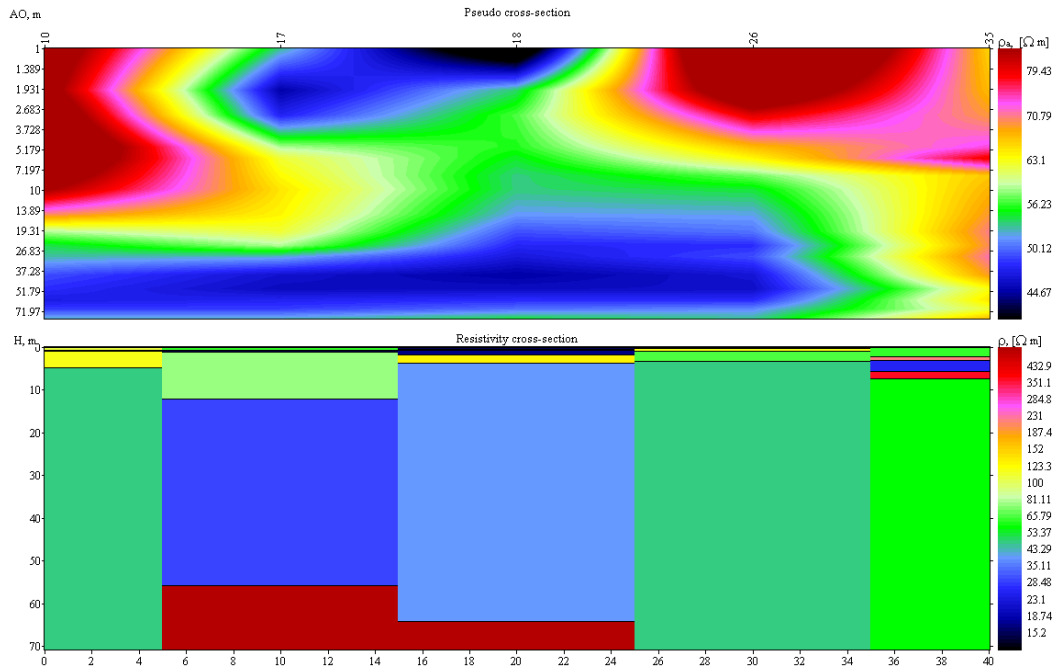


Fig. 6.12. 2-D subsurface images of Vertical profiles 10-17-18-26-35

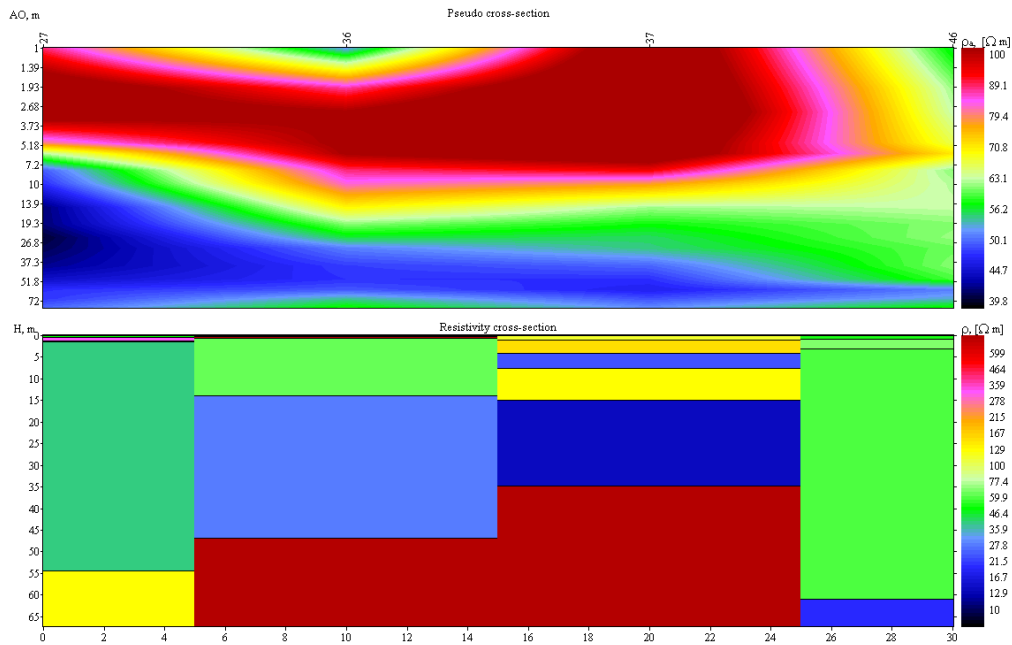


Fig. 6.13. 2-D subsurface images of Vertical profiles 27-36-37-46

6.2 Results and Data Processing

To understand the shallow subsurface geological and aquifer conditions in the area extending up to 70-90 meters depth, vertical electrical soundings (VES) were conducted at seven different locations and all the sounding data were modeled for the existing sections. Using IPI2 WINDOW based software the data obtained from field was processed which helps in interactive semi-automated interpretation of the field data. The VES data on apparent resistivity values was modeled by using above software to get different geological layers depicting their thickness, depth and true resistivity. As discussed above the sounding points with typical curves at selected sites give point information, which was further utilized to build comprehensive picture of subsurface geological situation depth-wise by preparing 2-D geoelectrical sections (Table 6.2). The geoelectrical cross-sections passing through various points have been presented in the above figures along with table. It is to be noted that these are apparent resistivity L sections, which broadly match the true resistivity of formations. Using IPI2 software, the values of true resistivity of strata (ρ), its thickness (h) and depth (d) have been obtained after modeling of data

and are depicted in table form besides graphs (Table 6.2).

It can be seen that at VES 2 and 8 there is a substantial drop in the resistivity at a depth of 53 to 55 meters these locations are good for siting bore wells. At VES 2 there is a continuous drop in modeled resistivity values. Moreover, the point is on the lowest possible site on the NIASM site and it is envisaged that all groundwater flow paths will converge towards this point. Hence, the Location 2 is most ideal for sinking a bore well. Location 2 is also surrounded by discontinuous pockets of low resistivity strata. At VES location 9 the strata is soft up to a depth of 75 meters beyond which massive hard rock is envisaged and hence this location is ideal for siting rain water harvesting structure such as recharging well or recharge pit. Similarly, point 11 is also recommended for rain water harvesting structure such as recharging well or recharge pit. At VES locations 18, the rock strata is conducive as potential aquifer up to depth of 20 meters respectively beyond which the strata encountered is hard compact and massive. These points if suitably treated 9 (bore blasting/ hydrofracturing) can be utilized for either purpose i.e. siting

exploitation bore wells or as recharging

wells or recharge pits.

Table 6.2. Modelled electrical resistivity data output at various locations (1-45) of NIASM site

Site No	Value					Graph																															
1.	<table border="1"> <thead> <tr> <th>N</th> <th>ρ</th> <th>h</th> <th>d</th> <th>Alt</th> </tr> </thead> <tbody> <tr> <td>1</td> <td>691.5</td> <td>0.4372</td> <td>0.4372</td> <td>0.43719</td> </tr> <tr> <td>2</td> <td>130.7</td> <td>1.03</td> <td>1.467</td> <td>-1.4673</td> </tr> <tr> <td>3</td> <td>39.22</td> <td>7.241</td> <td>8.709</td> <td>-8.7087</td> </tr> <tr> <td>4</td> <td>111.3</td> <td>4.584</td> <td>13.29</td> <td>-13.293</td> </tr> <tr> <td>5</td> <td>26.8</td> <td></td> <td></td> <td></td> </tr> </tbody> </table>	N	ρ	h	d	Alt	1	691.5	0.4372	0.4372	0.43719	2	130.7	1.03	1.467	-1.4673	3	39.22	7.241	8.709	-8.7087	4	111.3	4.584	13.29	-13.293	5	26.8									
N	ρ	h	d	Alt																																	
1	691.5	0.4372	0.4372	0.43719																																	
2	130.7	1.03	1.467	-1.4673																																	
3	39.22	7.241	8.709	-8.7087																																	
4	111.3	4.584	13.29	-13.293																																	
5	26.8																																				
2.	<table border="1"> <thead> <tr> <th>N</th> <th>ρ</th> <th>h</th> <th>d</th> <th>Alt</th> </tr> </thead> <tbody> <tr> <td>1</td> <td>219.5</td> <td>0.3615</td> <td>0.3615</td> <td>0.36147</td> </tr> <tr> <td>2</td> <td>43.98</td> <td>1.266</td> <td>1.627</td> <td>-1.627</td> </tr> <tr> <td>3</td> <td>35.08</td> <td>54.36</td> <td>55.99</td> <td>-55.986</td> </tr> <tr> <td>4</td> <td>2.66</td> <td></td> <td></td> <td></td> </tr> </tbody> </table>	N	ρ	h	d	Alt	1	219.5	0.3615	0.3615	0.36147	2	43.98	1.266	1.627	-1.627	3	35.08	54.36	55.99	-55.986	4	2.66														
N	ρ	h	d	Alt																																	
1	219.5	0.3615	0.3615	0.36147																																	
2	43.98	1.266	1.627	-1.627																																	
3	35.08	54.36	55.99	-55.986																																	
4	2.66																																				
3.	<table border="1"> <thead> <tr> <th>N</th> <th>ρ</th> <th>h</th> <th>d</th> <th>Alt</th> </tr> </thead> <tbody> <tr> <td>1</td> <td>93</td> <td>1.179</td> <td>1.179</td> <td>-1.179</td> </tr> <tr> <td>2</td> <td>33.52</td> <td>0.6429</td> <td>1.822</td> <td>-1.8219</td> </tr> <tr> <td>3</td> <td>210.2</td> <td>2.46</td> <td>4.281</td> <td>-4.2815</td> </tr> <tr> <td>4</td> <td>1.773</td> <td>0.2829</td> <td>4.564</td> <td>-4.5643</td> </tr> <tr> <td>5</td> <td>38.49</td> <td></td> <td></td> <td></td> </tr> </tbody> </table>	N	ρ	h	d	Alt	1	93	1.179	1.179	-1.179	2	33.52	0.6429	1.822	-1.8219	3	210.2	2.46	4.281	-4.2815	4	1.773	0.2829	4.564	-4.5643	5	38.49									
N	ρ	h	d	Alt																																	
1	93	1.179	1.179	-1.179																																	
2	33.52	0.6429	1.822	-1.8219																																	
3	210.2	2.46	4.281	-4.2815																																	
4	1.773	0.2829	4.564	-4.5643																																	
5	38.49																																				
4.	<table border="1"> <thead> <tr> <th>N</th> <th>ρ</th> <th>h</th> <th>d</th> <th>Alt</th> </tr> </thead> <tbody> <tr> <td>1</td> <td>50.39</td> <td>2.44</td> <td>2.44</td> <td>-2.4402</td> </tr> <tr> <td>2</td> <td>158.4</td> <td>0.7975</td> <td>3.238</td> <td>-3.2377</td> </tr> <tr> <td>3</td> <td>56.79</td> <td>13.8</td> <td>17.04</td> <td>-17.036</td> </tr> <tr> <td>4</td> <td>31.21</td> <td></td> <td></td> <td></td> </tr> </tbody> </table>	N	ρ	h	d	Alt	1	50.39	2.44	2.44	-2.4402	2	158.4	0.7975	3.238	-3.2377	3	56.79	13.8	17.04	-17.036	4	31.21														
N	ρ	h	d	Alt																																	
1	50.39	2.44	2.44	-2.4402																																	
2	158.4	0.7975	3.238	-3.2377																																	
3	56.79	13.8	17.04	-17.036																																	
4	31.21																																				
5.	<table border="1"> <thead> <tr> <th>N</th> <th>ρ</th> <th>h</th> <th>d</th> <th>Alt</th> </tr> </thead> <tbody> <tr> <td>1</td> <td>566.2</td> <td>0.448</td> <td>0.448</td> <td>0.44804</td> </tr> <tr> <td>2</td> <td>148.1</td> <td>1.401</td> <td>1.849</td> <td>-1.8492</td> </tr> <tr> <td>3</td> <td>24.7</td> <td>2.448</td> <td>4.298</td> <td>-4.2976</td> </tr> <tr> <td>4</td> <td>81.22</td> <td>6.388</td> <td>10.69</td> <td>-10.686</td> </tr> <tr> <td>5</td> <td>11.86</td> <td>4.685</td> <td>15.37</td> <td>-15.371</td> </tr> </tbody> </table>	N	ρ	h	d	Alt	1	566.2	0.448	0.448	0.44804	2	148.1	1.401	1.849	-1.8492	3	24.7	2.448	4.298	-4.2976	4	81.22	6.388	10.69	-10.686	5	11.86	4.685	15.37	-15.371						
N	ρ	h	d	Alt																																	
1	566.2	0.448	0.448	0.44804																																	
2	148.1	1.401	1.849	-1.8492																																	
3	24.7	2.448	4.298	-4.2976																																	
4	81.22	6.388	10.69	-10.686																																	
5	11.86	4.685	15.37	-15.371																																	
6.	<table border="1"> <thead> <tr> <th>N</th> <th>ρ</th> <th>h</th> <th>d</th> <th>Alt</th> </tr> </thead> <tbody> <tr> <td>1</td> <td>215.5</td> <td>0.4529</td> <td>0.4529</td> <td>0.45293</td> </tr> <tr> <td>2</td> <td>93.82</td> <td>4.201</td> <td>4.654</td> <td>-4.654</td> </tr> <tr> <td>3</td> <td>18.12</td> <td>1.916</td> <td>6.571</td> <td>-6.5705</td> </tr> <tr> <td>4</td> <td>143.8</td> <td>6.091</td> <td>12.66</td> <td>-12.662</td> </tr> <tr> <td>5</td> <td>6.864</td> <td>10.68</td> <td>23.34</td> <td>-23.343</td> </tr> <tr> <td>6</td> <td>962.6</td> <td></td> <td></td> <td></td> </tr> </tbody> </table>	N	ρ	h	d	Alt	1	215.5	0.4529	0.4529	0.45293	2	93.82	4.201	4.654	-4.654	3	18.12	1.916	6.571	-6.5705	4	143.8	6.091	12.66	-12.662	5	6.864	10.68	23.34	-23.343	6	962.6				
N	ρ	h	d	Alt																																	
1	215.5	0.4529	0.4529	0.45293																																	
2	93.82	4.201	4.654	-4.654																																	
3	18.12	1.916	6.571	-6.5705																																	
4	143.8	6.091	12.66	-12.662																																	
5	6.864	10.68	23.34	-23.343																																	
6	962.6																																				
7.	<table border="1"> <thead> <tr> <th>N</th> <th>ρ</th> <th>h</th> <th>d</th> <th>Alt</th> </tr> </thead> <tbody> <tr> <td>1</td> <td>263.2</td> <td>0.555</td> <td>0.555</td> <td>0.55496</td> </tr> <tr> <td>2</td> <td>21.21</td> <td>0.05457</td> <td>0.6095</td> <td>0.60954</td> </tr> <tr> <td>3</td> <td>72.32</td> <td>6.017</td> <td>6.627</td> <td>-6.6269</td> </tr> <tr> <td>4</td> <td>47.55</td> <td></td> <td></td> <td></td> </tr> </tbody> </table>	N	ρ	h	d	Alt	1	263.2	0.555	0.555	0.55496	2	21.21	0.05457	0.6095	0.60954	3	72.32	6.017	6.627	-6.6269	4	47.55														
N	ρ	h	d	Alt																																	
1	263.2	0.555	0.555	0.55496																																	
2	21.21	0.05457	0.6095	0.60954																																	
3	72.32	6.017	6.627	-6.6269																																	
4	47.55																																				

8.	<table border="1"> <thead> <tr> <th>N</th> <th>p</th> <th>h</th> <th>d</th> <th>Alt</th> </tr> </thead> <tbody> <tr> <td>1</td> <td>96.49</td> <td>1.341</td> <td>1.341</td> <td>-1.3411</td> </tr> <tr> <td>2</td> <td>38.42</td> <td>2.654</td> <td>3.995</td> <td>-3.9947</td> </tr> <tr> <td>3</td> <td>195.5</td> <td>1.034</td> <td>5.029</td> <td>-5.0286</td> </tr> <tr> <td>4</td> <td>45.29</td> <td>48.67</td> <td>53.7</td> <td>-53.699</td> </tr> <tr> <td>5</td> <td>1.74</td> <td></td> <td></td> <td></td> </tr> </tbody> </table>	N	p	h	d	Alt	1	96.49	1.341	1.341	-1.3411	2	38.42	2.654	3.995	-3.9947	3	195.5	1.034	5.029	-5.0286	4	45.29	48.67	53.7	-53.699	5	1.74				
N	p	h	d	Alt																												
1	96.49	1.341	1.341	-1.3411																												
2	38.42	2.654	3.995	-3.9947																												
3	195.5	1.034	5.029	-5.0286																												
4	45.29	48.67	53.7	-53.699																												
5	1.74																															
9.	<table border="1"> <thead> <tr> <th>N</th> <th>p</th> <th>h</th> <th>d</th> <th>Alt</th> </tr> </thead> <tbody> <tr> <td>1</td> <td>474</td> <td>1.26</td> <td>1.26</td> <td>-1.259</td> </tr> <tr> <td>2</td> <td>186</td> <td>3.79</td> <td>5.05</td> <td>-5.047</td> </tr> <tr> <td>3</td> <td>32.7</td> <td>70.5</td> <td>75.6</td> <td>-75.57</td> </tr> <tr> <td>4</td> <td>878</td> <td></td> <td></td> <td></td> </tr> </tbody> </table>	N	p	h	d	Alt	1	474	1.26	1.26	-1.259	2	186	3.79	5.05	-5.047	3	32.7	70.5	75.6	-75.57	4	878									
N	p	h	d	Alt																												
1	474	1.26	1.26	-1.259																												
2	186	3.79	5.05	-5.047																												
3	32.7	70.5	75.6	-75.57																												
4	878																															
10.	<table border="1"> <thead> <tr> <th>N</th> <th>p</th> <th>h</th> <th>d</th> <th>Alt</th> </tr> </thead> <tbody> <tr> <td>1</td> <td>104.9</td> <td>0.5683</td> <td>0.5683</td> <td>0.56829</td> </tr> <tr> <td>2</td> <td>47.18</td> <td>0.3278</td> <td>0.896</td> <td>0.89602</td> </tr> <tr> <td>3</td> <td>119.2</td> <td>3.939</td> <td>4.835</td> <td>-4.8349</td> </tr> <tr> <td>4</td> <td>47.71</td> <td></td> <td></td> <td></td> </tr> </tbody> </table>	N	p	h	d	Alt	1	104.9	0.5683	0.5683	0.56829	2	47.18	0.3278	0.896	0.89602	3	119.2	3.939	4.835	-4.8349	4	47.71									
N	p	h	d	Alt																												
1	104.9	0.5683	0.5683	0.56829																												
2	47.18	0.3278	0.896	0.89602																												
3	119.2	3.939	4.835	-4.8349																												
4	47.71																															
11.	<table border="1"> <thead> <tr> <th>N</th> <th>p</th> <th>h</th> <th>d</th> <th>Alt</th> </tr> </thead> <tbody> <tr> <td>1</td> <td>39.94</td> <td>0.4081</td> <td>0.4081</td> <td>0.40809</td> </tr> <tr> <td>2</td> <td>292</td> <td>0.2433</td> <td>0.6514</td> <td>0.65136</td> </tr> <tr> <td>3</td> <td>46.39</td> <td>7.549</td> <td>8.2</td> <td>-8.2</td> </tr> <tr> <td>4</td> <td>33.59</td> <td>32.43</td> <td>40.63</td> <td>-40.634</td> </tr> <tr> <td>5</td> <td>81.72</td> <td></td> <td></td> <td></td> </tr> </tbody> </table>	N	p	h	d	Alt	1	39.94	0.4081	0.4081	0.40809	2	292	0.2433	0.6514	0.65136	3	46.39	7.549	8.2	-8.2	4	33.59	32.43	40.63	-40.634	5	81.72				
N	p	h	d	Alt																												
1	39.94	0.4081	0.4081	0.40809																												
2	292	0.2433	0.6514	0.65136																												
3	46.39	7.549	8.2	-8.2																												
4	33.59	32.43	40.63	-40.634																												
5	81.72																															
12.	<table border="1"> <thead> <tr> <th>N</th> <th>p</th> <th>h</th> <th>d</th> <th>Alt</th> </tr> </thead> <tbody> <tr> <td>1</td> <td>46.71</td> <td>0.4222</td> <td>0.4222</td> <td>0.42216</td> </tr> <tr> <td>2</td> <td>29.13</td> <td>0.7732</td> <td>1.195</td> <td>-1.1954</td> </tr> <tr> <td>3</td> <td>51.65</td> <td>18.81</td> <td>20.01</td> <td>-20.009</td> </tr> <tr> <td>4</td> <td>16.38</td> <td>10.01</td> <td>30.02</td> <td>-30.017</td> </tr> <tr> <td>5</td> <td>66.21</td> <td></td> <td></td> <td></td> </tr> </tbody> </table>	N	p	h	d	Alt	1	46.71	0.4222	0.4222	0.42216	2	29.13	0.7732	1.195	-1.1954	3	51.65	18.81	20.01	-20.009	4	16.38	10.01	30.02	-30.017	5	66.21				
N	p	h	d	Alt																												
1	46.71	0.4222	0.4222	0.42216																												
2	29.13	0.7732	1.195	-1.1954																												
3	51.65	18.81	20.01	-20.009																												
4	16.38	10.01	30.02	-30.017																												
5	66.21																															
13.	<table border="1"> <thead> <tr> <th>N</th> <th>p</th> <th>h</th> <th>d</th> <th>Alt</th> </tr> </thead> <tbody> <tr> <td>1</td> <td>29.3</td> <td>0.717</td> <td>0.717</td> <td>-0.717</td> </tr> <tr> <td>2</td> <td>169</td> <td>1.01</td> <td>1.73</td> <td>-1.728</td> </tr> <tr> <td>3</td> <td>54.7</td> <td>9.03</td> <td>10.8</td> <td>-10.75</td> </tr> <tr> <td>4</td> <td>65.1</td> <td></td> <td></td> <td></td> </tr> </tbody> </table>	N	p	h	d	Alt	1	29.3	0.717	0.717	-0.717	2	169	1.01	1.73	-1.728	3	54.7	9.03	10.8	-10.75	4	65.1									
N	p	h	d	Alt																												
1	29.3	0.717	0.717	-0.717																												
2	169	1.01	1.73	-1.728																												
3	54.7	9.03	10.8	-10.75																												
4	65.1																															
14.	<table border="1"> <thead> <tr> <th>N</th> <th>p</th> <th>h</th> <th>d</th> <th>Alt</th> </tr> </thead> <tbody> <tr> <td>1</td> <td>33.19</td> <td>0.5</td> <td>0.5</td> <td>0.49994</td> </tr> <tr> <td>2</td> <td>63.44</td> <td>5.169</td> <td>5.669</td> <td>-5.6688</td> </tr> <tr> <td>3</td> <td>165.2</td> <td>3.556</td> <td>9.225</td> <td>-9.2247</td> </tr> <tr> <td>4</td> <td>8.901</td> <td>6.025</td> <td>15.25</td> <td>-15.249</td> </tr> <tr> <td>5</td> <td>73.56</td> <td></td> <td></td> <td></td> </tr> </tbody> </table>	N	p	h	d	Alt	1	33.19	0.5	0.5	0.49994	2	63.44	5.169	5.669	-5.6688	3	165.2	3.556	9.225	-9.2247	4	8.901	6.025	15.25	-15.249	5	73.56				
N	p	h	d	Alt																												
1	33.19	0.5	0.5	0.49994																												
2	63.44	5.169	5.669	-5.6688																												
3	165.2	3.556	9.225	-9.2247																												
4	8.901	6.025	15.25	-15.249																												
5	73.56																															
15.	<table border="1"> <thead> <tr> <th>N</th> <th>p</th> <th>h</th> <th>d</th> <th>Alt</th> </tr> </thead> <tbody> <tr> <td>1</td> <td>42.76</td> <td>1.196</td> <td>1.196</td> <td>-1.1964</td> </tr> <tr> <td>2</td> <td>100.9</td> <td>0.967</td> <td>2.163</td> <td>-2.1635</td> </tr> <tr> <td>3</td> <td>53.57</td> <td>23.63</td> <td>25.79</td> <td>-25.792</td> </tr> <tr> <td>4</td> <td>13.75</td> <td>17.37</td> <td>43.16</td> <td>-43.164</td> </tr> <tr> <td>5</td> <td>821.6</td> <td></td> <td></td> <td></td> </tr> </tbody> </table>	N	p	h	d	Alt	1	42.76	1.196	1.196	-1.1964	2	100.9	0.967	2.163	-2.1635	3	53.57	23.63	25.79	-25.792	4	13.75	17.37	43.16	-43.164	5	821.6				
N	p	h	d	Alt																												
1	42.76	1.196	1.196	-1.1964																												
2	100.9	0.967	2.163	-2.1635																												
3	53.57	23.63	25.79	-25.792																												
4	13.75	17.37	43.16	-43.164																												
5	821.6																															

16.	<table border="1"> <thead> <tr> <th>N</th> <th>p</th> <th>h</th> <th>d</th> <th>Alt</th> </tr> </thead> <tbody> <tr> <td>1</td> <td>32.99</td> <td>0.7942</td> <td>0.7942</td> <td>0.7941</td> </tr> <tr> <td>2</td> <td>47.04</td> <td>5.645</td> <td>6.439</td> <td>-6.4391</td> </tr> <tr> <td>3</td> <td>18.3</td> <td>0.9847</td> <td>7.424</td> <td>-7.4238</td> </tr> <tr> <td>4</td> <td>47.34</td> <td></td> <td></td> <td></td> </tr> </tbody> </table>	N	p	h	d	Alt	1	32.99	0.7942	0.7942	0.7941	2	47.04	5.645	6.439	-6.4391	3	18.3	0.9847	7.424	-7.4238	4	47.34														
N	p	h	d	Alt																																	
1	32.99	0.7942	0.7942	0.7941																																	
2	47.04	5.645	6.439	-6.4391																																	
3	18.3	0.9847	7.424	-7.4238																																	
4	47.34																																				
17.	<table border="1"> <thead> <tr> <th>N</th> <th>p</th> <th>h</th> <th>d</th> <th>Alt</th> </tr> </thead> <tbody> <tr> <td>1</td> <td>64.88</td> <td>0.656</td> <td>0.656</td> <td>0.6560</td> </tr> <tr> <td>2</td> <td>15.6</td> <td>0.3591</td> <td>1.015</td> <td>-1.0152</td> </tr> <tr> <td>3</td> <td>76.61</td> <td>11.13</td> <td>12.15</td> <td>-12.149</td> </tr> <tr> <td>4</td> <td>30.82</td> <td>43.53</td> <td>55.68</td> <td>-55.683</td> </tr> <tr> <td>5</td> <td>2359</td> <td></td> <td></td> <td></td> </tr> </tbody> </table>	N	p	h	d	Alt	1	64.88	0.656	0.656	0.6560	2	15.6	0.3591	1.015	-1.0152	3	76.61	11.13	12.15	-12.149	4	30.82	43.53	55.68	-55.683	5	2359									
N	p	h	d	Alt																																	
1	64.88	0.656	0.656	0.6560																																	
2	15.6	0.3591	1.015	-1.0152																																	
3	76.61	11.13	12.15	-12.149																																	
4	30.82	43.53	55.68	-55.683																																	
5	2359																																				
18.	<table border="1"> <thead> <tr> <th>N</th> <th>p</th> <th>h</th> <th>d</th> <th>Alt</th> </tr> </thead> <tbody> <tr> <td>1</td> <td>15.76</td> <td>0.3314</td> <td>0.3314</td> <td>0.3314</td> </tr> <tr> <td>2</td> <td>305.3</td> <td>0.3809</td> <td>0.7123</td> <td>0.7123</td> </tr> <tr> <td>3</td> <td>17.47</td> <td>1.102</td> <td>1.814</td> <td>-1.8139</td> </tr> <tr> <td>4</td> <td>127</td> <td>1.944</td> <td>3.758</td> <td>-3.7583</td> </tr> <tr> <td>5</td> <td>40.33</td> <td>60.4</td> <td>64.15</td> <td>-64.155</td> </tr> <tr> <td>6</td> <td>693.9</td> <td></td> <td></td> <td></td> </tr> </tbody> </table>	N	p	h	d	Alt	1	15.76	0.3314	0.3314	0.3314	2	305.3	0.3809	0.7123	0.7123	3	17.47	1.102	1.814	-1.8139	4	127	1.944	3.758	-3.7583	5	40.33	60.4	64.15	-64.155	6	693.9				
N	p	h	d	Alt																																	
1	15.76	0.3314	0.3314	0.3314																																	
2	305.3	0.3809	0.7123	0.7123																																	
3	17.47	1.102	1.814	-1.8139																																	
4	127	1.944	3.758	-3.7583																																	
5	40.33	60.4	64.15	-64.155																																	
6	693.9																																				
19.	<table border="1"> <thead> <tr> <th>N</th> <th>p</th> <th>h</th> <th>d</th> <th>Alt</th> </tr> </thead> <tbody> <tr> <td>1</td> <td>29.05</td> <td>0.5583</td> <td>0.5583</td> <td>0.5582</td> </tr> <tr> <td>2</td> <td>145.7</td> <td>0.8633</td> <td>1.422</td> <td>-1.4216</td> </tr> <tr> <td>3</td> <td>18.71</td> <td>0.9411</td> <td>2.363</td> <td>-2.3626</td> </tr> <tr> <td>4</td> <td>65.79</td> <td>11.38</td> <td>13.74</td> <td>-13.743</td> </tr> <tr> <td>5</td> <td>17.24</td> <td>11.5</td> <td>25.24</td> <td>-25.24</td> </tr> <tr> <td>6</td> <td>117.8</td> <td></td> <td></td> <td></td> </tr> </tbody> </table>	N	p	h	d	Alt	1	29.05	0.5583	0.5583	0.5582	2	145.7	0.8633	1.422	-1.4216	3	18.71	0.9411	2.363	-2.3626	4	65.79	11.38	13.74	-13.743	5	17.24	11.5	25.24	-25.24	6	117.8				
N	p	h	d	Alt																																	
1	29.05	0.5583	0.5583	0.5582																																	
2	145.7	0.8633	1.422	-1.4216																																	
3	18.71	0.9411	2.363	-2.3626																																	
4	65.79	11.38	13.74	-13.743																																	
5	17.24	11.5	25.24	-25.24																																	
6	117.8																																				
20.	<table border="1"> <thead> <tr> <th>N</th> <th>p</th> <th>h</th> <th>d</th> <th>Alt</th> </tr> </thead> <tbody> <tr> <td>1</td> <td>64.02</td> <td>0.662</td> <td>0.662</td> <td>-0.662</td> </tr> <tr> <td>2</td> <td>135.5</td> <td>0.4076</td> <td>1.07</td> <td>-1.0696</td> </tr> <tr> <td>3</td> <td>95.6</td> <td>7.933</td> <td>9.003</td> <td>-9.0026</td> </tr> <tr> <td>4</td> <td>41.96</td> <td></td> <td></td> <td></td> </tr> </tbody> </table>	N	p	h	d	Alt	1	64.02	0.662	0.662	-0.662	2	135.5	0.4076	1.07	-1.0696	3	95.6	7.933	9.003	-9.0026	4	41.96														
N	p	h	d	Alt																																	
1	64.02	0.662	0.662	-0.662																																	
2	135.5	0.4076	1.07	-1.0696																																	
3	95.6	7.933	9.003	-9.0026																																	
4	41.96																																				
21.	<table border="1"> <thead> <tr> <th>N</th> <th>p</th> <th>h</th> <th>d</th> <th>Alt</th> </tr> </thead> <tbody> <tr> <td>1</td> <td>12.99</td> <td>0.3264</td> <td>0.3264</td> <td>0.3263</td> </tr> <tr> <td>2</td> <td>455.3</td> <td>0.4092</td> <td>0.7355</td> <td>0.7355</td> </tr> <tr> <td>3</td> <td>18.52</td> <td>1.262</td> <td>1.998</td> <td>-1.9979</td> </tr> <tr> <td>4</td> <td>122.9</td> <td>11.95</td> <td>13.95</td> <td>-13.953</td> </tr> <tr> <td>5</td> <td>7.717</td> <td>12.25</td> <td>26.2</td> <td>-26.198</td> </tr> <tr> <td>6</td> <td>1278</td> <td></td> <td></td> <td></td> </tr> </tbody> </table>	N	p	h	d	Alt	1	12.99	0.3264	0.3264	0.3263	2	455.3	0.4092	0.7355	0.7355	3	18.52	1.262	1.998	-1.9979	4	122.9	11.95	13.95	-13.953	5	7.717	12.25	26.2	-26.198	6	1278				
N	p	h	d	Alt																																	
1	12.99	0.3264	0.3264	0.3263																																	
2	455.3	0.4092	0.7355	0.7355																																	
3	18.52	1.262	1.998	-1.9979																																	
4	122.9	11.95	13.95	-13.953																																	
5	7.717	12.25	26.2	-26.198																																	
6	1278																																				
22.	<table border="1"> <thead> <tr> <th>N</th> <th>p</th> <th>h</th> <th>d</th> <th>Alt</th> </tr> </thead> <tbody> <tr> <td>1</td> <td>42.69</td> <td>1.491</td> <td>1.491</td> <td>-1.4906</td> </tr> <tr> <td>2</td> <td>64.23</td> <td>20.03</td> <td>21.52</td> <td>-21.519</td> </tr> <tr> <td>3</td> <td>9.614</td> <td>10.82</td> <td>32.33</td> <td>-32.335</td> </tr> <tr> <td>4</td> <td>1627</td> <td></td> <td></td> <td></td> </tr> </tbody> </table>	N	p	h	d	Alt	1	42.69	1.491	1.491	-1.4906	2	64.23	20.03	21.52	-21.519	3	9.614	10.82	32.33	-32.335	4	1627														
N	p	h	d	Alt																																	
1	42.69	1.491	1.491	-1.4906																																	
2	64.23	20.03	21.52	-21.519																																	
3	9.614	10.82	32.33	-32.335																																	
4	1627																																				

23.	<table border="1"> <thead> <tr> <th>N</th> <th>p</th> <th>h</th> <th>d</th> <th>Alt</th> </tr> </thead> <tbody> <tr> <td>1</td> <td>8.463</td> <td>0.3017</td> <td>0.3017</td> <td>0.30167</td> </tr> <tr> <td>2</td> <td>311.3</td> <td>0.3908</td> <td>0.6924</td> <td>0.69244</td> </tr> <tr> <td>3</td> <td>10.42</td> <td>0.4627</td> <td>1.155</td> <td>-1.1552</td> </tr> <tr> <td>4</td> <td>64.85</td> <td>21.54</td> <td>22.7</td> <td>-22.698</td> </tr> <tr> <td>5</td> <td>35.96</td> <td></td> <td></td> <td></td> </tr> </tbody> </table>	N	p	h	d	Alt	1	8.463	0.3017	0.3017	0.30167	2	311.3	0.3908	0.6924	0.69244	3	10.42	0.4627	1.155	-1.1552	4	64.85	21.54	22.7	-22.698	5	35.96									
N	p	h	d	Alt																																	
1	8.463	0.3017	0.3017	0.30167																																	
2	311.3	0.3908	0.6924	0.69244																																	
3	10.42	0.4627	1.155	-1.1552																																	
4	64.85	21.54	22.7	-22.698																																	
5	35.96																																				
24.	<table border="1"> <thead> <tr> <th>N</th> <th>p</th> <th>h</th> <th>d</th> <th>Alt</th> </tr> </thead> <tbody> <tr> <td>1</td> <td>54.19</td> <td>7.491</td> <td>7.491</td> <td>-7.491</td> </tr> <tr> <td>2</td> <td>190.8</td> <td>1.693</td> <td>9.184</td> <td>-9.1843</td> </tr> <tr> <td>3</td> <td>45.36</td> <td>50.13</td> <td>59.32</td> <td>-59.316</td> </tr> <tr> <td>4</td> <td>4.816</td> <td></td> <td></td> <td></td> </tr> </tbody> </table>	N	p	h	d	Alt	1	54.19	7.491	7.491	-7.491	2	190.8	1.693	9.184	-9.1843	3	45.36	50.13	59.32	-59.316	4	4.816														
N	p	h	d	Alt																																	
1	54.19	7.491	7.491	-7.491																																	
2	190.8	1.693	9.184	-9.1843																																	
3	45.36	50.13	59.32	-59.316																																	
4	4.816																																				
25.	<table border="1"> <thead> <tr> <th>N</th> <th>p</th> <th>h</th> <th>d</th> <th>Alt</th> </tr> </thead> <tbody> <tr> <td>1</td> <td>32.28</td> <td>0.5357</td> <td>0.5357</td> <td>0.53564</td> </tr> <tr> <td>2</td> <td>242.2</td> <td>0.6519</td> <td>1.188</td> <td>-1.1876</td> </tr> <tr> <td>3</td> <td>84.9</td> <td>8.346</td> <td>9.533</td> <td>-9.5335</td> </tr> <tr> <td>4</td> <td>48.18</td> <td></td> <td></td> <td></td> </tr> </tbody> </table>	N	p	h	d	Alt	1	32.28	0.5357	0.5357	0.53564	2	242.2	0.6519	1.188	-1.1876	3	84.9	8.346	9.533	-9.5335	4	48.18														
N	p	h	d	Alt																																	
1	32.28	0.5357	0.5357	0.53564																																	
2	242.2	0.6519	1.188	-1.1876																																	
3	84.9	8.346	9.533	-9.5335																																	
4	48.18																																				
26.	<table border="1"> <thead> <tr> <th>N</th> <th>p</th> <th>h</th> <th>d</th> <th>Alt</th> </tr> </thead> <tbody> <tr> <td>1</td> <td>133.2</td> <td>0.7106</td> <td>0.7106</td> <td>0.71054</td> </tr> <tr> <td>2</td> <td>75.61</td> <td>1.743</td> <td>2.453</td> <td>-2.4531</td> </tr> <tr> <td>3</td> <td>50.54</td> <td>24.33</td> <td>26.79</td> <td>-26.787</td> </tr> <tr> <td>4</td> <td>17.9</td> <td>17.62</td> <td>44.41</td> <td>-44.406</td> </tr> <tr> <td>5</td> <td>835.3</td> <td></td> <td></td> <td></td> </tr> </tbody> </table>	N	p	h	d	Alt	1	133.2	0.7106	0.7106	0.71054	2	75.61	1.743	2.453	-2.4531	3	50.54	24.33	26.79	-26.787	4	17.9	17.62	44.41	-44.406	5	835.3									
N	p	h	d	Alt																																	
1	133.2	0.7106	0.7106	0.71054																																	
2	75.61	1.743	2.453	-2.4531																																	
3	50.54	24.33	26.79	-26.787																																	
4	17.9	17.62	44.41	-44.406																																	
5	835.3																																				
27.	<table border="1"> <thead> <tr> <th>N</th> <th>p</th> <th>h</th> <th>d</th> <th>Alt</th> </tr> </thead> <tbody> <tr> <td>1</td> <td>71.66</td> <td>0.6995</td> <td>0.6995</td> <td>-0.6995</td> </tr> <tr> <td>2</td> <td>365</td> <td>0.6583</td> <td>1.358</td> <td>-1.3578</td> </tr> <tr> <td>3</td> <td>8.477</td> <td>1.06</td> <td>2.417</td> <td>-2.4174</td> </tr> <tr> <td>4</td> <td>125.8</td> <td>3.331</td> <td>5.748</td> <td>-5.7482</td> </tr> <tr> <td>5</td> <td>11.84</td> <td>5.093</td> <td>10.84</td> <td>-10.841</td> </tr> <tr> <td>6</td> <td>64.4</td> <td></td> <td></td> <td></td> </tr> </tbody> </table>	N	p	h	d	Alt	1	71.66	0.6995	0.6995	-0.6995	2	365	0.6583	1.358	-1.3578	3	8.477	1.06	2.417	-2.4174	4	125.8	3.331	5.748	-5.7482	5	11.84	5.093	10.84	-10.841	6	64.4				
N	p	h	d	Alt																																	
1	71.66	0.6995	0.6995	-0.6995																																	
2	365	0.6583	1.358	-1.3578																																	
3	8.477	1.06	2.417	-2.4174																																	
4	125.8	3.331	5.748	-5.7482																																	
5	11.84	5.093	10.84	-10.841																																	
6	64.4																																				
28.	<table border="1"> <thead> <tr> <th>N</th> <th>p</th> <th>h</th> <th>d</th> <th>Alt</th> </tr> </thead> <tbody> <tr> <td>1</td> <td>44.206</td> <td>1.4662</td> <td>1.4662</td> <td>1.46614</td> </tr> <tr> <td>2</td> <td>219.55</td> <td>0.71789</td> <td>2.184</td> <td>2.18405</td> </tr> <tr> <td>3</td> <td>14.086</td> <td>2.03</td> <td>4.214</td> <td>4.21404</td> </tr> <tr> <td>4</td> <td>310.25</td> <td>2.841</td> <td>7.0551</td> <td>7.05504</td> </tr> <tr> <td>5</td> <td>54.648</td> <td></td> <td></td> <td></td> </tr> </tbody> </table>	N	p	h	d	Alt	1	44.206	1.4662	1.4662	1.46614	2	219.55	0.71789	2.184	2.18405	3	14.086	2.03	4.214	4.21404	4	310.25	2.841	7.0551	7.05504	5	54.648									
N	p	h	d	Alt																																	
1	44.206	1.4662	1.4662	1.46614																																	
2	219.55	0.71789	2.184	2.18405																																	
3	14.086	2.03	4.214	4.21404																																	
4	310.25	2.841	7.0551	7.05504																																	
5	54.648																																				
29.	<table border="1"> <thead> <tr> <th>N</th> <th>p</th> <th>h</th> <th>d</th> <th>Alt</th> </tr> </thead> <tbody> <tr> <td>1</td> <td>63.17</td> <td>0.7556</td> <td>0.7556</td> <td>0.75554</td> </tr> <tr> <td>2</td> <td>122.8</td> <td>1.236</td> <td>1.991</td> <td>-1.9913</td> </tr> <tr> <td>3</td> <td>53.28</td> <td>18.2</td> <td>20.19</td> <td>-20.189</td> </tr> <tr> <td>4</td> <td>64.97</td> <td></td> <td></td> <td></td> </tr> </tbody> </table>	N	p	h	d	Alt	1	63.17	0.7556	0.7556	0.75554	2	122.8	1.236	1.991	-1.9913	3	53.28	18.2	20.19	-20.189	4	64.97														
N	p	h	d	Alt																																	
1	63.17	0.7556	0.7556	0.75554																																	
2	122.8	1.236	1.991	-1.9913																																	
3	53.28	18.2	20.19	-20.189																																	
4	64.97																																				
30.	<table border="1"> <thead> <tr> <th>N</th> <th>p</th> <th>h</th> <th>d</th> <th>Alt</th> </tr> </thead> <tbody> <tr> <td>1</td> <td>66.45</td> <td>0.4556</td> <td>0.4556</td> <td>-0.4556</td> </tr> <tr> <td>2</td> <td>50.75</td> <td>9.614</td> <td>10.07</td> <td>-10.069</td> </tr> <tr> <td>3</td> <td>143</td> <td>5.448</td> <td>15.52</td> <td>-15.518</td> </tr> <tr> <td>4</td> <td>7.824</td> <td>10.33</td> <td>25.85</td> <td>-25.851</td> </tr> <tr> <td>5</td> <td>919.4</td> <td></td> <td></td> <td></td> </tr> </tbody> </table>	N	p	h	d	Alt	1	66.45	0.4556	0.4556	-0.4556	2	50.75	9.614	10.07	-10.069	3	143	5.448	15.52	-15.518	4	7.824	10.33	25.85	-25.851	5	919.4									
N	p	h	d	Alt																																	
1	66.45	0.4556	0.4556	-0.4556																																	
2	50.75	9.614	10.07	-10.069																																	
3	143	5.448	15.52	-15.518																																	
4	7.824	10.33	25.85	-25.851																																	
5	919.4																																				

31.	<table border="1"> <thead> <tr> <th>N</th> <th>p</th> <th>h</th> <th>d</th> <th>Alt</th> </tr> </thead> <tbody> <tr> <td>1</td> <td>22.7</td> <td>2.12</td> <td>2.12</td> <td>-2.123</td> </tr> <tr> <td>2</td> <td>464</td> <td>1.54</td> <td>3.66</td> <td>-3.663</td> </tr> <tr> <td>3</td> <td>4.06</td> <td>2.28</td> <td>5.94</td> <td>-5.941</td> </tr> <tr> <td>4</td> <td>105</td> <td></td> <td></td> <td></td> </tr> </tbody> </table>	N	p	h	d	Alt	1	22.7	2.12	2.12	-2.123	2	464	1.54	3.66	-3.663	3	4.06	2.28	5.94	-5.941	4	105														
N	p	h	d	Alt																																	
1	22.7	2.12	2.12	-2.123																																	
2	464	1.54	3.66	-3.663																																	
3	4.06	2.28	5.94	-5.941																																	
4	105																																				
32.	<table border="1"> <thead> <tr> <th>N</th> <th>p</th> <th>h</th> <th>d</th> <th>Alt</th> </tr> </thead> <tbody> <tr> <td>1</td> <td>90.71</td> <td>3.232</td> <td>3.232</td> <td>-3.2319</td> </tr> <tr> <td>2</td> <td>74.87</td> <td>11.71</td> <td>14.94</td> <td>-14.944</td> </tr> <tr> <td>3</td> <td>53.38</td> <td>53.61</td> <td>68.55</td> <td>-68.552</td> </tr> <tr> <td>4</td> <td>180.9</td> <td></td> <td></td> <td></td> </tr> </tbody> </table>	N	p	h	d	Alt	1	90.71	3.232	3.232	-3.2319	2	74.87	11.71	14.94	-14.944	3	53.38	53.61	68.55	-68.552	4	180.9														
N	p	h	d	Alt																																	
1	90.71	3.232	3.232	-3.2319																																	
2	74.87	11.71	14.94	-14.944																																	
3	53.38	53.61	68.55	-68.552																																	
4	180.9																																				
33.	<table border="1"> <thead> <tr> <th>N</th> <th>p</th> <th>h</th> <th>d</th> <th>Alt</th> </tr> </thead> <tbody> <tr> <td>1</td> <td>118.2</td> <td>1.483</td> <td>1.483</td> <td>-1.4827</td> </tr> <tr> <td>2</td> <td>39.82</td> <td>8.137</td> <td>9.619</td> <td>-9.6194</td> </tr> <tr> <td>3</td> <td>206.6</td> <td>6.254</td> <td>15.87</td> <td>-15.874</td> </tr> <tr> <td>4</td> <td>9.757</td> <td>9.893</td> <td>25.77</td> <td>-25.766</td> </tr> <tr> <td>5</td> <td>1466</td> <td></td> <td></td> <td></td> </tr> </tbody> </table>	N	p	h	d	Alt	1	118.2	1.483	1.483	-1.4827	2	39.82	8.137	9.619	-9.6194	3	206.6	6.254	15.87	-15.874	4	9.757	9.893	25.77	-25.766	5	1466									
N	p	h	d	Alt																																	
1	118.2	1.483	1.483	-1.4827																																	
2	39.82	8.137	9.619	-9.6194																																	
3	206.6	6.254	15.87	-15.874																																	
4	9.757	9.893	25.77	-25.766																																	
5	1466																																				
34.	<table border="1"> <thead> <tr> <th>N</th> <th>p</th> <th>h</th> <th>d</th> <th>Alt</th> </tr> </thead> <tbody> <tr> <td>1</td> <td>92.06</td> <td>1.788</td> <td>1.788</td> <td>-1.7883</td> </tr> <tr> <td>2</td> <td>164.1</td> <td>0.851</td> <td>2.639</td> <td>-2.6393</td> </tr> <tr> <td>3</td> <td>49.7</td> <td>9.193</td> <td>11.83</td> <td>-11.832</td> </tr> <tr> <td>4</td> <td>13.64</td> <td>5.807</td> <td>17.64</td> <td>-17.639</td> </tr> <tr> <td>5</td> <td>88.58</td> <td></td> <td></td> <td></td> </tr> </tbody> </table>	N	p	h	d	Alt	1	92.06	1.788	1.788	-1.7883	2	164.1	0.851	2.639	-2.6393	3	49.7	9.193	11.83	-11.832	4	13.64	5.807	17.64	-17.639	5	88.58									
N	p	h	d	Alt																																	
1	92.06	1.788	1.788	-1.7883																																	
2	164.1	0.851	2.639	-2.6393																																	
3	49.7	9.193	11.83	-11.832																																	
4	13.64	5.807	17.64	-17.639																																	
5	88.58																																				
35.	<table border="1"> <thead> <tr> <th>N</th> <th>p</th> <th>h</th> <th>d</th> <th>Alt</th> </tr> </thead> <tbody> <tr> <td>1</td> <td>65.23</td> <td>2.236</td> <td>2.236</td> <td>-2.2365</td> </tr> <tr> <td>2</td> <td>209.6</td> <td>0.8219</td> <td>3.058</td> <td>-3.0584</td> </tr> <tr> <td>3</td> <td>26.26</td> <td>2.632</td> <td>5.69</td> <td>-5.6904</td> </tr> <tr> <td>4</td> <td>356.5</td> <td>1.693</td> <td>7.383</td> <td>-7.383</td> </tr> <tr> <td>5</td> <td>57.96</td> <td></td> <td></td> <td></td> </tr> </tbody> </table>	N	p	h	d	Alt	1	65.23	2.236	2.236	-2.2365	2	209.6	0.8219	3.058	-3.0584	3	26.26	2.632	5.69	-5.6904	4	356.5	1.693	7.383	-7.383	5	57.96									
N	p	h	d	Alt																																	
1	65.23	2.236	2.236	-2.2365																																	
2	209.6	0.8219	3.058	-3.0584																																	
3	26.26	2.632	5.69	-5.6904																																	
4	356.5	1.693	7.383	-7.383																																	
5	57.96																																				
36.	<table border="1"> <thead> <tr> <th>N</th> <th>p</th> <th>h</th> <th>d</th> <th>Alt</th> </tr> </thead> <tbody> <tr> <td>1</td> <td>18.21</td> <td>0.2964</td> <td>0.2964</td> <td>0.2963</td> </tr> <tr> <td>2</td> <td>1230</td> <td>0.2256</td> <td>0.522</td> <td>0.5219</td> </tr> <tr> <td>3</td> <td>63.49</td> <td>13.37</td> <td>13.89</td> <td>-13.892</td> </tr> <tr> <td>4</td> <td>29.2</td> <td>32.86</td> <td>46.76</td> <td>-46.757</td> </tr> <tr> <td>5</td> <td>1376</td> <td></td> <td></td> <td></td> </tr> </tbody> </table>	N	p	h	d	Alt	1	18.21	0.2964	0.2964	0.2963	2	1230	0.2256	0.522	0.5219	3	63.49	13.37	13.89	-13.892	4	29.2	32.86	46.76	-46.757	5	1376									
N	p	h	d	Alt																																	
1	18.21	0.2964	0.2964	0.2963																																	
2	1230	0.2256	0.522	0.5219																																	
3	63.49	13.37	13.89	-13.892																																	
4	29.2	32.86	46.76	-46.757																																	
5	1376																																				
37.	<table border="1"> <thead> <tr> <th>N</th> <th>p</th> <th>h</th> <th>d</th> <th>Alt</th> </tr> </thead> <tbody> <tr> <td>1</td> <td>117.8</td> <td>1.049</td> <td>1.049</td> <td>-1.0485</td> </tr> <tr> <td>2</td> <td>150.7</td> <td>2.972</td> <td>4.021</td> <td>-4.021</td> </tr> <tr> <td>3</td> <td>24.12</td> <td>3.538</td> <td>7.559</td> <td>-7.5591</td> </tr> <tr> <td>4</td> <td>128.6</td> <td>7.472</td> <td>15.03</td> <td>-15.031</td> </tr> <tr> <td>5</td> <td>14.51</td> <td>19.68</td> <td>34.71</td> <td>-34.713</td> </tr> <tr> <td>6</td> <td>1205</td> <td></td> <td></td> <td></td> </tr> </tbody> </table>	N	p	h	d	Alt	1	117.8	1.049	1.049	-1.0485	2	150.7	2.972	4.021	-4.021	3	24.12	3.538	7.559	-7.5591	4	128.6	7.472	15.03	-15.031	5	14.51	19.68	34.71	-34.713	6	1205				
N	p	h	d	Alt																																	
1	117.8	1.049	1.049	-1.0485																																	
2	150.7	2.972	4.021	-4.021																																	
3	24.12	3.538	7.559	-7.5591																																	
4	128.6	7.472	15.03	-15.031																																	
5	14.51	19.68	34.71	-34.713																																	
6	1205																																				
38.	<table border="1"> <thead> <tr> <th>N</th> <th>p</th> <th>h</th> <th>d</th> <th>Alt</th> </tr> </thead> <tbody> <tr> <td>1</td> <td>56.46</td> <td>0.4137</td> <td>0.4137</td> <td>0.4136</td> </tr> <tr> <td>2</td> <td>42.33</td> <td>3.734</td> <td>4.148</td> <td>-4.148</td> </tr> <tr> <td>3</td> <td>106.8</td> <td>6.917</td> <td>11.07</td> <td>-11.065</td> </tr> <tr> <td>4</td> <td>20.18</td> <td>27.09</td> <td>38.16</td> <td>-38.156</td> </tr> <tr> <td>5</td> <td>1910</td> <td></td> <td></td> <td></td> </tr> </tbody> </table>	N	p	h	d	Alt	1	56.46	0.4137	0.4137	0.4136	2	42.33	3.734	4.148	-4.148	3	106.8	6.917	11.07	-11.065	4	20.18	27.09	38.16	-38.156	5	1910									
N	p	h	d	Alt																																	
1	56.46	0.4137	0.4137	0.4136																																	
2	42.33	3.734	4.148	-4.148																																	
3	106.8	6.917	11.07	-11.065																																	
4	20.18	27.09	38.16	-38.156																																	
5	1910																																				

39.	<table border="1"> <thead> <tr> <th>N</th> <th>p</th> <th>h</th> <th>d</th> <th>Alt</th> </tr> </thead> <tbody> <tr> <td>1</td> <td>176</td> <td>0.858</td> <td>0.858</td> <td>-0.8583</td> </tr> <tr> <td>2</td> <td>639</td> <td>0.338</td> <td>1.2</td> <td>-1.196</td> </tr> <tr> <td>3</td> <td>76.3</td> <td>14.2</td> <td>15.4</td> <td>-15.44</td> </tr> <tr> <td>4</td> <td>39.4</td> <td></td> <td></td> <td></td> </tr> <tr> <td></td> <td></td> <td></td> <td></td> <td></td> </tr> </tbody> </table>	N	p	h	d	Alt	1	176	0.858	0.858	-0.8583	2	639	0.338	1.2	-1.196	3	76.3	14.2	15.4	-15.44	4	39.4														
N	p	h	d	Alt																																	
1	176	0.858	0.858	-0.8583																																	
2	639	0.338	1.2	-1.196																																	
3	76.3	14.2	15.4	-15.44																																	
4	39.4																																				
40.	<table border="1"> <thead> <tr> <th>N</th> <th>p</th> <th>h</th> <th>d</th> <th>Alt</th> </tr> </thead> <tbody> <tr> <td>1</td> <td>104</td> <td>1.22</td> <td>1.22</td> <td>-1.222</td> </tr> <tr> <td>2</td> <td>51.9</td> <td>3.3</td> <td>4.52</td> <td>-4.521</td> </tr> <tr> <td>3</td> <td>247</td> <td>3.16</td> <td>7.68</td> <td>-7.677</td> </tr> <tr> <td>4</td> <td>6.56</td> <td>5.32</td> <td>13</td> <td>-13</td> </tr> <tr> <td>5</td> <td>164</td> <td></td> <td></td> <td></td> </tr> </tbody> </table>	N	p	h	d	Alt	1	104	1.22	1.22	-1.222	2	51.9	3.3	4.52	-4.521	3	247	3.16	7.68	-7.677	4	6.56	5.32	13	-13	5	164									
N	p	h	d	Alt																																	
1	104	1.22	1.22	-1.222																																	
2	51.9	3.3	4.52	-4.521																																	
3	247	3.16	7.68	-7.677																																	
4	6.56	5.32	13	-13																																	
5	164																																				
41.	<table border="1"> <thead> <tr> <th>N</th> <th>p</th> <th>h</th> <th>d</th> <th>Alt</th> </tr> </thead> <tbody> <tr> <td>1</td> <td>101.8</td> <td>1.994</td> <td>1.994</td> <td>-1.9939</td> </tr> <tr> <td>2</td> <td>46.42</td> <td>1.436</td> <td>3.43</td> <td>-3.4301</td> </tr> <tr> <td>3</td> <td>537.2</td> <td>0.3357</td> <td>3.766</td> <td>-3.7659</td> </tr> <tr> <td>4</td> <td>64.44</td> <td></td> <td></td> <td></td> </tr> </tbody> </table>	N	p	h	d	Alt	1	101.8	1.994	1.994	-1.9939	2	46.42	1.436	3.43	-3.4301	3	537.2	0.3357	3.766	-3.7659	4	64.44														
N	p	h	d	Alt																																	
1	101.8	1.994	1.994	-1.9939																																	
2	46.42	1.436	3.43	-3.4301																																	
3	537.2	0.3357	3.766	-3.7659																																	
4	64.44																																				
42.	<table border="1"> <thead> <tr> <th>N</th> <th>p</th> <th>h</th> <th>d</th> <th>Alt</th> </tr> </thead> <tbody> <tr> <td>1</td> <td>145.9</td> <td>1.051</td> <td>1.051</td> <td>-1.0506</td> </tr> <tr> <td>2</td> <td>83.39</td> <td>10.46</td> <td>11.51</td> <td>-11.515</td> </tr> <tr> <td>3</td> <td>43.78</td> <td>9.602</td> <td>21.12</td> <td>-21.117</td> </tr> <tr> <td>4</td> <td>71.53</td> <td></td> <td></td> <td></td> </tr> </tbody> </table>	N	p	h	d	Alt	1	145.9	1.051	1.051	-1.0506	2	83.39	10.46	11.51	-11.515	3	43.78	9.602	21.12	-21.117	4	71.53														
N	p	h	d	Alt																																	
1	145.9	1.051	1.051	-1.0506																																	
2	83.39	10.46	11.51	-11.515																																	
3	43.78	9.602	21.12	-21.117																																	
4	71.53																																				
43.	<table border="1"> <thead> <tr> <th>N</th> <th>p</th> <th>h</th> <th>d</th> <th>Alt</th> </tr> </thead> <tbody> <tr> <td>1</td> <td>165.3</td> <td>1.272</td> <td>1.272</td> <td>-1.2723</td> </tr> <tr> <td>2</td> <td>233.5</td> <td>1.127</td> <td>2.399</td> <td>-2.3989</td> </tr> <tr> <td>3</td> <td>72.72</td> <td>11.01</td> <td>13.41</td> <td>-13.412</td> </tr> <tr> <td>4</td> <td>38.76</td> <td>42.73</td> <td>56.14</td> <td>-56.14</td> </tr> <tr> <td>5</td> <td>1288</td> <td></td> <td></td> <td></td> </tr> </tbody> </table>	N	p	h	d	Alt	1	165.3	1.272	1.272	-1.2723	2	233.5	1.127	2.399	-2.3989	3	72.72	11.01	13.41	-13.412	4	38.76	42.73	56.14	-56.14	5	1288									
N	p	h	d	Alt																																	
1	165.3	1.272	1.272	-1.2723																																	
2	233.5	1.127	2.399	-2.3989																																	
3	72.72	11.01	13.41	-13.412																																	
4	38.76	42.73	56.14	-56.14																																	
5	1288																																				
44.	<table border="1"> <thead> <tr> <th>N</th> <th>p</th> <th>h</th> <th>d</th> <th>Alt</th> </tr> </thead> <tbody> <tr> <td>1</td> <td>81.63</td> <td>1.544</td> <td>1.544</td> <td>-1.5444</td> </tr> <tr> <td>2</td> <td>139</td> <td>1.279</td> <td>2.823</td> <td>-2.8233</td> </tr> <tr> <td>3</td> <td>33.36</td> <td>2.831</td> <td>5.654</td> <td>-5.6544</td> </tr> <tr> <td>4</td> <td>338.7</td> <td>4.253</td> <td>9.908</td> <td>-9.9077</td> </tr> <tr> <td>5</td> <td>44.85</td> <td>34.02</td> <td>43.93</td> <td>-43.931</td> </tr> <tr> <td>6</td> <td>2854</td> <td></td> <td></td> <td></td> </tr> </tbody> </table>	N	p	h	d	Alt	1	81.63	1.544	1.544	-1.5444	2	139	1.279	2.823	-2.8233	3	33.36	2.831	5.654	-5.6544	4	338.7	4.253	9.908	-9.9077	5	44.85	34.02	43.93	-43.931	6	2854				
N	p	h	d	Alt																																	
1	81.63	1.544	1.544	-1.5444																																	
2	139	1.279	2.823	-2.8233																																	
3	33.36	2.831	5.654	-5.6544																																	
4	338.7	4.253	9.908	-9.9077																																	
5	44.85	34.02	43.93	-43.931																																	
6	2854																																				
45.	<table border="1"> <thead> <tr> <th>N</th> <th>p</th> <th>h</th> <th>d</th> <th>Alt</th> </tr> </thead> <tbody> <tr> <td>1</td> <td>54.6</td> <td>0.7632</td> <td>0.7632</td> <td>0.76311</td> </tr> <tr> <td>2</td> <td>70.21</td> <td>2.348</td> <td>3.112</td> <td>-3.1116</td> </tr> <tr> <td>3</td> <td>61.23</td> <td>57.89</td> <td>61</td> <td>-60.997</td> </tr> <tr> <td>4</td> <td>20.72</td> <td></td> <td></td> <td></td> </tr> </tbody> </table>	N	p	h	d	Alt	1	54.6	0.7632	0.7632	0.76311	2	70.21	2.348	3.112	-3.1116	3	61.23	57.89	61	-60.997	4	20.72														
N	p	h	d	Alt																																	
1	54.6	0.7632	0.7632	0.76311																																	
2	70.21	2.348	3.112	-3.1116																																	
3	61.23	57.89	61	-60.997																																	
4	20.72																																				

7. Development of Piezometers and Groundwater Management

Maharashtra is predominantly an agrarian State and most of its area constitutes the hard-rock terrain. The rain-shadow drought prone region (DPR) constitutes an important agroclimatic region of the state. In general, depleting groundwater levels and over-exploitation due to repeated droughts have characterized the DPR. However, with the advent of the irrigated agriculture in the DPR the water levels in some of the command areas began to rise. The lava flows belonging to the Deccan Trap aquifers from this region have complex geometries, low storativity, low hydraulic conductivity and uncertain groundwater yields. The recharge of these aquifers is primarily dependent on the precipitation from the monsoon. The vagaries of monsoon and frequency and irregularities of the inter spell showers have a profound impact on the run off – recharge relationship. It follows that all these contributed to the low yields of water abstraction structures in the trappean aquifers. Over dependence on groundwater in the DPR has led to its overexploitation, falling water levels and degrading groundwater quality (e.g. Duraiswami et al., 2012).

The NIASM site at Malegaon khurd in Baramati Taluka of Pune District belongs to the rain-shadow drought prone region of the State. On the basis of PET and Moisture Index, the climate of the area can be classified into the Arid Megathermal type (Paranjpe, 2001). The total annual average rainfall is around 600 mm with 25-30 days gap between consecutive rain spells (Dhokariker, 1991). Thus, although the quantum of rainfall is adequate to recharge, the long gap between rain spells and the barren hard rock terrain with limited soil cover is conducive to large surface run-off with little or no infiltration and percolation into the sub-surface. Moreover the presence of a low weathered mantle on shallow hard

rock and un-jointed nature of the lava flows prove to be impediments to occurrence and movement of the groundwater at the NIASM site. This aspect is further complicated by the fact that the NIASM site is on ridge-like mound (water divide) which encourages the away movement of the groundwater leading to the absence of a phreatic water table below. Hence, the region below the NIASM site has a low groundwater potential and is not suitable for the exploration and development of water abstraction structures. The absence of any water abstraction structures within and in the near vicinity of the NIASM site is bears testimony to low groundwater potential of the site. Most of the water abstraction structure around the NIASM site is restricted to the adjacent low-lying water courses and are probably tapping the base flow and limited shallow phreatic aquifer.

Management of Groundwater Resources is of vital importance in the DPR region of Maharashtra State. Several schemes related to Watershed Development have been implemented by various line Departments of the State and Central Government and the Voluntary Organisations for the conservation on soil and surface run-off. Traditional watershed development interventions such as continuous contour trenches, contour bunds, loose boulder structure, vegetative filter strips, and other area treatment measures have been implemented in many places. Drainage treatment interventions like loose boulder structures, gabion structures, cement nala bunds are in vogue. Many of these interventions have proved their utility based on the merits of their siting and the quality of the civil works. The NIASM watershed has received considerable attention as far as the Watershed Development is concerned, but as the drainage are low order streams the detailed interventions have not been

implemented. The water divide on which the NIASM site is located is already been contour trenched and harrowed which will go a long way in hastening the soil formation process, reduce surface runoff and improve percolation of rainwater in the monsoon months.

In light of the agroclimatic zone, terrain characteristics and hydrogeology of the lava flows exposed at the NIASM sites the limited groundwater potential within the site calls for some management interventions. These are enlisted below:

1. Excavation of a series of Recharge Trenches filled with appropriate filter medium in areas where recharge potential is high e.g. along the down slope side of the road leading to the Main Building. Recharge trench can have a depth of about 1.5 m, 1-2 m wide and 3-4 m long. The slopes of the trench can be sloping to avoid collapse. These trenches may be filled with large boulders at the base followed by cobbles, pebbles and coarse sand as filter medium. Similarly, the Main Pit can be converted into a recharge point by drilling a borehole at its base and collecting runoff water within the Main Pit. Preparation of such recharge trenches will augment groundwater in the downstream side of the NIASM site.
2. A series of two large Farm Ponds admeasuring 20 x 20 x 3 m each is recommended to the southeast of the Main Building where the terrain slopes by ~5%. This structure may be stone pitched on all four sides but the bottom may be left to augment percolation. The monsoon runoff can be stored in these ponds and the excess may be used for artificial recharge.
3. Geophysical Surveys for groundwater exploration were

carried out using Electrical Resistivity Method for the delineation of potential/ suitable/ favorable zones for sinking of water abstraction structures (dug well / bore well) for water supply to farm land, plots and other utilities on the NIASM campus. Based on electrical resistivity survey most area below the NIASM is unfavourable for siting suitable sites for groundwater exploration. However, based on the moderate potential and urgent need for groundwater at the NIASM site an exploratory bore well is suggested in the southwest corner of the NIASM site at VES spot 2. This bore is expected to be low yielding but it can be augmented by increasing recharge towards its catchment through recharging trenches and recharge pits. Also the unconventional techniques like bore blasting, hydrofracturing, etc. developed by the Groundwater Surveys and Development Agency can be implemented subsequently. The bore well can be used for irrigational purposes if the yield is significant or may be converted into a piezometer for the continuous monitoring of the water table fluctuations. This information can be integrated with the meteorological data collected at the NIASM station to calculate the water budget of the area.

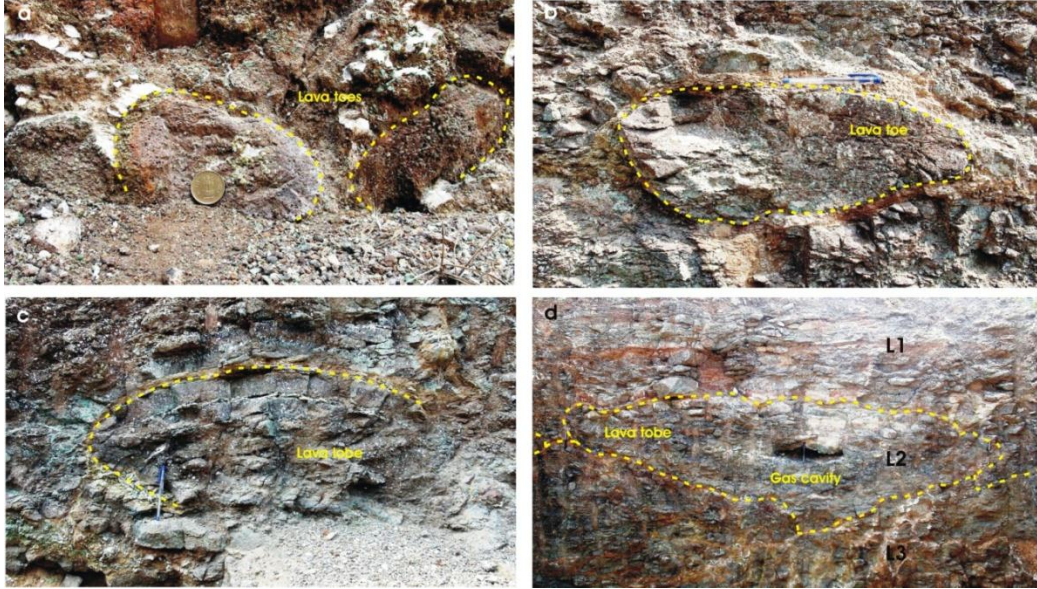
4. The NIASM site is to be landscaped into a beautiful campus with elaborate buildings. These civil structures can be used for roof top harvesting. The drain water can also be utilized to replenish the Farm ponds and the surplus can be diverted for artificial recharge into the recharge trench, pits, etc. The detail plan of the roof top rainwater harvesting will be finalised once the civil structures have been built.

8. References

- APHA, AWWA and WPCF (1981) Standard methods for the examination of water and wastewaters. American Public Health Association, 14th Edition, pp. 1193.
- Aubele, J.C., Crumpler, L.S. and Elston W.E. (1988) Vesicle zonation and vertical structure of basalt flows. *Jour. Volcanol. Geotherm. Res.*, v. 35, pp.349–374.
- Beane, J.E., Turner, C.A., Hooper, P.R., Subbarao, K.V. and Walsh, J.N. (1986) Stratigraphy, composition and form of the Deccan basalts, Western Ghats, India. *Bull. Volcanol.*, v. 48, pp. 61–83.
- Bhosale, U.R. (1982) Physical Environment of the Karha river basin, Pune district, Western Maharashtra, Unpublished M.Phil thesis, University of Poona, Pune. 67 p.
- Bhosale, U.R. and Patil, D.N. (1982) Physical Determinants of the environment in Karha basin, Maharashtra and their impact on land use. *Proc. of National Symposium on Environmental Management*, Allahabad. 75 p.
- Bondre N.R., Duraiswami, R.A. and Dole, G. (2004) Morphology and emplacement of flows from the Deccan Volcanic Province, India; *Bull. Volcanol.*, v. 66, pp. 29–45.
- Bureau of Indian Standards (1991) Drinking water specification (First Revision), IS 10500.
- Desai A. G. and Warriar S. (1987) Mineralogy and geochemistry of the calcretes in alluvial sediments from Pune, India. *Jour. Geol. Soc. India*, v. 24, pp. 584-593.
- Dhokariker, B.G. (1991) Groundwater Resource Development in Basaltic Rock Terrain of Maharashtra. Water Industry Publication, Pune.
- Duraiswami, R.A. (2000) Retrospective on the role of surface morphology and internal flow structure on the hydrogeology of basaltic aquifers in the Deccan Volcanic Province. In: *Groundwater Surveys and Development Agency Seminar volume “Integrated approach for strengthening and protecting drinking water sources”*, IUCCA, Pune, 1999, pp. 310-320.
- Duraiswami, R.A. (2008) Changing geohydrological scenario in the hard-rock terrain of Maharashtra: issues, concerns and way forward. In: *Changing Geohydrological Scenario-Hard rock terrain of Peninsular India* (Ed.) Subhajyoti Das. *Geol. Soc. India Golden Jubilee volume*, pp. 86-121.
- Duraiswami, R.A. (2009) Pulsed inflation in the hummocky lava flow near Morgaon, Western Deccan Volcanic Province and its significance. *Current Science*, v. 97, no. 3, pp. 313-316
- Duraiswami, R.A., Bondre, N.R. and Managave, S. (2008a) Morphology of rubbly pahoehoe (simple) flows from the Deccan Volcanic Province: implications for style of emplacement. *Jour. Volcanol. Geotherm. Res.*, v. 177, pp. 822-836.
- Duraiswami, R.A., Krishnamurthy, V., Mitra, D. and Joshi, V.B. (2008b) Modeling salinity in the Karha River Basin: a Remote Sensing and GIS approach. *Jour. Applied Hydrology*, v. 20, no. 3, pp.37-50.
- Duraiswami, R.A., Dumale, V. and Shetty, U. (2009) Geospatial mapping of potential recharge zones in the Pune University, Shivajinagar-Kothrud area, Pune, Maharashtra, India. *Jour. Geol. Soc. Ind.*, v.73, pp. 621-630.
- Duraiswami, R.A., Babaji Maskare and Patankar, U.R. (2012) Geochemistry of groundwaters in the arid regions of Deccan Trap country, Maharashtra, India. *Special Publication of Indian Society of Applied Geochemists*, Hyderabad. In Press.
- Eggleton, R.E., Foudoulis, C. and Varkevissier (1987) Weathering of basalt: changes in rock chemistry and mineralogy. *Clays and Clay Minerals*, v. 35, 161-169.
- Gadgil, A., Deosthali, V. and Soibam, H. (1990) Analysis of agricultural dry spells in Pune District. In: *Modern techniques of rainwater harvesting, water conservation and artificial recharge for drinking water, afforestation, horticulture and agriculture*. GSDA Proceeding Volume, pp.73-84.
- Geological Survey of India (1998) Quadrangle Geological Map of Baramati Quadrangle. Government of India Press.
- Ghodke S.S, Powar K.B. and Kanegoankar, N.B. (1984) Trace elements distribution in Deccan Trap flows in Dive Ghat area, Pune district, Maharashtra. *Proc. Symp. on Deccan Traps and Bauxites*, Geological Survey of India. Special Publication No. 14, pp.55-62.
- Ghosh A.K., Sarkar, D., Bhattacharyya, P., Maurya, U.K. and Nayak, D.C. (2006). Mineralogical study of some arsenic contaminated soils of West Bengal, India. *Geoderma*, v. 136, pp. 300-309.
- Godbole, S.M., Rana, R. S., Natu, S.R. (1996) Lava stratigraphy of Deccan basalts of western Maharashtra. *Gondwana Geol. Mag. Spl. Publ.*, v. 2,125-134.
- Godbole, S.M., Rana, R.S., Natu, S.R. (1996) Lava stratigraphy of Deccan basalts of western Maharashtra. *Gondwana Geol. Mag. Spl. Publ.*, v. 2, 125-134.
- Goldich (1938) as quoted in Rankama and Sahama (1949)
- GSDA, (1992) A report of the salinity problem in Pune District. Unpub. GSDA Report, pp1-14.
- GSDA and Unicef (1999) Jalsandhan Margadarhika. Water Supply and Sanitation Department,

- Government of Maharashtra, Second Edition, pp. 1-116.
- Joshi, V.B. (2005) Environment impact assessment related to the drinking water quality deterioration from parts of the Karha river basin, Western Maharashtra, India. Unpubl. M.Sc. Dissertation, Sikkim Manipal University, New Delhi.
- Kale, M.G. and Dasgupta, S. (2009) Petrography of Quaternary sediments of Morgaon area, Pune District, Maharashtra, India. *Gond. Geol. Mag.*, v.24 (1), pp. 1-10.
- Kale, V.S. and Joshi, V. (2002) Field Guide. Global Continental Paleohydrology 1 (GLOCOPH-2002), CIRT, Pune, 6-14.
- Kale, V.S., Patil, D.N., Pawar, N.J., Rajaguru, S.N. (1993) Discovery of volcanic ash bed in the alluvial sediments at Morgaon, Maharashtra. *Man and Environment*, v. 18 (2), pp. 141-143.
- Kale, V.S. and Rajaguru, S.N. (1987) Late Quaternary alluvial history of the northwestern Deccan Upland Region. *Nature*, v. 325, pp. 612-614.
- Kanegaonkar N.B, Powar K.B (1978) Genesis of Plagioclase megacrysts in porphyritic basalts of Purandhar hills, Western Maharashtra. *Recent Res. Geol.*, Hindustan Publ. Corp, Delhi., v. 4, pp. 313-332.
- Kar, P.F. (1977) *Optical Mineralogy*. McGraw Hill, pp. 1-442.
- Khadri, S.R.F, Subbarao, K.V. and Walsh, J.N. (1999) Stratigraphy, form and structure of the east Pune basalts, western Deccan Basalt Province, India. *Geol. Soc. Ind. Mem.* v. 43, pp. 172-202.
- Korisettar, R., Venkatesan, T.R, Mishra, S., Rajaguru, S.N., Somayajulu, B. L. K., Tandon, S.K., Gogte, V.D., Ganjoo, R. K., and Kale, V.S. (1989) Discovery of tephra bed in the Quaternary alluvial sediments of Pune district (Maharashtra), Peninsular India. *Curr. Sci*, 58, pp. 564-567.
- Kothavala, R. (1991) The Wagholi cavansite locality near Poona, India. *Mineral. Record*, 22, 415-420.
- Krishnamurthy, V., Duraiswami, R.A. and Joshi, V.B. (2004) Application of Remote Sensing tools in the delineation of saline groundwater zones in hard rock areas: a case study from Pune district. *Global Spatial Data Infrastructure 7th Conference*, February 2-6, 2004, Bangalore.
- Makki, M.F., "Collecting cavansite in the Wagholi quarry complex, Pune, Maharashtra, India", *The Mineralogical Record*, v. 36, No. 6, pp. 507-512, Nov-Dec 2005.
- Maurya, U.K. and Vittal, K.P.R. (2010). *Geology of the NIAM Site. NIAM Technical Bulletin - 1*, National Institute of Abiotic Stress Management (ICAR), Baramati, 13p.
- Maurya, U.K. and Vittal, K.P.R. (2011a). Identification of Abiotic Edaphic Stressors at NIASM Site, Malegaon, A Geotechnical and Geological Study. NIASM Technical Bulletin - 2. National Institute of Abiotic Stress Management (ICAR), Baramati, 40pp.
- Maurya, U.K. and Vittal, K.P.R. (2011b). Forms and Development of Zeolites and its Application in Edaphic Stress Management. NIASM Technical Bulletin-3. National Institute of Abiotic Stress Management (ICAR), Baramati, 43pp (in Press).
- Middlemost, (1989) LeBas, M. J., LeMaitre, R.W., Streckeisen, A. and Zanettin, B. (1986) A chemical classification of volcanic rocks based on the total alkali-silica diagram. *Jour. Petrol.*, v. 27, pp. 745-750.
- Parker, A. (1970) An index of weathering for silicate rocks. *Geol. Mag.*, v. 107, pp. 501-504.
- Paranjpe, S. C. (2001) Climatic classification of the Maharashtra State based on methods proposed by Thornwaite. In: *An integrated approach for strengthening and protecting drinking water sources*, GSDA Seminar Volume, 489-498.
- Pawar, N. J. and Nikhumb, J. (2000) Hydrochemistry of groundwater from Behedi Basin, Deccan Trap Hydrologic Province, India. In: A. M. Pathan and S. S. Thigale (eds.) *Contribution to Environmental Geoscience*. Prof. K. B. Powar Commemorative Volume, Aravali Books International, New Delhi. 131-150.
- Piper, A.M. (1994) A graphic procedure in the geochemical interpretation of water analyses. *Am. Geophys. Union Trans.*, v. 25, pp. 914-923.
- Powar K. B., Thigale, S. S., Patil, D. N., Sukthankar, R. K., Bhosale, V. N., Gupte, S. C., Kannalkar, P. R., Gadgil, A. S. and Kelkar, M. B. (1984) A study of physical detenninants of Indrayani, Mula-Mutha and Kara river basins and the impact on land use. A preliminary report submitted to the Department of Science and Technology, Government of India. 10 p.
- Price, J. and Velbel, M.A. (2003) Chemical weathering indices applied to weathering profiles developed on heterogeneous felsic metamorphic parent rocks. *Chem. Geol.*, v.202, pp. 397-416.
- Rajguru, S.N., Kale, V.S. and Badam, G.L. (1993) Quaternary fluvial systems in upland Maharashtra. *Current Science*, v. 64, pp. 817-822.
- Rankama, K. and Sahama, Th. G. (1949) *Geochemistry*. The University of Chicago Press, Chicago, p. 1-911.
- Read, H.H. (1963) *Rutley's Elements of Mineralogy*. Twenty – Fifth Edition, Thomas Murby Publication, London, 525pp
- Richards, L.A. (1954) *Diagnosis and improvement of saline and alkali soils*. U.S. Department of Agriculture Handbook 60.
- Saleh, A., Al-Ruwaih, F. and Shehata, M. (1999) Hydrochemical processes operating within the main aquifers of Kuwait. *Jour Arid Environ.*, v. 42, pp. 195-209.

- Scerbina, V.V. (1939) Oxidation-reduction potentials as applied to the study of the paragenesis of minerals. *Compt. Rend. (Doklady) Acad. Sci. U.R.S.S.*, v. 22, p. 503.
- Sowani, P. V. and Peshwa, V. V. (1966) An olivine bearing basalt flow at Purandhar. *Jour. Univ. Pune, Science and Tech. Section 30*, pp. 113-116.
- Sowani, P. V. and Peshwa, V. V. (1970) Iddigsite from basalt flows at Purandhar, District Pune, *Jour. Univ. Pune, Science and Tech. Section 38*, pp. 85-88.
- Surana, A. (1988) Genesis of Calcrete deposits of Saswad-Nira tract, Western Maharashtra, India. Unpub M. Phil Thesis, University of Pune.
- Verma, S.P., Torres-Alvarado, I.S. and Sotelo-Rodríguez, Z.T. (2002) SINCLAS: standard Igneous norm and volcanic rock classification system. *Computers & Geosciences*, v. 28, pp. 711-715.
- Wilcox, L.V. (1948) The quality of water for irrigation use. *US Department of Agriculture, Tech. Bull.*, 1962, Washington DC, pp. 1-19.
- Wilmoth R.A., Walker, G.P.L. (1993) P-type and S-type pahoehoe: a study of vesicle distribution patterns in Hawaiian lava flows. *Jour. Volcanol Geotherm Res.*, v. 55, pp.129-142



National Institute of Abiotic Stress Management
(Deemed University)
Indian Council of Agricultural Research
Malegaon, Baramati - 413115, Pune, Maharashtra